GRAVITY WAVES ON WATER
WITH NON-UNIFORM DEPTH AND CURRENT

PROEFSCHRIFT

TER VERKRIJGING VAN DE GRAAD VAN DOCTOR IN
DE   TECHNISCHE   WETENSCHAPPEN   AAN   DE
TECHNISCHE HOGESCHOOL DELFT, OP GEZAG VAN DE
RECTOR MAGNIFICUS PROF.IR. B.P.TH. VELTMAN,
HOOGLERAAR IN DE AFDELING DER TECHNISCHE
NATUURKUNDE, VOOR EEN COMMISSIE AANGEWEZEN
DOOR HET COLLEGE VAN DEKANEN TE VERDEDIGEN
OP DINSDAG 19 MEI 1981 TE 14.00 UUR.

door

Nico BOOIJ
wiskundig ingenieur
geboren te Leiden

Dit proefschrift is goedgekeurd door de promotor prof. dr.
ir. J. A. Battjes

SUMMARY

A mathematical model for the combined refraction-diffraction
of linear periodic gravity waves on water is developed, in
which the influence of inhomogeneities of depth and current
is taken into account.
The model is used to compute partial reflection of waves
crossing a gully or an undersea slope, with influence of a
current. The model is also applied to prismatic wave
channels with reflecting side-walls. For a gully bounded by
shallows the model predicts the decay of wave height due to
radiation of energy in lateral direction.
For practical application in regions with arbitrary bottom
and current topography a parabolic approximation of the
model is derived. This is used as a basis for numerical
calculation of waves in a sea region near the coast.

Stellingen

I

Nagegaan dient te worden voor welke eindtermen het indienen van stellingen dienstig is, en vervolgens of stellingen het meest doelmatige middel vormen ter toetsing van deze eindtermen.

II

De vergelijking voor refractie-diffractie met stroming, afgeleid in dit proefschrift, kan toegepast worden bij berekening van brandings-stromen en muistromen.

III

De methode van de gewogen residuen biedt een goed aanknopings-punt voor het berekenen van een overgangslaag met eindige dikte tussen zoet en zout grondwater, als compromis tussen het rekenen met een scherp grensvlak en het rekenen met een volledige dichtheidsverdeling over de vertikaal.

IV

Bij de numerieke berekening van een aantal beginwaardeproblemen kan de predictor-corrector-methode een gunstig alternatief vormen voor de methode van Lax of Lax-Wendroff. Hierbij wordt bijvoorbeeld gedacht aan de vergelijking voor bodemverandering in rivieren.

V

Bij de berekening van hoogwatergolven in rivieren is een expliciet reken-schema mogelijk, dat niet onderhevig is aan een stabiliteitsvoorwaarde. Dit wordt verwezenlijkt door een benadering van de verhangterm, waar-door ook de richting van de karakteristieken verandert. Deze aanpak is ook dienstig bij netwerken waarin takken met supercritische stroming voorkomen.

VI

Ontwikkelaars van applicatie-software dienen niet slechts te streven naar gebruikersvriendelijkheid van hun produkten; zij zouden hun ontwerpen ergonomisch moeten bekijken. Deze aanpak is van belang voor het gemak van de gebruiker, maar ook voor de voorkoming van gebruikersfouten, en voor een tijdige opsporing daarvan.

VII

In sommige industrieën is men afgestapt van het lopende-band systeem, en heeft men dit vervangen door teams van mensen die samen een compleet produkt maken. Het verdient aanbeveling te onderzoeken of voor het onderwijssysteem aan de Technische Hogeschool een analoge wijziging voordelen zou bieden.

VIII

In de basisstudie van de studierichting der Civiele Techniek dient een cursus betreffende de ontwikkeling en het gebruik van mathematische modellen opgenomen te worden.

IX

Bij diverse terreinen van overheidsbeleid, met name dat betreffende de volkshuisvesting, kan de beleidsvoorbereiding worden verbeterd door toepassing van System Dynamics.

X

Het landschap in de Krimpener- en Alblasserwaard is van zo grote waarde dat het beschermd moet worden, o.a. door de bestaande verkeerstoegangen bij Krimpen en Alblasserdam niet te verruimen.

<u>ERRATA</u>

De tekst op het midden van de titelpagina dient als volgt te luiden:

PROEFSCHRIFT

TER VERKRIJGING VAN DE GRAAD VAN DOCTOR IN DE TECHNISCHE WETENSCHAPPEN AAN DE TECHNISCHE HOGESCHOOL DELFT, OP GEZAG VAN DE RECTOR MAGNIFICUS PROF. IR. B.P.TH. VELTMAN, VOOR EEN COMMISSIE AANGEWEZEN DOOR HET COLLEGE VAN DEKANEN TE VERDEDIGEN OP DINSDAG 19 MEI 1981 TE 14.00 UUR.

In eq. (3.20) the symbol α is to be replaced by: a.
In eq. (4.8) the symbol κ is to be replaced by: k.
On page 44, 7th line from bottom, 'the coefficient :' is to be replaced by 'the coefficient κ'.
In eq. (5.1) the symbol $\underline{x}$ is to be replaced by: x.

CONTENTS

NOTATIONS

The summation convention is employed, i.e. if a subscript appears twice in the same term, summation over this subscript is understood.

Greek symbols α, β etc. used as subscript, indicate components of a vectorial quantity in the 3-dimensional space. Latin characters i, j, k etc. used as subscript, indicate components of a vectorial quantity in the propagation space (Chapter 2), or in the two horizontal dimensions (other chapters). x_1 and x_2 are the horizontal coordinates, $z=x_3$ is the vertical coordinate.

Differentiation in the horizontal direction is denoted by the operator ∇, or by adding a Latin subscript preceded by a comma: $\phi_{,j}$. Differentiation in the 3-dimensional space is denoted by the operator D , or by adding a Greek subscript preceded by a comma: $\phi_{,\alpha}$

L_t denotes the partial derivative of the quantity L with respect to t, all other variables kept constant, even if dependent on t. $\partial L/\partial t$ denotes the partial derivative taking into account such dependence on t. Therefore if L is a function of x, t and p: $L(p,x,t)$, then

$$\frac{\partial L}{\partial t} = L_t + L_p \frac{\partial p}{\partial t} .$$

$p_{,j}$ denotes the partial derivative of p with respect to x_j. The distinction between $L_{,j}$ and ∇L is analogous to the distinction between L_t and $\partial L/\partial t$ resp..

List of Symbols
----

a   product of phase and group velocity, $a = cc_g$

A   amplitude of the wave potential

c   phase velocity,

c_g group velocity,

D   3-dimensional differential operator

e   base of natural logarithm

f   function of z, giving the vertical structure of the waves

g   acceleration due to gravity

G   dispersion relation: $G(\omega, k)$

h'   vertical position of the bottom with respect to datum: $z = -h'(\underline{x})$.

h   local depth; $h = h' + \eta$

i   (unless used as subscript) imaginary unit

k   (unless used as subscript) wave number

l   component of the vectorial wave number

L   Lagrangian function

$\mathcal{L}$ Lagrangian function averaged over the phase

m   (unless used as subscript) component of the vectorial wave number

p   pressure

s   coordinate (roughly) in the direction of wave propagation

S   outer surface of the volume V

t   time

$\underline{u}$ unsteady part of the particle velocity

$\underline{U}$ steady part of the velocity, i.e. current velocity

$\underline{v}$ total particle velocity, $\underline{v} = \underline{U} + \underline{u}$

V   a control volume

W   function relating wave number and frequency

$\underline{x}$ coordinate vector

z   vertical coordinate

δ variation symbol

δ_{jk} Kronecker symbol, $=1$ if $j=k$, and $=0$ if $j \neq k$

ζ unsteady part of the position of the free surface

η vertical position of the free surface with respect to datum,

$\bar{\eta}$ mean vertical position of the free surface

θ phase function

κ wave number

σ frequency as observed when moving with the current

ϕ wave potential

ω frequency observed from a fixed point

CHAPTER 1. INTRODUCTION

Knowledge of wave conditions is of great importance to coastal engineering practice, mainly with regard to coastal defense works and the building and maintenance of harbors. In the problem of the determination of the wave conditions two aspects can be distinguished, viz. the generation of the waves by the wind in the largest deeper part of the sea, and the propagation of waves over shallows near the coast. Mathematical models which consider both aspects of the problem, do exist (e.g. CAVALERI and MALANOTTE RIZZOLI, 1977). Usually however, the two aspects are considered separately, in which case the necessary data concerning the waves coming in from the sea are obtained from either wave generation formulas, or from measurements. Such measurements are often performed with wave buoys located in a part of the sea that can be considered as deep for the most relevant wave frequencies.

The propagation of the waves over shallows is frequently calculated using the refraction or ray method. This method works well for those parts of the coast which are reasonably regular. In irregularly shaped regions, such as exist near the entrance of an estuary (see for instance figure 6.2), this method yields results which are hard to interpret. This is due to the sensitivity of the rays to every bottom irregularity. This sensitivity even causes appreciable differences between the results of different computer programs based on the ray method. A problem related with the existence of irregular shallows is that diffraction of the waves becomes important. This is clearly true for caustics that arise in such regions, but also for ray bundles which diverge. This shows the need for the development of a com-

bined refraction and diffraction model. A first step in this process was made by SVENDSEN (1967) who derived an equation for the propagation of gravity waves on water in one dimension. Later SCHONFELD (1972) and BERKHOFF (1972, 1976) derived a similar equation for two dimensions. Their equation is known as the mild-slope equation. RADDER (1979) developed a parabolic approximation to the mild-slope equation whereby he provided a method for carrying out practical calculations in the nearshore region.

The mild-slope equation included only the effect of bottom inhomogeneities. The effect of a current was neglected. In practice however, the regions that have the most irregular bottom topographies, are the entrances to estuaries, at the same time regions with strong currents due to tidal motion. A valuable contribution would be to add terms to the mild-slope equation representing the effect of a current. This thesis presents a derivation of such terms. The resulting model is applied to a number of problems concerning wave propagation across or along channels with prismatic bottom configuration, and with a current velocity constant in axial direction.

For the computation of wave fields in regions of arbitrary bathymetry and with an arbitrary current pattern, occurring in coastal engineering practice, a parabolic approximation to the above refraction-diffraction model is developed. A numerical model based on this approximation is shown to be applicable in practice.

CHAPTER 2. DISCUSSION OF EXISTING WAVE MODELS

2.1. Discussion of basic assumptions in relation with prac-
     tical applications.

The common refraction model is subject to a large number of
restrictions. In essence it is based on a potential flow
model in connection with small-amplitude sinusoidal waves
over a bottom with very small slope, and if a current is
taken into account, a current velocity field which varies
slowly both in space and time. In addition to this the
influence of differences in wave amplitude on the propaga-
tion (the diffraction effect) has been neglected. Due to the
assumed linearity one can and does consider one elementary
wave at a time.

In reality one is confronted with an irregular wave field
which can be considered as a superposition of many elemen-
tary sinusoidal wave components, each with different fre-
quency and direction. These components interact due to non-
linearities in the wave equations. The interaction becomes
pronounced with strongly nonlinear effects such as breaking.
Moreover the energy dissipation caused by breaking and by
bottom friction is inconsistent with the assumption of
potential flow. The assumption of a small bottom slope is
better justified than the others, at least for a sea with a
sandy bottom.

Several steps have been taken to overcome the rather severe
restrictions of the refraction model. Energy dissipation
due to bottom friction was introduced (SKOVGAARD, JONSSON
and BERTELSEN, 1975) as well as another nonlinear effect,
viz. the influence of the wave amplitude on the propagation
velocity (WALKER, 1976). Although in this way some non-li-

nearity is introduced, the refraction method still ignores
any interaction between wave components. With these addi-
tions the model can be classified according to PEREGRINE and
THOMAS (1976) as a near-linear wave model.

The introduction of an effect like breaking of waves is
theoretically inconsistent with several assumptions:
linearity, sinusoidal shape, potential flow. Due to this
the shape of the waves is far from correctly described by
the refraction model, if breaking etc. is included. At best
the model is fit to describe overall wave conditions, such
as the amount of energy per unit surface, and the direction
of propagation of the waves. Other models would have to be
used to establish the local wave shape or other quantities
of interest, as for instance the orbital velocities.

The main difference between the refraction and the refrac-
tion-diffraction models as far as basic assumptions are con-
cerned, is that the latter type of models do take into
account the influence of differences in wave amplitude on
the propagation. A related difference is that the restric-
tion on the bottom slope is less strict with the refraction-
diffraction models.

The refraction-diffraction equation developed by BERKHOFF
(1972, 1976), also known as the mild-slope equation, is
strictly linear and non-dissipative. This hampers the use
in regions containing beaches, because a linear and non-dis-
sipative model will predict an infinite wave height at a
beach. In the parabolic approximation to the mild-slope
equation by RADDER (1979) this had to be remedied, since it
was designed for such regions. In this model breaking is
included, as well as the influence of the wave height on the
propagation velocity, also a nonlinear effect. Theoreti-
cally the same effects could be built into the mild-slope
equation as well, but for computational reasons a parabolic

model can cope better with nonlinear effects, due to the
fact that it is solved in a step-wise manner. It must be
added that the parabolic method is subject to a more severe
restriction on the other hand. It ignores reflections from
the field, which is allowed only for very small slopes.

The aim of the present study is to develop an equation which
is analogous to the existing mild-slope equation with some
terms added which model the influence of the current. It is
therefore an obvious choice to start with similar assump-
tions: linear wave theory, and use of a velocity potential.

The use of linear wave theory is neither more, nor less
justified for waves in flowing water than it is for waves
entering still water. An exception must be made for regions
where the waves meet a countercurrent which is so strong
that it prevents propagation any further into that region.
In such a case on the one hand diffraction effects come into
play, which is legitimate in a refraction-diffraction equa-
tion, on the other hand wave breaking may occur. Wave
breaking, being a nonlinear as well as a dissipative pheno-
menon, is not included in the model, at least not at the
outset. It must be remarked that the wave model to be
developed will only be valid for moderate current veloci-
ties, so that the problem mentioned above will be excluded.

The use of a velocity potential is far more questionable.
Theory shows that waves entering still water remain free of
rotation if they are not subject to shear stresses. Of
course waves which 'feel the bottom' have an appreciable
orbital velocity at the bottom and will therefore experience
shear. Still a velocity potential is often used, mainly
because the region in which the fluid is rotating is res-
tricted to a boundary layer near the bottom. A similar
argument can be used for waves in a flowing water body. A
current in restricted depth can also for a large part be

considered as having little rotation. Only in the lower region the velocity gradient and thus the rotation is large. This means that most of the wave motion takes place in that part of the fluid which has small rotation. The conclusion is that the use of a velocity potential is not as firmly based as for waves in water with zero mean velocity, but it seems a usable starting point.

For those cases in which the assumption of an irrotational current leads to unacceptable results, the approach by JONS-SON, BRINK-KJAER and THOMAS (1978) could provide a solution, at least for rotation in a vertical plane.

The rotation in the horizontal plane will be much smaller than that in the vertical plane, since the length scale of depth and current inhomogeneities is much larger than the depth itself. Moreover the equation for wave propagation derived in this thesis, although it is based on the use of a velocity potential, conforms well to the refraction equation with current, which is also valid for a current with rotation in the horizontal plane.

2.2. Use of the variational method for wave problems.

The variational method provides a framework of great gener-
ality for wave models, as for other physical phenomena. Not
only the partial differential equation governing the wave
motion can immediately be derived from the variational
statement, but also the important law of conservation of
wave action. Furthermore the method gives a deeper insight
in the connection between the refraction model and the
refraction-diffraction model. In the present study the
method is used in the first place to derive a vertically
integrated model from the three-dimensional equations. In
this section a brief account is given of aspects of the var-
iational method, which will be important in later chapters.

The variational principle generally states that the varia-
tion of a certain quantity, often an integral, vanishes if
the function that describes the evolution of the physical
process is subject to small variations. It is often written
as the integral of the so-called Lagrangian function:

$$\delta \int_{X'} \int_{T} L \, d\underline{x} \, dt = 0 \quad . \tag{2.1}$$

The region over which the integration extends is a part of
the propagation space $X'*T$, i.e. the Cartesian product of a
subspace of the physical space X, and time. The propagation
space is the space in which the waves propagate. If the
propagation space is of lower dimension than the physical
space, there also exists a so-called cross space X''. In the
case of gravity waves on water the propagation space con-
sists of time and both horizontal dimensions. The vertical
dimension acts as cross space. If a cross space is present
one is dealing with modal waves, in the terminology of HAYES
(1970), whereas the waves are called local if the propaga-
tion space fills the entire physical space.

The Lagrangian function L appearing in the integral (2.1) depends on the functions describing the state of the physical process, and on their spatial and temporal derivatives. If there is no cross space the wave equation can easily be derived as the Eulerian relation resulting from the variational principle (see e.g. MIKHLIN, 1964). Let the Lagrangian be dependent on the function ϕ and its first derivatives:

$$L = L \,(\phi, \ \phi_t, \ \phi_{,j}). \tag{2.2}$$

It is understood that Latin subscripts i or j refer to coordinates in the propagation space, whereas Greek subscripts α or β indicate coordinates in the whole physical space.

Then
$$L_\phi - \frac{\partial}{\partial t} L_{\phi_t} - \nabla_j \, L_{\phi_{,j}} = 0 \tag{2.3}$$

is the partial differential equation describing the wave motion. If L contains second powers of ϕ or its derivatives, the corresponding wave equation is linear. The procedure can however just as well be used for nonlinear waves. An important example is the variational principle for gravity waves proposed by LUKE (1967):

$$L = \int_{-h'}^{\eta} \{\phi_t - \tfrac{1}{2}(\phi_{,\alpha} \, \phi_{,\alpha}) - gz\} \ dz \ . \tag{2.4}$$

The Lagrangian function is integrated over the cross space, as usual. It is noted that the state variables are η , the vertical position of the free surface, and ϕ , the velocity potential.

The fact that one is dealing with waves comes out more pregnantly by realizing the existence of periodic or nearly periodic solutions. This is expressed by

$$\phi = P(\theta), \qquad (2.5)$$

θ being the phase function. The frequency ω and the wave number $\underline{k}$ are derivatives of the phase function:

$$\omega = -\theta_t, \qquad (2.6)$$

$$\underline{k} = \nabla \theta.$$

In periodic or nearly periodic waves these functions are constant or slowly varying.

The shape of the function P is derived from the variational principle.

Let $\qquad L(P, -\omega P', \underline{k} P') = L^*(P, P'),$

where P' denotes the derivative of P with respect to θ.

Then $\qquad L_P^* - \dfrac{\partial}{\partial \theta} L_{P'}^* = 0. \qquad (2.7)$

There exists a first integral of this differential equation:

$$L^* - P' L_{P'}^* = A' = \text{const.} \qquad (2.8)$$

Eq. (2.7) is the differential equation by which the function $P(\theta)$ can be established. In (2.8) a quantity A' appears that is independent of the phase, and that is related to the wave amplitude.

An important step in this theory was made by WHITHAM (1965, 1971), when he introduced the averaging of the Lagrangian over the phase:

$$\mathcal{L} = \frac{1}{2\pi} \int_0^{2\pi} L \, d\theta. \qquad (2.9)$$

Thereby he obtained a Lagrangian which depends on the frequency, the wave number and the amplitude A. So

$$\mathcal{L} = \mathcal{L} (\omega, \underline{k}, A) \qquad (2.10)$$

with an additional consistency relation:

$$\frac{\partial \underline{k}}{\partial t} + \nabla \omega = 0 . \qquad (2.11)$$

On the basis of the averaged Lagrangian (2.10) a set of equations is formed by which ω, $\underline{k}$ and A can be determined. The Eulerian equation that results by considering the variation of A is:

$$\mathcal{L}_A = 0 .$$

This equation has the character of a dispersion relation, a fact that can be seen more clearly with linear waves. For linear waves L is quadratic in ϕ, and therefore $\mathcal{L}$ is quadratic in A. It can thus be written:

$$\mathcal{L} = \tfrac{1}{2} G(\omega, \underline{k}) A^2 . \qquad (2.12)$$

So $$\mathcal{L}_A = A G(\omega, \underline{k}) = 0$$

or simply $$G (\omega, \underline{k}) = 0 , \qquad (2.13)$$

since evidently the amplitude should not vanish everywhere. For linear waves the dispersion relation turns out to be independent of the wave amplitude, a natural property of this class of waves.

If the non-averaged or primitive Lagrangian is related to a refraction-diffraction equation, the averaged Lagrangian is related to the refraction model for the same type of waves.

In the refraction method the dispersion relation is used first to determine the wave rays, and then, if needed, the amplitude is determined using a conservation equation. This relation results from considering the variation with respect to θ :

$$\frac{\partial}{\partial t} \mathcal{L}_\omega - \nabla_i \mathcal{L}_{k_i} = 0 \ . \tag{2.14}$$

This equation is in the form of a conservation equation. It represents the law of conservation of wave action, a generalisation of the adiabatic invariant. ANDREWS and McINTYRE (1978b) showed its validity in a completely different way for waves in a moving medium. The quantity $\mathcal{L}_\omega$ is interpreted as the wave action density, and $\mathcal{L}_{k_i}$ as the transport of wave action. The equation of conservation of wave action can be used to determine A. This too can be seen more clearly for the linear subcase:

$$\frac{\partial}{\partial t} (G_\omega A^2) - \nabla_i (G_{k_i} A^2) = 0 \ . \tag{2.15}$$

The group velocity, being the velocity with which the wave energy is transported, emerges from the conservation equation:

$$c_{g_i} = - \frac{G_{k_i}}{G_\omega} \ . \tag{2.16}$$

The group velocity can also be introduced by means of the dispersion relation. This relation is a partial differential equation of the first order in θ :

$$G (-\theta_t, \theta_{,i}) = 0 \ . \tag{2.17}$$

Equations of this type have characteristic curves, along which the following relations hold:

$$\frac{dt}{d\gamma} = G_{\theta_t} = -G_\omega$$

$$\frac{dx_i}{d\gamma} = G_{\theta,i} = G_{k_i} \quad .$$

One of the merits of the variational method is that it clarifies why the propagation velocity associated with these characteristics, equals the group velocity.

From the line of reasoning pursued so far it would seem that the conservation of wave action can only be arrived at via the averaged Lagrangian. HAYES (1970) however showed that the conservation principle can also be obtained from the primitive Lagrangian directly. A family of periodic solutions is introduced:

$$\phi = P (\theta, \underline{x}, t) \quad . \tag{2.18}$$

Periodicity is expressed by

$$P (\theta + 2\pi, \underline{x}, t) = P (\theta, \underline{x}, t) \quad .$$

Hayes defines the wave action density and wave action transport as resp.

$$A_w = \overline{L_{\phi_t} P_\theta} = \frac{1}{2\pi} \oint L_{\phi_t} \, dP \, , \tag{2.19}$$

$$\underline{B_w} = \overline{L_{\phi,i} P_\theta} = \frac{1}{2\pi} \oint L_{\phi,i} \, dP \, . \tag{2.20}$$

The local conservation law is then readily obtained:

$$\frac{\partial A_w}{\partial t} + \nabla \cdot \underline{B_w} = 0 \quad . \tag{2.21}$$

Similarly in this thesis a conservation principle will not only be derived for refraction-like models, but also for refraction-diffraction models, for instance in the next sec-

tion. The method uses a multiplication with the complex conjugate of the wave potential. Superficially it appears to be different, but it is in fact a special case of Hayes' method.

The present study is concerned with the following elements of the variational theory. An averaged Lagrangian for waves on currents does exist, and the aim is to develop a primitive Lagrangian for this phenomenon. It is to be in a form corresponding to a local wave equation with the horizontal coordinates and time spanning the propagation space. To this end a modal wave equation is developed first, with the vertical dimension acting as cross space. This is subsequently reduced to the desired equation (chapter 3). By averaging the Lagrangian thus obtained it is shown to be in accordance with the refraction model (chapter 4).

2.3. Existing refraction-diffraction equations

The model of greatest generality for gravity waves in an irrotational fluid is provided by the variational model of LUKE (1967). The Lagrangian appearing in this model is:

$$L = \int_{-h'}^{\eta} \{\phi_t - \tfrac{1}{2} (\phi_{,\alpha} \phi_{,\alpha}) - gz\} \, dz .$$

This model describes nonlinear waves which need not be periodic and the bottom is allowed to have arbitrarily steep slopes. In this very general form it can hardly be used for practical computations since it comprises three space dimensions and time. It is used often as a starting-point for more specialized models, that do lend themselves to the solution of practical problems.

One model that can be considered as a special case of the above model, is the mild-slope equation (BERKHOFF, 1972, 1976). It is only a two-dimensional model. The time coordinate has disappeared because the wave motion is assumed sinusoidal in time and the vertical coordinate has disappeared because the model is vertically integrated. The equation reads

$$\nabla . (c \, c_g \nabla \tilde{\Phi}) + \kappa^2 c \, c_g \tilde{\Phi} = 0 . \tag{2.22}$$

As its name indicates it is valid for small bottom slopes. Furthermore the waves are linear. The function $\tilde{\Phi}$ is the complex potential at the mean free surface (z=0 in this case). The three-dimensional potential is related to $\tilde{\Phi}$ in the following way:

$$\phi (\underline{x}, z, t) = \frac{\cosh \kappa (z + h)}{\cosh \kappa h} \, \mathrm{Re} \, \{e^{-i\omega t} \tilde{\Phi} (\underline{x})\} .$$

The coefficients κ, c and c_g are calculated from the given

frequency ω and depth h by:

$$\omega^2 = g\kappa \tanh(\kappa h)$$

$$c = \omega / \kappa$$

$$c_g = g \ \frac{\frac{1}{4}\sinh(2\kappa h) + \frac{1}{2}\kappa h}{\omega\{\cosh(\kappa h)\}^2} \ .$$

In a region with homogeneous depth κ can be interpreted as the wave number associated with a homogeneous wave field, c as the phase velocity, and c_g as the group velocity associated with the same wave field.

BERKHOFF (1972, 1976) does not explicitly use variational methods in his derivation of (2.22) but closer examination reveals that he in fact used the Galerkin method. He explicitly takes care that the wave energy is conserved.

A refraction-diffraction model developed almost simultaneously with the mild-slope equation is proposed by ITO and TANIMOTO (1972). Unlike the mild-slope equation it is in the form of an initial value problem:

$$\frac{\partial u_j}{\partial t} = -g \ \nabla_j \ \zeta \ ,$$

$$\frac{\partial \zeta}{\partial t} = - \frac{1}{\kappa} \tanh(\kappa h) \ \nabla_j \ u_j \ . \tag{2.23}$$

The notations have been modified to conform with this thesis. After elimination of $\underline{u}$ there results

$$\frac{\partial^2 \zeta}{\partial t^2} - g \ \frac{\tanh(\kappa h)}{\kappa} \nabla^2 \zeta = 0 \ .$$

For a purely harmonic wave this is easily transformed into an equation for the potential $\tilde{\phi}$:

$$\kappa^2 \ \tilde{\phi} + \nabla^2 \ \tilde{\phi} = 0 \ , \tag{2.24}$$

which deviates from the mild-slope equation. The disagreement is mainly due to a different treatment of the boundary condition at the bottom. According to Ito and Tanimoto this condition is

$$\frac{\partial \phi}{\partial z} = 0 \ ,$$

whereas the slope of the bottom, although it is small, is taken into account more accurately in the mild-slope equation. As a consequence the law of conservation of wave energy is obeyed accurately by the mild-slope equation. This is verified by multiplying the equation with the complex conjugate of $\tilde{\phi}$ (denoted by $\tilde{\phi}^{\mathbf{x}}$) and then taking the imaginary part of the product:

$$\text{Im} \ \{\tilde{\phi}^{\mathbf{x}} \ (\nabla \ . \ c \ c_g \ \nabla . \tilde{\phi} + c \ c_g \ \kappa^2 \ \tilde{\phi})\} =$$

$$= \text{Im} \ \{\nabla \ . \ (\tilde{\phi}^{\mathbf{x}} \ c \ c_g \ \nabla \ \tilde{\phi}) - c \ c_g \ \nabla \ \tilde{\phi}^{\mathbf{x}} \ . \ \nabla \ \tilde{\phi}\} =$$

$$= \nabla \ . \ \{\text{Im} \ (c \ c_g \ \tilde{\phi}^{\mathbf{x}} \ \nabla \ \tilde{\phi})\} = 0 \ .$$

It is noted that $\tilde{\phi}\tilde{\phi}^{\mathbf{x}}$ and $\nabla\tilde{\phi}.\nabla\tilde{\phi}^{\mathbf{x}}$ are real and therefore disappear. If one substitutes $\tilde{\phi}=\hat{\phi}\exp(i\theta)$, this relation transforms into an expression which is more easily recognizable as the divergence of the transport of wave action:

$$\nabla \ . \ (c \ c_g \ \hat{\phi}^2 \ \nabla \ \theta) = \nabla \ . \ (k \ c \ c_g \ \frac{\nabla\theta}{k} \ \hat{\phi}^2) = \nabla \ . \ (\omega \ \underline{c}_g \ \hat{\phi}^2) = 0 \ .$$

where the vector $\underline{c}_g$ is defined by $c_g \nabla\theta/\kappa$.

The same procedure applied to eq. (4.3) leads to

$$\nabla \ . \ (\hat{\phi}^2 \ \nabla \ \theta) = \nabla \ . \ (\underline{k} \ \hat{\phi}^2) = 0 \ .$$

which is not in agreement with the conservation of wave action.

Although it must be concluded that eq. (2.23) is not

entirely correct, the method of finding the periodic motion
as a limit of an unsteady process is valuable when con-
structing a numerical solution. The solution can be found
in an iterative manner, avoiding the solution of a large
system of linear equations. It is admitted that there are
other iterative solution methods, but the method discussed
above is relatively efficient. Therefore the equation which
will be derived in the next chapter will also be in time-de-
pendent form instead of a harmonic form.

CHAPTER 3. A MATHEMATICAL MODEL FOR WAVE PROPAGATION

3.1. Differential equations and boundary conditions.

In this section the equations for wave propagation in the
presence of a current appear. The usual assumptions for
linear wave theory have been applied:
- the wave motion is irrotational,
- the waves are linear, so all terms in which the wave
  amplitude or a related quantity appears in higher than the
  first order, will be disregarded, if first order terms are
  present.
In addition to this it is assumed that the spatial variation
of the current velocity and the mean free surface are very
small. Although this study is concerned with the influence
of a current on the waves, the opposite effect of the waves
on the current is neglected, or assumed known. Then, if the
effect of the waves on the current is important, the current
description can be improved by means of time-averaged equa-
tions, and a next iteration towards the wave state can be
carried out. Thus in an iterative procedure both the waves
and the current can be determined.

In the following derivation it is assumed that the waves are
almost periodic with a frequency in the neighbourhood of ω_0.
The equations are kept in transient form instead of harmonic
form. Later on this will result in a wave model in the form
of an initial value problem, which enables one to use time-
dependent computational methods in the solution of the wave
equation.

The total particle velocity $\underline{v}$ consists of a steady part $\underline{U}$

and an unsteady periodic part $\underline{u}$ with zero mean. It is assumed that the motion due to waves is irrotational, so there exists a velocity potential ϕ for which

$$u_\alpha = D_\alpha \phi \qquad\qquad \alpha = 1, 2, 3 . \qquad\qquad (3.1)$$

D is the three-dimensional differential operator. The water is assumed to be incompressible as usual. Therefore we have in the interior of the fluid:

$$D_\alpha u_\alpha = D^2 \phi = 0 . \qquad\qquad (3.2)$$

For the same reason the current velocity field is divergence-free:
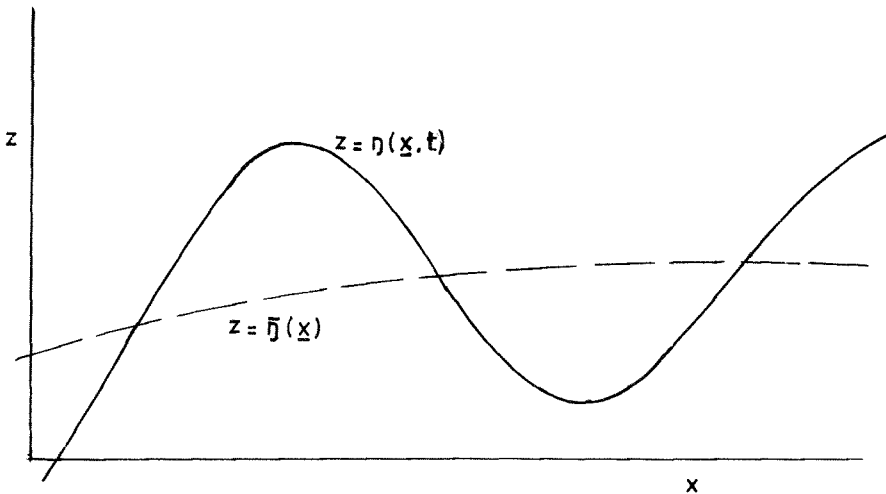
$$\underline{D}.\underline{U} = 0.$$

Figure 3.1. Definition sketch of the free surface

In addition to this the boundary conditions are needed. Now a distinction is needed between the two horizontal coordi-

nates x_1 and x_2 , and the vertical coordinate z. The coordinate x_3 which is occasionally used, is identical with z. The bottom, which is defined by:

$$z = - h'(\underline{x}) \qquad (3.3)$$

is assumed to be rigid and impermeable so that the derivative of ϕ in the direction normal to the bottom vanishes:

$$n_\alpha u_\alpha = n_\alpha D_\alpha \phi = 0 \qquad \text{on} \quad z = -h'(\underline{x}) . \qquad (3.4)$$

On the upper (free) surface two conditions hold, viz. the kinematic and the dynamic boundary conditions. A definition sketch of the free surface is rendered in figure 3.1. The surface is defined by:

$$z = \eta(\underline{x}, t) = \bar{\eta}(\underline{x}) + \zeta(\underline{x}, t) .$$

The last term of the right hand side, representing the variable part of the position of the surface, is an unknown function as yet. The term $\bar{\eta}(\underline{x})$ is the mean vertical position of the free surface. It is assumed to be a known function, in other words the set-down due to waves is neglected.

The kinematic boundary condition states that the velocity component normal to the free surface is equal to the speed with which this surface travels in the same direction. So

$$n_\alpha v_\alpha = n_3 \frac{\partial \eta}{\partial t} \qquad \text{on} \quad z = \eta(\underline{x}, t) .$$

The unit normal vector $\underline{n}$ is related to the gradient of the surface:

$$n_j = -n_3 \nabla_j \eta \qquad j = 1, 2 .$$

So

$$\frac{\partial \eta}{\partial t} + v_j \nabla_j \eta - v_3 = 0 \qquad \text{on} \quad z = \eta(\underline{x}, t) .$$

In this equation both variables $\underline{v}$ and η are separated into

their steady and fluctuating parts. After the steady terms
have been dropped, there remains

$$\frac{\partial \zeta}{\partial t} + U_j \nabla_j \zeta + u_j \nabla_j \bar{\eta} + u_j \nabla_j \zeta - \frac{\partial \phi}{\partial z} = 0 \qquad \text{on} \quad z = \eta \ (\underline{x}, t) \ .$$

In this equation the term

$$u_j \nabla_j \zeta$$

is deleted, being a term of second order. Also because of
the linearity of the waves, the boundary conditions are
taken on the mean free surface instead of the free surface
itself. The term

$$u_j \nabla_j \bar{\eta}$$

can be neglected. In deep water or water of intermediate
depth the horizontal component of $\underline{u}$ is of the same order of
magnitude as the vertical component. Because the slope of
the mean free surface is very small, for this range of
depths the following relation holds

$$\frac{|u_j \nabla_j \bar{\eta}|}{|u_3|} \simeq |\nabla \bar{\eta}| << 1 \ .$$

Another argument, also valid for smaller depths, is that the
same term is small compared with

$$U_j \nabla_j \zeta$$

The reason is that the gradient operator appearing in this
term is applied to a quantity that varies over a wavelength,
whereas in the neglected term the gradient of the mean free
surface appears. The neglected term is much smaller since
the wavelength is assumed to be small compared with the
characteristic length of the variation of the mean quanti-
ties.

Altogether the kinematic boundary condition becomes:

$$\frac{\partial \zeta}{\partial t} + U_j \, \nabla_j \, \zeta - \frac{\partial \phi}{\partial z} = 0 \qquad \text{on} \quad z = \bar{\eta}(\underline{x}) \tag{3.5}$$

The second condition for the free surface derives from the equation of motion. This equation reads:

$$\rho \left\{ \frac{\partial v_\alpha}{\partial t} + v_\beta \, D_\beta \, v_\alpha \right\} + D_\alpha \, (p + \rho g z) = 0 \qquad \left. \begin{array}{c} \alpha \\ \beta \end{array} \right\} = 1, \, 2, \, 3 \, .$$

So:

$$\rho \left\{ \frac{\partial}{\partial t} \, D_\alpha \, \phi + (U_\beta + D_\beta \, \phi) \, D_\beta \, (U_\alpha + D_\alpha \, \phi) \right\} + D_\alpha \, (p + \rho g z) = 0 \, . \tag{3.6}$$

It is remarked that to first order the steady part of the sum $p + \rho g z$ is equal to $\rho g \bar{\eta}$.

Deleting the steady part of eq. (3.6) as well as the higher order terms one is left with:

$$\rho \left\{ \frac{\partial}{\partial t} \, D_\alpha \, \phi + U_\beta \, D_\beta \, D_\alpha \, \phi + (D_\beta \, \phi) \, (D_\beta \, U_\alpha) \right\} + D_\alpha \, \{ p + \rho g \, (z - \bar{\eta}) \} = 0 \, .$$

If one substitutes $D_\alpha U_\beta$ for $D_\beta U_\alpha$ this leads to

$$D_\alpha \left\{ \rho \, \frac{\partial \phi}{\partial t} + \rho \, D_\beta \, (U_\beta \, \phi) + p + \rho g \, (z - \bar{\eta}) \right\} = 0 \, . \tag{3.7}$$

The above substitution is correct if $\underline{U}$ is a potential flow field. This will in general not be true. However, the mean flow varies slowly in space, so the substitution amounts to substituting one small term by another.

Eq. (3.7) holds everywhere in the fluid, and also on the free surface. The vertical component of $\underline{U}$ on the free surface is very small. Furthermore the boundary condition is taken at the mean free surface, as usual in linear wave theory.

Therefore

$$\frac{\partial \phi}{\partial t} + \nabla_k \ (U_k \ \phi) + g \zeta = 0 \quad \text{on} \quad z = \bar{\eta}(\underline{x}) \ . \qquad (3.8)$$

Comparing the free surface conditions (3.5) and (3.8) with the ones holding for the case of zero mean flow, it appears that the time derivative is replaced by a material derivative for a quantity moving with the current velocity. Both boundary conditions can be combined into one:

$$(\frac{\partial}{\partial t} + U_j \ \nabla_j) \ (\frac{\partial \phi}{\partial t} + \nabla_k \ (U_k \ \phi)) + g \frac{\partial \phi}{\partial z} = 0 \quad \text{on} \quad z = \bar{\eta}(\underline{x}) \qquad (3.9)$$

3.2. A variational principle for the wave model

In this section it will appear that a variational principle can be derived from the differential equation (3.2) together with the boundary conditions at the bottom (3.4) and at the mean free surface (3.9).

In the wave propagation problem considered in this chapter, the domain is a volume V bounded by the bottom $z=-h'(\underline{x})$ and the mean free surface $z=\overline{\eta}(\underline{x})$. A region M in the $\underline{x}$-plane is assumed. Then the volume V is the set of points $(\underline{x},z)$ such that $\underline{x}$ is in M, and $-h'(\underline{x})<z<\overline{\eta}(\underline{x})$.
Since everywhere in the fluid Laplace's equation holds, the following must be true for every arbitrary function $\delta\phi$:

$$\iiint\limits_{V} \delta\phi \ D^2\phi \ dV = 0 \ .$$

Applying Gauss' divergence theorem one obtains

$$\iint\limits_{S} \delta\phi \ \underline{n} \ . \ \nabla\phi \ dS - \iiint\limits_{V} (D\delta\phi) \ . \ (D\phi) \ dV = 0 \ . \qquad (3.10)$$

Here S is the outer surface of V, and $\underline{n}$ is the outward normal to S. The boundary conditions are introduced into the integral over S. The integral over the bottom vanishes, since the normal derivative of ϕ vanishes on the bottom. Over that portion of S whose projection on the $\underline{x}$-plane is the outer edge of M, the boundary value of ϕ is known. For this reason the variation $\delta\phi =0$, so that this part of the integral vanishes too.
In the integral over the upper surface (S_u) boundary condition (3.9) is used. As before the slope of this surface is very small so that the normal derivative can be replaced by the derivative with respect to z. Altogether (3.10) becomes

$$- \frac{1}{g} \iint\limits_{S_u} \delta\phi \ (\frac{\partial}{\partial t} + U_j \ \nabla_j) \ (\frac{\partial\phi}{\partial t} + \nabla_k \ (U_k\phi)) \ dS - \iiint\limits_{V} (D\delta\phi) \ . \ (D\phi) \ dV = 0 \ .$$

Gauss' divergence theorem is applied again, this time to the
integral over S_u. This results in an integral over the edge
of S_u, which vanishes due to the boundary value of ϕ, and
another integral over S_u. The following variational princi-
ple follows:

$$\delta \left[\frac{1}{2g} \iint\limits_{S_u} (\frac{\partial \phi}{\partial t} + \nabla_k (U_k \phi))^2 \, dS - \frac{1}{2} \iiint\limits_V (D \phi)^2 \, dV \right] = 0 .$$

The integral over S_u is replaced by an integral over M, its
projection on the (x_1, x_2)-plane. Since the slope of S_u is
small, dS is replaced by $dx_1 * dx_2$. The variational principle
becomes

$$\delta \iint\limits_M L \, dx_1 \, dx_2 = 0 ,$$

in which

$$L = \frac{1}{2g} (\frac{\partial \phi}{\partial t} + \nabla \cdot (\underline{U} \phi))^2 \Big|_{z = \bar{\eta}} - \frac{1}{2} \int_{-h'}^{\bar{\eta}} (D \phi)^2 \, dz . \qquad (3.11.)$$

Variational principles have been used already long ago to
find approximate solutions by applying the variational
method in a restricted class of solutions. This method is
known as the Ritz method; it forms the basis for the finite
element method. The idea of the Ritz method will be
explored in the next section.

3.3. Approximation leading to a vertically integrated equation.

A well-known property of time-harmonic linear waves propagating in a region with a horizontal bottom and a homogeneous current field is that a separation of variables of the form

$$\phi \,(\underline{x},\, z,\, t) = \text{Re} \,\{e^{-i\omega_o t} \, f\,(z) \, \tilde{\Phi}\,(\underline{x})\} \qquad (3.12)$$

is possible. f(z) is a hyperbolic function of z:

$$f\,(z) = \frac{\cosh\{\kappa\,(h' + z)\}}{\cosh\{\kappa\,(h' + \bar{\eta})\}}\,. \qquad (3.13)$$

Furthermore it turns out that the wave number κ obeys the following relationship:

$$\sigma_o^2 = g\,\kappa\,\tanh(\kappa\,h) \qquad , \qquad (3.14)$$

where
$$\sigma_o = \omega_o - \underline{\kappa} \cdot \underline{U} \qquad (3.15)$$

and
$$h = h' + \bar{\eta} \qquad . \qquad (3.16)$$

It is noted here that κ appears as a vectorial quantity whose direction is related to the direction of propagation of the waves. One can use eq. (3.14) and (3.15) if this direction is known in advance. What is to be done if this is not so, is dicussed later in this section.

The above relations have been derived under very severe restrictions. In the refraction theory most of these restrictions can be alleviated: the bottom may be nearly horizontal, the current velocity field is allowed to vary slowly, and the waves are assumed to be nearly periodic, i.e. the

frequency changes slowly. In the following analysis similar
restrictions will apply, with the additional restriction
that the frequency is allowed to vary only within a narrow
band around ω_0. A variable frequency is useful if one tries
to determine a periodic motion as the limit of an instation-
ary process ,as was done by ITO and TANIMOTO (1972) and by
ABBOTT et al. (1978). The reduction to the equation for the
purely periodic motion is easily carried out.

Using eq. (3.14) and (3.15) κ can from now on be considered
as a known quantity. It is based on the known constant ω_0,
so variations of the frequency do not affect this coeffi-
cient, or other coefficients based on κ. κ is usually vari-
able in space due to its dependence on the depth h and the
current velocity $\underline{U}$. The function f is therefore no longer
independent of $\underline{x}$. However, since the bottom is mildly slop-
ing, the derivatives with respect to $\underline{x}$ will be small.

In order to encompass the case in which the frequency is not
entirely constant, a function Φ will be used in which the
total dependence on t is incorporated. In other words

$$\phi\ (\underline{x},\ z,\ t) = f\ (z,\ h)\ \Phi\ (\underline{x},\ t) \tag{3.17}$$

It is noted that due to the choice of f, $\Phi = \phi$ on the surface
S_u. Deleting the derivatives of f with respect to $\underline{x}$, the
Lagrangian (3.11) can be rewritten as

$$L = \frac{1}{2g}\ \{\frac{\partial\Phi}{\partial t} + \nabla\ .\ (\underline{U}\ \Phi)\}^2 - \frac{1}{2}\int_{-h'}^{\bar{\eta}}\ \{\Phi^2\ (\frac{\partial f}{\partial z})^2 + f^2\ (\nabla\Phi)^2\}\ dz =$$

$$= \frac{1}{2g}\ \{\frac{\partial\Phi}{\partial t} + \nabla\ .\ (\underline{U}\ \Phi)\}^2 - \frac{1}{2}\ \Phi^2\int_{-h'}^{\bar{\eta}}(\frac{\partial f}{\partial z})^2\ dz - \frac{1}{2}\ (\nabla\Phi)^2\int_{-h'}^{\bar{\eta}}\ f^2\ dz\ .$$

The integrals over z appearing in this expression can be
expressed in the parameter κ after some simple calculation.

$$g \int_{-h'}^{\bar{\eta}} f^2 \, dz = g \; \frac{\frac{1}{4} \sinh(2\kappa h) \; + \frac{1}{2} \kappa h}{\kappa \{\cosh(\kappa h)\}^2} \equiv c \; c_g \equiv a \; , \qquad (3.18)$$

$$g \int_{-h'}^{\bar{\eta}} (\frac{\partial f}{\partial z})^2 \, dz = g\kappa \; \frac{\frac{1}{4} \sinh(2\kappa h) - \frac{1}{2} \kappa h}{\{\cosh(\kappa h)\}^2} = \sigma_o^2 - \kappa^2 a \; . \qquad (3.19)$$

Here a is the product of the phase velocity and the group velocity of the waves.

With the above the Lagrangian appears as:

$$L = \frac{1}{2} \{ (\frac{\partial \Phi}{\partial t} + \nabla.(\underline{U} \; \Phi))^2 - \alpha \; (\nabla \; \Phi)^2 - (\sigma_o^2 - \kappa^2 \; a) \; \Phi^2 \} \; . \qquad (3.20)$$

The differential equation describing the wave motion follows immediately from the Lagrangian function by means of the Euler-Lagrange relation

$$L_\Phi - \frac{\partial}{\partial t} L_{\Phi_t} - \nabla_i L_{\Phi,i} = 0 \qquad .$$

which gives

$$(\frac{\partial}{\partial t} + \underline{U}.\nabla) (\frac{\partial \Phi}{\partial t} + \nabla.(\underline{U} \; \Phi)) + \nabla.(a\nabla\Phi) + (\sigma_o^2 - \kappa^2 \; a) \; \Phi = 0 \; . \quad (3.21)$$

This equation is the main result of the study. It is a par-tial differential equation of the hyperbolic type.   The equation can be classified as a linear Klein-Gordon equation for a moving medium.   In this form the equation could be used for a wave with a frequency different from ω_0 , and con-sequently a wave number different from κ .
A version of the equation for purely periodic waves with frequency ω_0 , for which

$$\Phi \; (\underline{x}, \; t) = \text{Re} \; \{e^{-i\omega_o t} \; \tilde{\Phi} \; (\underline{x})\} \; , \qquad (3.22)$$

reads $\quad - i\omega_o \ (\underline{U}.\nabla\tilde{\Phi} + \nabla.(\underline{U}\,\tilde{\Phi})) + (\underline{U}.\nabla)\,\nabla.(\underline{U}\,\tilde{\Phi})$

$$- \nabla.(a\,\nabla\tilde{\Phi}) + (\omega_o^2 + \omega_o^2 - \kappa^2 a)\,\tilde{\Phi} = 0 \quad . \qquad (3.23)$$

(3.23) is a partial differential equation of elliptic type. In a region of constant depth and current velocity, (3.21) and (3.23) allow a solution in the form of a plane wave. A plane wave is described by:

$$\Phi = \hat{\Phi} \exp\,(-i\omega t + i\,\underline{k}.\underline{x}) \qquad (3.24)$$

Eq. (3.21) yields the following relation for such a wave:

$$(\omega - \underline{k}\,.\,\underline{U})^2 - a\,k^2 - (\sigma_o^2 - a\,\kappa^2) = 0 \qquad (3.25)$$

This relation can be considered as the dispersion relation for waves determined by eq. (3.21). It is noted that if $\omega = \omega_0$, and if κ obeys (3.14) and (3.15), the wave number of the plane wave system $\underline{k}$ is equal to $\underline{\kappa}$.

In situations for which eq. (3.21) is intended, crossing waves and reflection of waves can occur, so that in one point waves from more than one direction may exist simultaneously. In such cases eq. (3.14) and (3.15) cannot be used. Since the value of κ depends on the direction of the waves, it might be concluded that eq. (3.21) cannot be used at all in such situations. This conclusion is too pessimistic: if an approximate value for κ is used to estimate the coefficients in eq.(3.21), this equation can still provide a very good approximation of the wave field. To see this, it is essential to distinguish between κ , a coefficient in (3.21); and $\underline{k}$, the wave number associated with the wave field that is found by solving the partial differential equation (3.21). If the first one is not exact, the second one will in general differ from the first. Now the most

interesting point is not how large the error in the coeffi-
cients of (3.21) is, but how much its solution is in error.
Therefore the error in $\underline{k}$ is to be studied.

Often the main direction of wave propagation is known, so
that (3.15) still can be used to some extent. Equations
(5.7) and (6.11) give examples of such use of (3.15). In
the worst case, if no information of this kind is available,
one could estimate the coefficients in (3.21) by using the
expression for κ that is valid for a zero mean velocity:

$$\omega_o^2 = g \kappa_o \tanh(\kappa_o h) \tag{3.26}$$

This approximation to κ is subject to a relative error of
the order of $|U|/c$, and consequently the coefficients used
in (3.21) have a similar error. It is noted that the value
of κ_0 is independent of the direction of wave propagation.
k however is not, since $\underline{U}$ appears in (3.25).

If in (3.21) and (3.25) the coefficients κ_0 and a_0 are used,
it follows that the relative error in the wave number k is
of the order of $(|U|/c)^2$. The value of $\underline{k}$ is found from
(3.25); in this case σ_0 is assumed equal to ω_0, so:

$$(\omega_o - \underline{k}.\underline{U})^2 = a_o + (\omega_o^2 - a_o \kappa_o^2) \quad .$$

The value of $\underline{k}$ is to be compared with the exact value κ,
under the assumption that a wave in one and the same direc-
tion is considered. κ obeys the relationship:

$$(\omega_o - \underline{\kappa}.\underline{U})^2 = g \kappa \tanh(\kappa h) \quad .$$

In order to find an estimate of k-κ the second equation is
subtracted from the first. The left hand side of the
resulting equation is:

$$(\omega_o - \underline{k}.\underline{U})^2 - (\omega_o - \underline{\kappa}.\underline{U})^2 = 2\omega_o \underline{U}.(\underline{\kappa}-\underline{k}) + 0(U/c)^2 \quad .$$

Since $\underline{k}$ and $\underline{\kappa}$ have the same direction

$$2\omega_o \; \underline{U} \cdot (\underline{\kappa} - \underline{k}) \;=\; 2\omega_o \underline{U} \cdot \underline{\kappa} \;\; (\kappa - k)/\kappa$$

Regarding the right hand side it is noted, that

$$\omega_o^2 \;=\; g \; \kappa_o \; \tanh(\kappa_o h) \quad .$$

Furthermore

$$a_o \;=\; \frac{d}{d(k^2)} \; g \; k \; \tanh(kh) \; \Big|_{k=\kappa_o}$$

A development into powers of $\kappa_0^2 - \kappa^2$ leads to:

$$g \; \kappa_o \; \tanh(\kappa_o h) \;-\; g \; \kappa \; \tanh(\kappa h) \;=$$

$$=\; a_o \; (\kappa_o^2 - \kappa^2) \;+\; 0(\kappa_o^2 - \kappa^2)^2$$

It is noted that $\kappa_0^2 - \kappa^2$ is of order U/c, so that the full equation reads:

$$2 \; \omega_o \; \underline{U} \cdot \underline{\kappa} \;\; (\underline{\kappa} - \underline{k})/\kappa \;+\; 0(U/c)^2 \;=$$

$$=\; a_o \; (k^2 - \kappa_o^2) \;+\; a_o \; (\kappa_o^2 - \kappa^2) \;+\; 0(U/c)^2 \;=$$

$$=\; a_o \; (k^2 - \kappa^2) \;+\; 0(U/c)^2 \quad .$$

The first term of the left hand side is smaller than the first term of the right hand side by a factor of U/c. Consequently the latter term is the main term of the equation. It must be of the order of $(U/c)^2$.

It is concluded that $\kappa - k$ is of the order of $(U/c)^2$. In other words, the wave model (3.21) with coefficients following from (3.26) predicts a solution which exhibits a wave number deviating $0(U/c)^2$ from the one resulting from the coefficients, in which the wave direction is correctly taken into account. So the solution of the differential equation is better than the error of κ_0 suggests. Table 3.1 gives some figures of k and the exact value for different depths and current velocities. The value of κ_0 is found in the column corresponding to zero velocity. The current direction is assumed to be collinear with the propagation direction, since this leads to the largest errors. All quanti-

ties in the table have been non-dimensionalized by means of ω_0 and g.

TABLE 3.1

depth	current velocity $(U\omega_0/g)$ ->								
	-0.15	-0.10	-0.05	0.00	0.05	0.10	0.15	0.20	0.25
0.20	3.85	3.11	2.65	2.31	2.06	1.86	1.70	1.56	1.45
	3.65	3.07	2.64	2.31	2.06	1.85	1.68	1.54	1.42
0.40	2.48	2.13	1.88	1.69	1.55	1.43	1.32	1.24	1.16
	2.37	2.10	1.88	1.69	1.54	1.42	1.31	1.21	1.13
0.60	2.03	1.76	1.58	1.44	1.32	1.23	1.15	1.08	1.02
	1.93	1.73	1.57	1.44	1.32	1.22	1.13	1.05	0.99
0.80	1.81	1.57	1.41	1.29	1.19	1.11	1.04	0.98	0.93
	1.71	1.55	1.41	1.29	1.19	1.10	1.02	0.96	0.90
1.00	1.68	1.46	1.31	1.20	1.11	1.04	0.97	0.92	0.87
	1.58	1.43	1.31	1.20	1.11	1.02	0.95	0.89	0.83

Table of computed wave numbers. Upper value is exact, from (3.14) and (3.15), lower is k from (3.25), using κ_0 from (3.26).

Inspection of the table shows that for small non-dimensional current velocities the wave number of the wave field computed with approximate coefficients is only a few percents in error. In fact, the current velocity non-dimensionalized by means of ω_0 and g is in practice usually below 0.1, so that the approximation is allowable. Moreover it should be borne in mind that the case represented, is the most pessimistic. Often a main direction of propagation can be identified so that a better approximation is possible. See chapters 5 and 6 for examples of such an approximation.

CHAPTER 4. DISCUSSION OF THE PROPOSED MODEL

4.1. Introduction.

The validity of the proposed model is hard to verify experi-
mentally. For the current-free mild-slope equation such an
investigation has been performed by BERKHOFF, RADDER and
BOOIJ (not yet published), but the setting-up of laboratory
experiments with a non-trivial bottom topography as well as
a controlled current pattern is difficult. Even more diffi-
cult is the measurement of waves in nature, including wave
directions and current velocities.

In this thesis it is chosen to do the verification by means
of a comparison with related mathematical models for wave
propagation. A number of them are available, such as the
variational principle of Luke, the refraction model for
waves in a region with current, a model for shallow water
waves and the refraction-diffraction model without current.

Since the study aims at adding terms to the mild-slope equa-
tion which model the influence of a current, this equation
is an obvious candidate for the comparison. If in eq.
(3.21) the terms containing $\underline{U}$ are deleted, and if a time
dependence of purely harmonic character is assumed, as in
(3.22), the mild-slope equation (2.22) is found indeed.

A comparison with Luke's variational principle for irrota-
tional waves is treated in the next section. A comparison
with the refraction model with current is dealt with in sec.
4.3.

LOZANO and MEYER(1976) showed that the mild-slope equation reduces to the shallow-water equation if it is assumed that κ h<<1. A similar procedure can be applied to eq. (3.21), which results in a linearized form of the shallow-water equation. Details are given in sec. 4.4..

4.2. Comparison with Luke's variational principle for water wave propagation.

LUKE (1967) developed a variational principle for nonlinear irrotational waves:

$$\delta \int_{t_1}^{t_2} \iiint_{V'} \{\phi_t' + \tfrac{1}{2} (D \phi')^2 + gz\} \, dz \, dx_1 \, dx_2 \, dt = 0 \ . \qquad (4.1)$$

The volume V' over which the integration is performed, is the volume which is occupied by the fluid at any moment, whereas the volume V appearing in the foregoing chapter is steady, since it lies between the bottom and the mean free surface. It is possible to reduce Luke's principle to a principle for linear waves such as (3.20). In order that the reduction can be performed, the total potential (ϕ') is split into a potential for the current and one for the waves (ϕ) :

$$D \phi' = \underline{U} + D \phi \ ,$$

$$\frac{\partial \phi'}{\partial t} = \frac{\partial \phi}{\partial t} \ .$$

The fact that $\underline{U}$ has a potential, implies that the current has to be irrotational. With the above substitution the Lagrangian for Luke's principle reads:

$$L = \int_{-h'}^{\eta} \{\phi_t + \tfrac{1}{2} (\underline{U} + D \phi)^2 + gz\} \, dz =$$

$$(4.2)$$

$$= \int_{-h'}^{\bar{\eta}} \{\phi_t + \tfrac{1}{2} (\underline{U} + D \phi)^2 + gz\} \, dz + \int_{\bar{\eta}}^{\eta} \{\phi_t + \tfrac{1}{2} (\underline{U} + D \phi)^2 + gz\} \, dz \ .$$

In this way the integral over the total unsteady volume is split into an integral over the steady volume between the

bottom and the mean free surface, and an integral between the mean free surface and the free surface itself. In the above expression the terms

$$\int_{-h'}^{\bar{\eta}} \phi_t \, dz \ , \qquad \int_{-h'}^{\bar{\eta}} gz \, dz \ , \qquad \int_{-h'}^{\bar{\eta}} \tfrac{1}{2} \, U^2 \, dz \ , \qquad \int_{-h'}^{\bar{\eta}} \underline{U} \cdot D \phi \, dz$$

do not contribute to the Euler equation and are therefore deleted. The term

$$\int_{\bar{\eta}}^{\bar{\eta}+\zeta} \tfrac{1}{2} \, U^2 \, dz$$

contributes only to the equation for the steady motion and is thus not of interest now. The term

$$\int_{\bar{\eta}}^{\bar{\eta}+\zeta} \tfrac{1}{2} \, (D \, \phi)^2 \, dz$$

is of third order in the wave amplitude and can be deleted since a model for linear waves is sought.

The remaining terms from the second integral of the right hand side in (4.2) are approximated by the assumption that the variation of the potential ϕ is small in the interval $(\bar{\eta}, \bar{\eta}+\zeta)$. This results in

$$\int_{\bar{\eta}}^{\bar{\eta}+\zeta} \phi_t \, dz = \zeta \, \phi_t + O \, (\hat{\phi}^3) \ ,$$

$$\int_{\bar{\eta}}^{\bar{\eta}+\zeta} \underline{U} \cdot D \phi \, dz = \int_{\bar{\eta}}^{\bar{\eta}+\zeta} D \cdot (\underline{U} \, \phi) \, dz$$

The vertical component of the mean velocity $\underline{U}$ is much smaller than the horizontal components, at least near the free surface. Thus the last term is nearly equal to

$$\zeta \, \nabla \cdot (\underline{U} \, \phi) \ .$$

Furthermore

$$\int_{\bar{\eta}}^{\bar{\eta}+\zeta} gz \, dz = \tfrac{1}{2} g \{(\bar{\eta} + \zeta)^2 - \bar{\eta}^2\} = \tfrac{1}{2} g \zeta^2 + g \bar{\eta} \zeta \, .$$

The term $g\bar{\eta}\zeta$ contributes only to the steady terms in the Euler equation. The reduced Lagrangian reads:

$$L = \int_{-h'}^{\bar{\eta}} (D \phi)^2 \, dz + \zeta \phi_t \;\; + \;\; \zeta \nabla.(\underline{U} \, \phi) + \tfrac{1}{2} g \, \zeta^2 \, .$$

After substitution of the vertical structure described by eq. (3.12) and (3.13) there results

$$L = \tfrac{1}{2} a (\nabla \Phi)^2 + \tfrac{1}{2}(\sigma_o^2 - \kappa^2 a)\Phi^2 + g \zeta \Phi t + g \, \zeta \nabla.(\underline{U} \phi) + \tfrac{1}{2} g^2 \zeta^2 \, . \qquad (4.3)$$

By varying the integral with respect to ζ one finds the Euler equation which represents the dynamic boundary condition at the free surface:

$$L_\zeta = \Phi_t \;\; + \;\; \nabla.(\underline{U} \, \phi) + g \, \zeta = 0 \, . \qquad (4.4)$$

Varying with respect to Φ results in:

$$L_\Phi - \frac{\partial}{\partial t} L_{\Phi_t} - \nabla_j L_{\Phi_{,j}} = \qquad\qquad\qquad (4.5)$$

$$= -g \, (\frac{\partial \zeta}{\partial t} + U.\nabla\zeta) - \nabla.(a \nabla\Phi) + (\sigma_o^2 - \kappa^2 a)\Phi = 0 \, .$$

The set of equations (4.4) and (4.5) is identical with (3.21), but it has the advantage that the vertical position of the free surface appears explicitly. In some cases this is useful.

4.3. Comparison with the refraction model

In order to be able to compare (3.21) with the refraction
model, at first the diffraction terms must be removed from
the latter equation. An attractive way to obtain a refrac-
tion-like model is by averaging the Lagrangian (3.20) over
the phase (WHITHAM, 1971). In Whitham's procedure the aver-
aging of a linear model is accomplished by substitution of:

$$\Phi = A \cos \theta \tag{4.6}$$

with
$$\omega = - \theta_t$$

$$\underline{k} = \nabla \theta$$

In the averaging process ω, $\underline{k}$ and A are kept constant. By
definition:
$$\mathcal{L} = \frac{1}{2\pi} \int_0^{2\pi} L \, d\theta$$

Substitution of (3.20) for L gives

$$\mathcal{L} = \frac{1}{2\pi} \int_0^{2\pi} \{(\omega - \underline{U}.k)^2 A^2 (\sin \theta)^2 - a k^2 A^2 (\sin \theta)^2 -$$

$$(\sigma_o^2 - \kappa^2 a) A^2 (\cos \theta)^2\} \, d\theta =$$

$$= \frac{1}{2} A^2 \{(\omega - \underline{U}.\underline{k})^2 - a k^2 - (\sigma_o^2 - \kappa^2 a)\} \,. \tag{4.7}$$

This is a special case of eq. (2.12).

There exists an averaged Lagrangian for the refraction model
itself as well. This too is a special case of (2.12). It
reads

$$\mathcal{L} = \frac{1}{2} A^2 \{(\omega - \underline{U}.\underline{k})^2 - g k \tanh(\kappa h)\} \,. \tag{4.8}$$

It was seen in sec. 2.2 that both the dispersion relation (2.13) and the conservation equation (2.15) follow from the averaged Lagrangian (2.12). If the two Lagrangians (4.7) and (4.8) themselves and their derivatives with respect to ω and $\underline{k}$ coincide for $k=\kappa$, the corresponding dispersion relations and the conservation equations coincide also for $k=\kappa$. An expansion of the expression gk.tanh(kh), based on the definition of σ_0 (3.14) shows that this is the case:

$$g \ k \ \tanh(kh) \ = a \ k^2 + (\sigma_0^2 - a \ \kappa^2) = g \ \kappa \ \tanh(\kappa h) \ + a \ (k^2 - \kappa^2) \ (4.9)$$

It is noted that $k=\kappa$ implies that $\omega=\omega_0$, since the equations (3.14) and (3.15) are identical with the dispersion relation following from (4.8).

It is concluded that eq. (3.21) reduces to the refraction model with current, if its coefficients are calculated by means of (3.14) and (3.15). If approximate coefficients have to be used in (3.21), e.g. due to crossing waves, it does not exactly agree with the refraction model any more. For instance if the coefficient κ was found from (3.26) the wave number of the solution deviates by $O(U/c)^2$; the amplitude is subject to a deviation of $O(U/c)$ due to the deviation in the coefficient : appearing in the conservation equation. This is of course less accurate than was found for the dispersion relation, but the dispersion relation determines among others the direction of the energy transport, so that the errors are cumulative. An error in the equation for the conservation of wave action has less grave consequences.

4.4. Comparison with the shallow-water equation

In this section the special case of (3.21) for shallow water is compared with the usual shallow-water equation. In shallow water $\kappa h \ll 1$. It follows from (3.14) and (3.18) that in that case:

$$\sigma_o^2 - a \kappa^2 = 0 , \qquad (4.10)$$

$$a = g h \qquad (4.11)$$

In this comparison it is fruitful to use the version of the equation which includes an expression for the elevation of the free surface, i.e. eq. (4.4) and (4.5). In shallow water these equations read

$$\Phi_t + \nabla.(\underline{U} \, \Phi) + g \zeta = 0 , \qquad (4.12)$$

and
$$- (\frac{\partial \zeta}{\partial t} + \underline{U}.\nabla \zeta) - \nabla.(h \nabla \Phi) = 0 . \qquad (4.13)$$

In shallow water the horizontal velocity $\underline{u} = \nabla \phi$ is uniform in vertical direction. Then eq. (4.13) is recognizable as a linearization of the continuity equation. In its original form this equation reads

$$\frac{\partial \zeta}{\partial t} + \nabla.(\underline{v} \, (h + \zeta)) =$$

$$= \frac{\partial \zeta}{\partial t} + \nabla.((\underline{U} + \underline{u}) \, (h + \zeta)) = 0 .$$

Deleting steady terms and terms of higher than the first order there remains

$$\frac{\partial \zeta}{\partial t} + \nabla.(\underline{U} \, \zeta) + \nabla.(\underline{u} \, h) = 0 .$$

Because $\nabla.\underline{U}$ was assumed small, the correspondence is corro-

borated.

Eq. (4.12) is related to the equation of motion, but it needs more elaboration to show the relationship. First the gradient of this equation is taken:

$$\nabla_i \Phi_t + \nabla_i (\nabla_k U_k \Phi) + g \nabla_i \zeta =$$

$$= \frac{\partial u_i}{\partial t} + \nabla_i (U_k u_k) + g \nabla_i \zeta = 0.$$

where again a term $\nabla . \underline{U}$ is ignored. In the derivation of condition (3.8) a term $D_\alpha U_\beta$ was replaced by $D_\beta U_\alpha$, justified by the assumption that $\underline{U}$ has small derivatives. Now the reverse is done, leading to:

$$\frac{\partial u_i}{\partial t} + U_k \nabla_k u_i + u_k \nabla_k U_i + g \nabla_i \zeta = 0 ,$$

which is a linearization of the equation of motion in shallow water, which reads:

$$\frac{\partial v_i}{\partial t} + v_k \nabla_k v_i + g \nabla_i (\bar{\eta} + \zeta) = 0 .$$

The temporal derivatives of $\underline{u}$ and $\underline{v}$ coincide, since these velocities differ only by a constant. The term $g \nabla \bar{\eta}$ is ignored, since only non-stationary terms are considered. For the middle term of the left hand side some further elaboration is needed:

$$v_k \nabla_k v_i = (U_k + u_k) \nabla_k (U_i + u_i) =$$

$$= U_k \nabla_k U_i + U_k \nabla_k u_i + u_k \nabla_k U_i + u_k \nabla_k u_i .$$

The first term of the lower line is deleted because it is a steady term, the last one because it is a higher order term. This shows that the model (3.21) is in agreement with the shallow water equation both with regard to the continuity

equation and the equation of motion.

This completes the comparison with the shallow-water equation. It is concluded that there is correspondence under some conditions which are consistent with assumptions made in the derivation of eq. (3.21).

4.5. Discussion of the implementation of the model with regard to engineering practice

The problem of constructing usable numerical solutions for a wave equation such as (3.21) in a rather general case is by no means simple. The straightforward approach of discretizing the equation and then solving the resulting set of equations by some linear equations solver is not feasible due to the extremely large number of unknowns encountered in a typical problem. A representative region for which one might want to do a wave computation is 20 km by 20 km. The wavelength of the waves considered could be about 100 m. In order to get a reasonable accuracy one should choose a mesh size of at most one tenth of the wavelength, which results in an array of 2000*2000 nodes. Let M be the number of meshes along one side of the computational area (M=2000 in this case). Then a system of M^2 linear equations must be solved, requiring of the order of M^4 operations. This takes an impossible amount of computer time on present-day computers. Moreover the matrix is far too large to be stored in the computer memory. BERKHOFF (1972, 1976) used the finite element method in the way described here, but understandably for regions only a few wavelengths in size.

A different approach was taken by ITO and TANIMOTO (1972) and by ABBOTT et al. (1978). They find the periodic motion as the limiting state of a transient process initially at rest, with periodic boundary conditions. For a region of the size indicated above this method requires the same number of nodes as mentioned before. One would have to compute over a time span at least roughly equal to the time it would take a group of waves to travel through the entire region, i.e. the length of one side divided by the group velocity. Thus the number of time steps is of the order of M, and the computation consists of about M^3 operations. Although this

is a considerable reduction compared with the preceding method, it is still not feasible. This is illustrated by the fact that for M=2000, the computational process is many times slower than the physical process.

It was shown by RADDER (1979) that the parabolic approximation, developed mainly in the field of acoustics, is applicable for waves in coastal regions. By this approximation the partial differential equation which is originally of elliptic nature, is transformed into a parabolic one. In other words, it has become an initial value problem, with the incoming wave acting as initial value. In this method the number of operations is proportional to the number of nodes, so of the order of M^2. This requires a feasible amount of computer time, and also the storage requirements are within reasonable bounds. Thus the parabolic method is the only feasible alternative for refraction-diffraction computations in a coastal zone. In Chapter 6 a parabolic approximation for eq. (3.21) will be derived, and a numerical model based on this approximation will be applied to a region in the entrance of an estuary.

Before this is done, the full equation is applied to some idealized, quasi two-dimensional cases in the next chapter.

CHAPTER 5. APPLICATION TO PRISMATIC SLOPES AND CHANNELS

5.1. Wave transmission over an undersea slope.

As was remarked in sec. 4.5 the numerical computation of a wave field for practical purposes is by no means a simple matter. In the course of this study it is useful to select a subclass of problems that can be treated more easily. One such subclass has the property that the wave field repeats itself in one direction, say the y-direction. The partial differential equation is then reduced to an ordinary differential equation in the other coordinate, x. This requires that the depth and current velocity are independent of y. A possible situation is sketched in figure 5.1.

This subclass of problems is useful in two respects: it provides solutions for a set of practical problems, viz. those concerning waves propagating over an undersea slope, or along a gully or channel, and it provides the possibility of comparing the vertically integrated model with a full three-dimensional model.

The x- and y-components of the current velocity will be denoted by U and V. U and V and the depth h are functions of x. The requirement that the wave field be periodic in t as well as y, is expressed by

$$\Phi = Re \; \{e^{-i\omega_o t \; + \; imy} \; \psi \; (\underline{x})\} \tag{5.1}$$
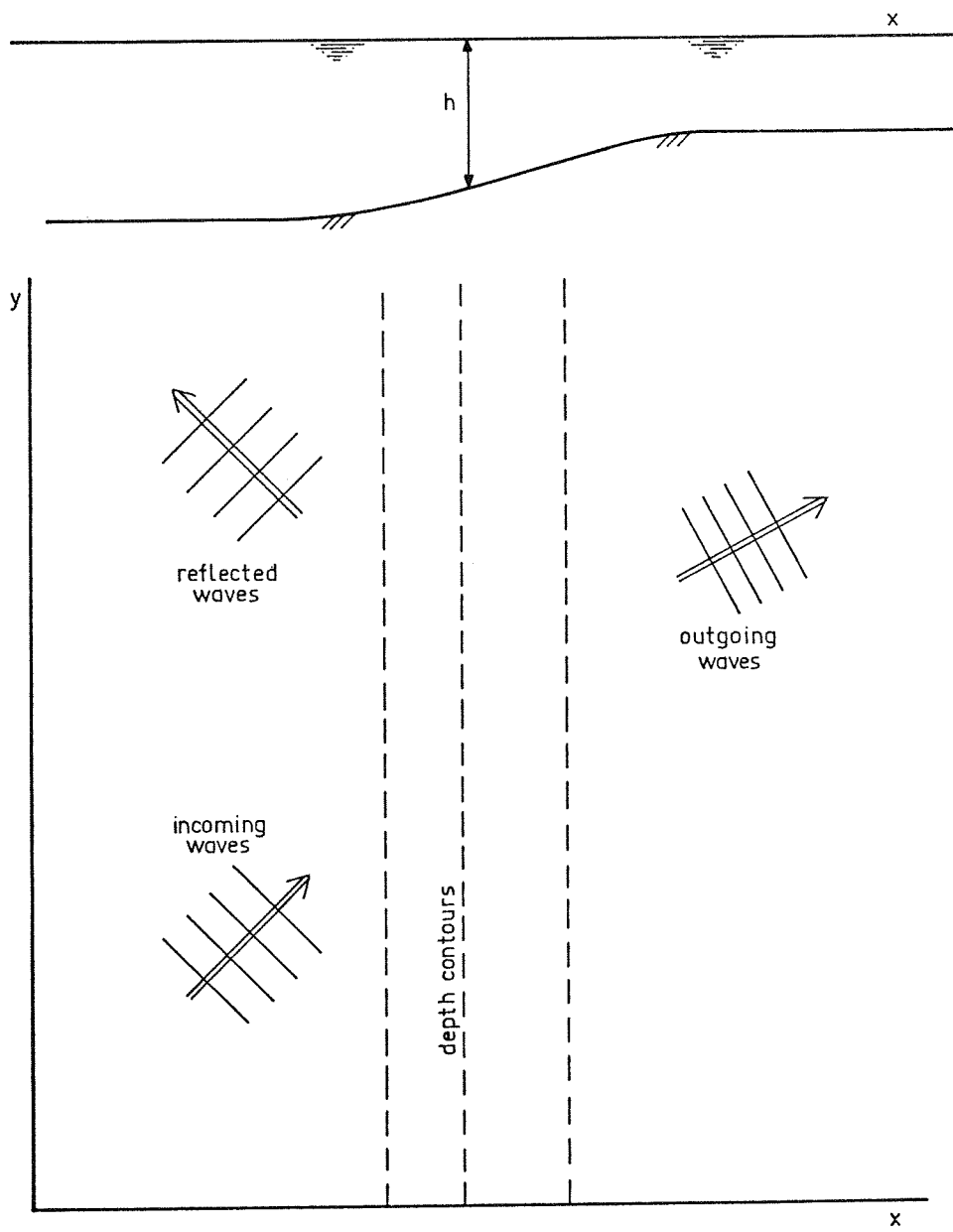
Figure 5.1. Cross-section and plan view
of waves crossing an undersea slope.

The general two-dimensional wave propagation model (3.21) now reduces to:

$$- (\omega_o - m\,V)^2\,\psi + i\,(\omega_o - m\,V)\,\{U\,\frac{\partial\psi}{\partial x} + \frac{\partial}{\partial x}\,(U\,\psi)\} + U\,\frac{\partial^2}{\partial x^2}\,(U\,\psi) +$$

$$U\,\frac{\partial}{\partial x}\,(im\,V\,\psi) - \frac{\partial}{\partial x}\,(a\,\frac{\partial\psi}{\partial x}) + (\sigma_o^2 - a\,\kappa^2 + a\,m^2)\,\psi = 0\;. \tag{5.2}$$

The necessary boundary conditions follow from assumptions concerning the incident waves and the waves radiated away from the model. This model consists of an undersea slope which forms the transition between two regions of constant depth and current. Thus it is assumed that for x<0 and for x>L the depth is constant, and $\underline{U}$=const. From the left, x<0, periodic waves are coming in under a given angle of incidence. The direction of these waves determines the wave number component m. At the other side of the model, x=L, there are no incident waves, only waves radiated outwards.

The condition that at x=L there are only waves in positive x-direction, is expressed by the following radiation condition:

$$\frac{\partial\psi}{\partial x}\,\bigg|_{x\,=\,L} = i\,l^{+}\,\psi\;. \tag{5.3}$$

The wave number component l^{+} is the positive root of an equation, that is derived from eq. (5.2) by substituting:

$$\psi\,(x) = \hat{\psi}\,e^{ilx}\;.$$

This equation reads

$$- (\omega_o - m\,V - l\,U)^2 + a\,(m^2 + l^2 - \kappa^2) + \sigma_o^2 = 0\;. \tag{5.4}$$

At x=0 there is an incident wave

$$\psi_i = \hat{\psi}_i\,e^{il^{+}x}\;,$$

and a reflected wave ψ_r for which

$$\frac{\partial \psi_r}{\partial x} = i1^- \; \psi_r \; .$$

The values of 1^+ and 1^- are the local values of the positive
and the negative root of eq. (5.4). For the function
itself the boundary condition follows from:

$$\psi = \psi_i + \psi_r \qquad ,$$

and the radiation condition given above. It reads:

$$\frac{\partial \psi}{\partial x} = i1^- \; \psi + (i1^+ - i1^-) \; \hat{\psi}_i \qquad \qquad at \quad x = 0 \; . \qquad \qquad (5.5)$$

The differential equation (5.2) is discretized by means of
the Finite Element Method (see ZIENKIEWICZ, 1977, or CONNOR
and BREBBIA, 1977). The unknown function is approximated by
linear shape functions, and the values at the nodal points
are determined by the Galerkin method. The numerical analy-
sis is described in more detail in appendix 1.

In the computer program based on this method the functions
$h(x)$ and $V(x)$ can be chosen by the user. $U(x)$ is determined
by

$$U = Q_x \; / \; h$$

Q_x being a constant chosen by the user. The value of σ_o can
be determined in one of the following ways

$$\sigma_o = \omega_o \qquad \qquad (5.6)$$

corresponding to eq. (3.26), or

$$\sigma_o = \omega_o - m \; V \; . \qquad \qquad (5.7)$$

representing a compromise between eq. (3.15) and (3.26). In
this compromise the y-component of the wave number is prop-
erly taken into account, whereas the x-component is not.
The y-component can be used because it is a given number in
this type of problem. In x-direction however, there will

exist two waves propagating in opposite directions, and hav-
ing wave numbers with opposite signs. Therefore the x-com-
ponent of the wave number cannot be used for the calculation
of σ_0 . By comparing the results obtained for the two
choices for σ_0 it can be investigated whether the solution
is very sensitive to changes in this value, or not (see for
instance figure 5.11).

Although the program can deal with dimensional variables,
all examples in this thesis have been done with non-dimen-
sional variables. All length measures have been non-dimen-
sionalized by means of the factor ω_0^2/g, and the velocities
by means of ω_0/g.

Figure 5.2 shows the cross-section that is used in the first
series of examples. Figures 5.3, 5.4 and 5.5 show the wave
functions for different angles of incidence. In all three
examples there is no current.   The quantities plotted are
the real and imaginary parts of the function ψ , written as
ψ_1 and ψ_2 respectively.   The amplitude of the incoming
wave ($\hat{\psi}_i$) is supposed to be unity. In the case of waves
progressing in positive x-direction ψ_1 and ψ_2 have a phase
difference of $\pi/2$ and they have the same amplitude.   In
standing waves on the other hand they have the same phase.
Figure 5.6 shows how the amplitude at the downwave side of
the model depends on the value of m.   According to the
refraction method there would be complete reflection or
standing waves for m>1.291, and complete transmission or
progressing waves for m<1.291. As figure 5.6 shows the
refraction-diffraction equation proves the existence of a
transition range from about 1.20 to 1.40, or from 31^0 to 37^0
in terms of angle of incidence. So, although there is a
range of angles for which the refraction method gives inac-
curate results, this range is quite small. Figures 5.3
through 5.5 show the wave function for m=1.20, m=1.30 and
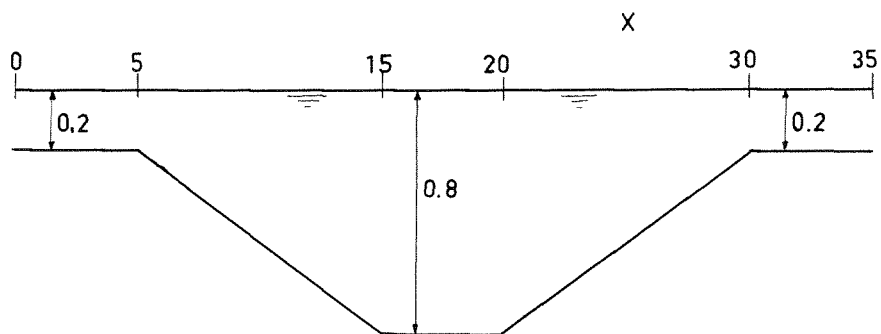m=1.40, respectively. The example m=1.30 is typical for the

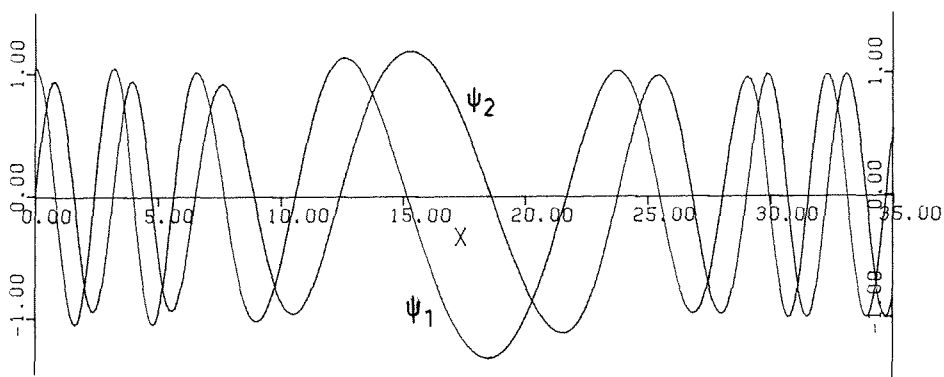Figure 5.2 Cross-section of a gully (distorted scale). Measures are non-dimensional.

Figure 5.3. Waves crossing the gully shown in figure 5.2, angle of incidence 31°, or m=1.20.
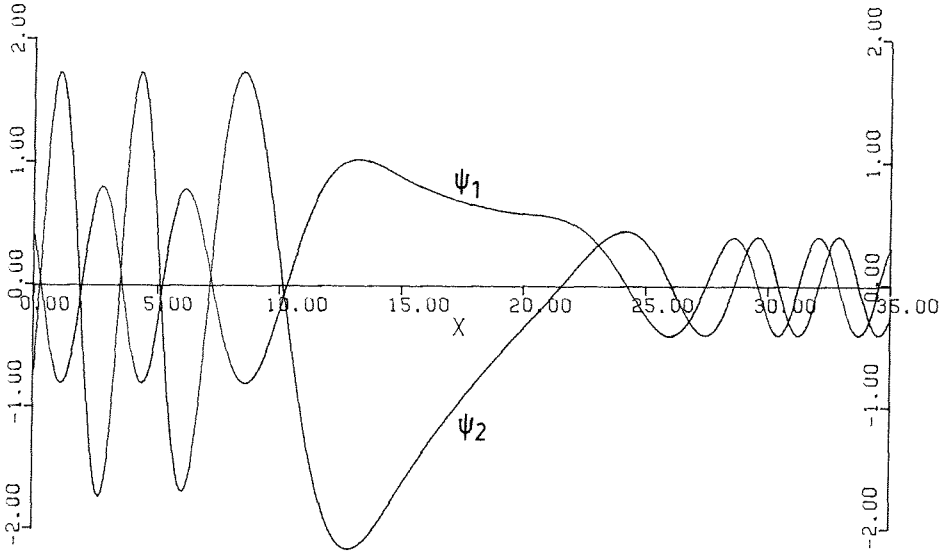
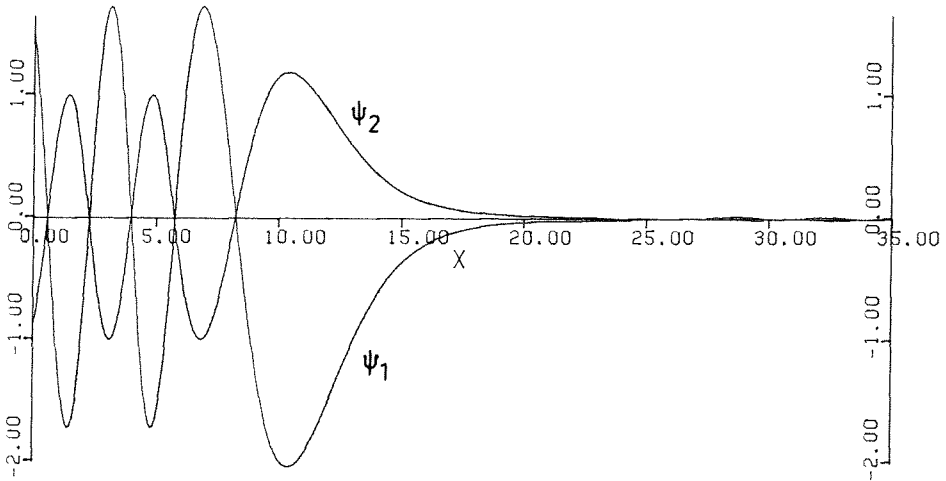Figure 5.4. Waves crossing the gully shown in figure 5.2, angle of incidence 34°, or m=1.30.

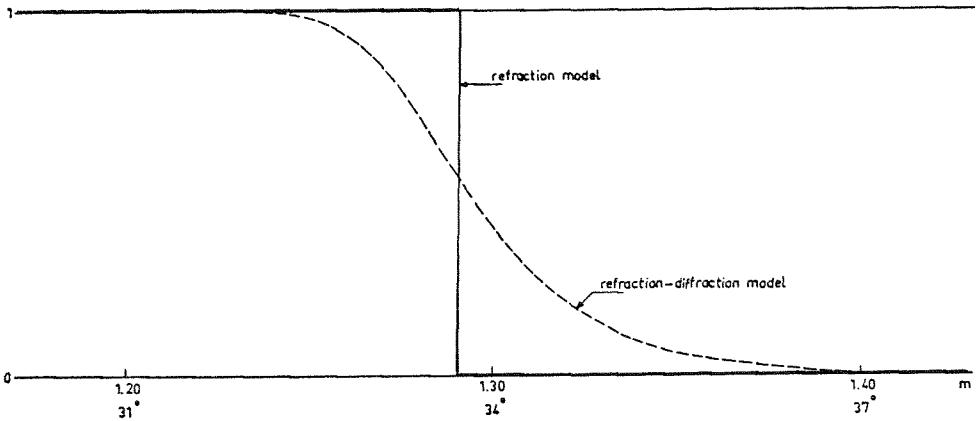Figure 5.5. Waves crossing the gully shown in figure 5.2, angle of incidence 37°, or m=1.40.

Figure 5.6. Wave amplitude at x=L as function of m, or as
        function of angle of incidence, for cross-section
        shown in figure 5.2.

transition cases. In the deepest part of the gully the wave
function varies slightly (it is nearly a negative exponen-
tial function there) and more to the right it becomes a pro-
gressive wave of reduced amplitude.

Partial reflection can also occur for waves incident nor-
mally to an undersea slope. The reflection is appreciable
only for rather steep slopes. In figure 5.7 it is shown how
the reflection coefficient depends on the bottom inclination
(tangent of the slope angle) for a certain cross-section.
In this cross-section the depth is uniformly 0.6 (non-dimen-
sional) at the upwave side of the slope, and 0.2 at the

downwave side.   The slope itself is plane.   The   length of
the slope (projected on the horizontal plane) is used as the
independent variable in figure 5.7.   The bottom inclination
is also indicated   in the graph.   It may be   argued that for
such steep slopes the mild-slope equation cannot be used.
In order to establish whether this is so, some computations
with a three-dimensional model have been carried out.

A brief account is given of the 3-dimensional wave computa-
tions that were carried out in order to check the   use of a
vertically integrated   model.   This 3-dimensional model   is
reduced to a 2-dimensional partial differential equation,
involving a horizontal and a vertical coordinate.   This
reduction is done   in the same way as   discussed in relation
with eq. (5.1) for the vertically integrated model:

$$\phi \ (x, \ y, \ z, \ t) = \text{Re} \ \{e^{-i\omega_o t \ + \ imy} \ P \ (x,z)\} \qquad . \qquad (5.8)$$

The function P is determined by means of the following equa-
tions, that are easily derived from the   3-dimensional wave
equations.   In the interior of the fluid:

$$\frac{\partial^2 P}{\partial x^2} + \frac{\partial^2 P}{\partial y^2} - m^2 \ P = 0 \ . \qquad (5.9)$$

The boundary condition on the bottom reads:

$$\frac{\partial P}{\partial n} = 0 \ . \qquad (5.10)$$

The 3-dimensional   computations have   only been   carried out
for the current-free case.   On   the mean free surface, which
is located in z=0, the following boundary condition holds:

$$\frac{\partial P}{\partial z} = \frac{\omega^2}{g} \ P \qquad . \qquad (5.11)$$

On x=0 and   x=L radiation conditions are   used, analogous to
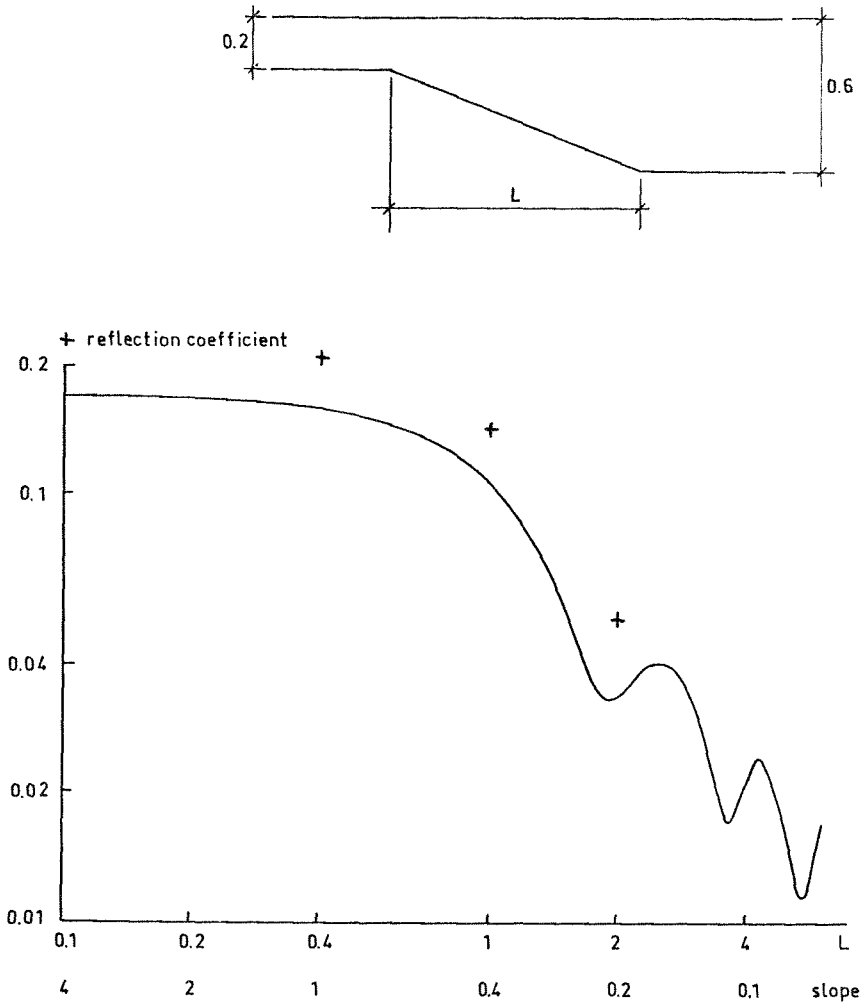(5.3) and (5.5):

Figure 5.7. Reflection coefficient as function of bottom
             inclination (normal incidence). The cross-section
             is shown in the upper part of the figure.
             curve: refraction-diffraction model.
             crosses: three-dimensional model.

$$\frac{\partial P}{\partial x} = i1^+ \, P \qquad\qquad \text{at} \quad x = L \qquad (5.12)$$

$$\frac{\partial P}{\partial x} = i1^- \, P + (i1^+ - i1^-) \, \hat{\psi}_i \; \frac{\cosh \kappa \, (z + h')}{\cosh (\kappa h)} \quad \text{at } x = 0 \qquad (5.13)$$

The partial differential equation (5.9) together with the boundary conditions is solved numerically by means of the Finite Element Method. The finite elements used are of triangular shape, with shape functions linear over each element. Appendix 1 discusses the method in more detail, but mainly for the vertically integrated model.

The reflection coefficients computed by the 3-dimensional model are plotted together with the results of the mild-slope equation in figure 5.7. The conclusion is that the mild-slope equation predicts a reflection coefficient of the right order of magnitude, even for slopes with a bottom inclination near to 1. In absolute sense the dicrepancy between the reflection coefficients decreases with decreasing bottom inclination, confirming that the refraction-diffraction equation is correct for mild slopes.

The second series (figure 5.8 to 5.11) gives examples of the influence of a current in the direction of the gully axis. The cross-section is sketched in figure 5.8. It is the same as the left half of the cross-section shown in figure 5.2. Figure 5.9 shows the wave field in absence of a current, figure 5.10 the wave field in the case of a current velocity in the same direction as the y-component of the wave propagation. The maximum current velocity (non-dimensional) is 0.1. Figure 5.11 shows the result for a current in the direction opposite to the y-component of the wave propagation. As in the preceding set of examples, figure 5.9 through 5.11 present graphs of the real and imaginary parts of the wave potential at the surface.

The example with current in positive y-direction shows a greater reflection than the one with current in negative y-direction. This should be expected on the ground of refraction calculations since the curvature of the wave rays is larger in the first of the two cases. It is seen that the influence of the current on the amount of reflection is large in this case. It must be remarked however, that the angle of incidence was deliberately chosen near to the critical angle.

In figure 5.11 two results are shown. The solid line is based on the use of eq. (5.6), the broken line on eq. (5.7). A small difference in amplitude and a very small phase difference are the consequences of the different formulas.

In the third series of examples (figure 5.12 and 5.13) the influence of a current in the x-direction is investigated. The depth profile is identical with the previous series (see figure 5.8). The wave system in absence of a current is also the same (see figure 5.9). The current velocity U is defined by $U=Q_x/h$. Due to the depth profile the current velocity is largest at x=0. Here the absolute value of the (non-dimensional) velocity is 0.2.

It is seen that the current has a strong influence on the wavelength of the solution, as it should according to the refraction method. Furthermore, the graphs show that the refraction-diffraction equation predicts that the reflection coefficient is much less influenced by a current perpendicular to the slope than by a current parallel to the slope.
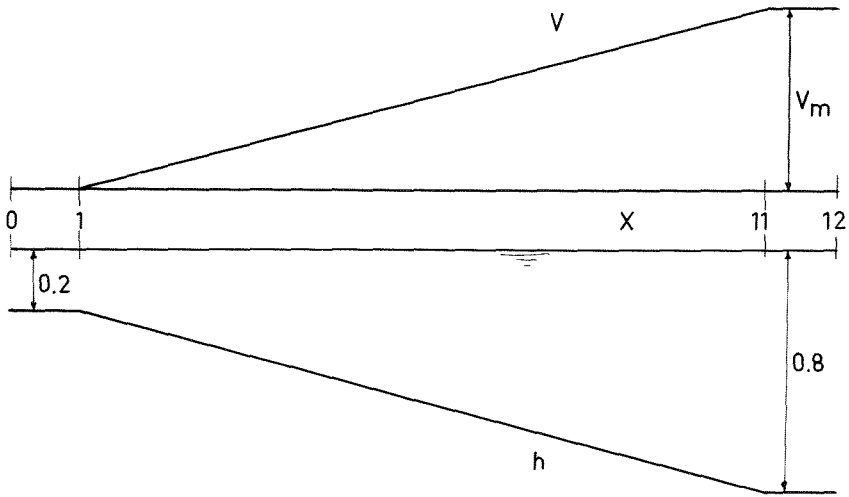
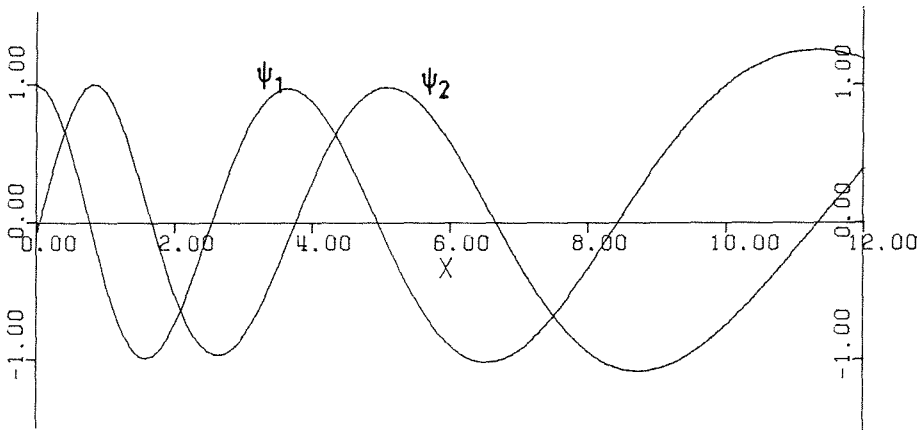Figure 5.8. Cross-section and velocity profile.

Figure 5.9. Wave system in absence of a current. angle of
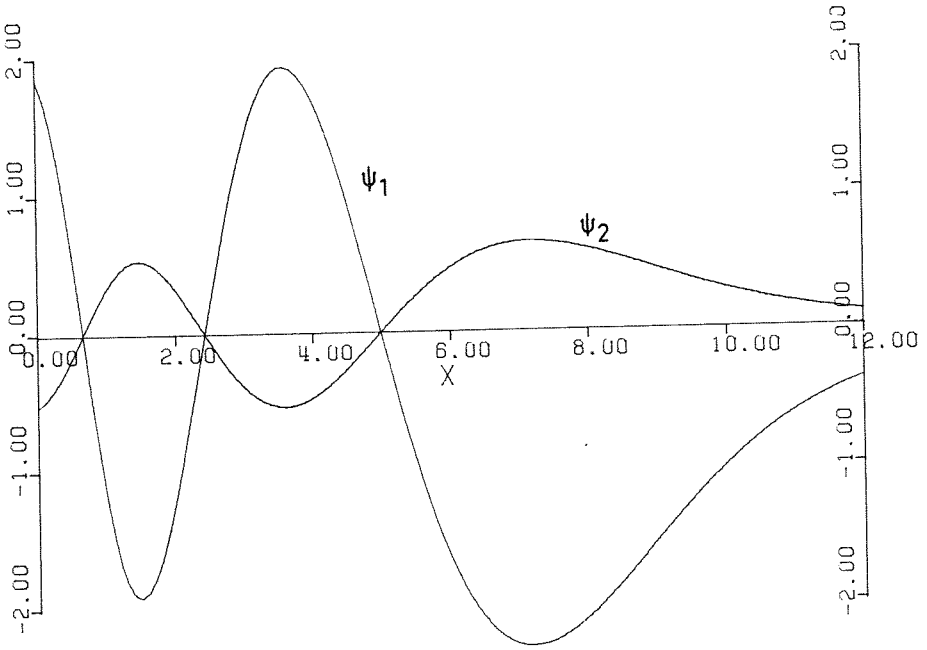incidence 31°, or m=1.20.

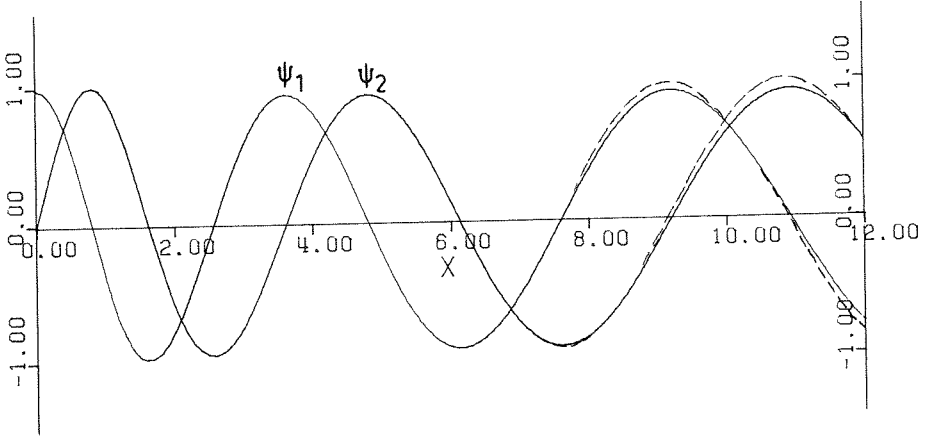Figure 5.10. Wave system with current in positive y-direction. m=1.20, Vm=0.1.

Figure 5.11. Wave system with current in negative y-direction. m=1.20, Vm=-0.1.
solid line: eq. (5.6) is used;
broken line: eq. (5.7) is used.

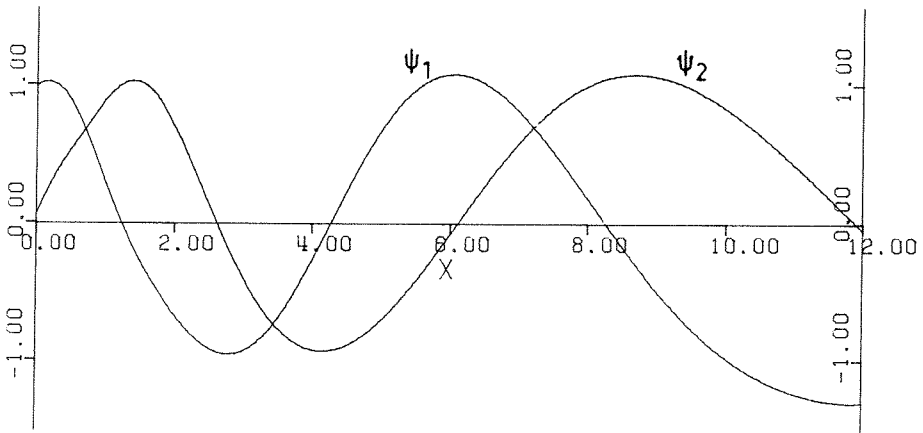Figure 5.12. Wave system with current velocity perpendicular
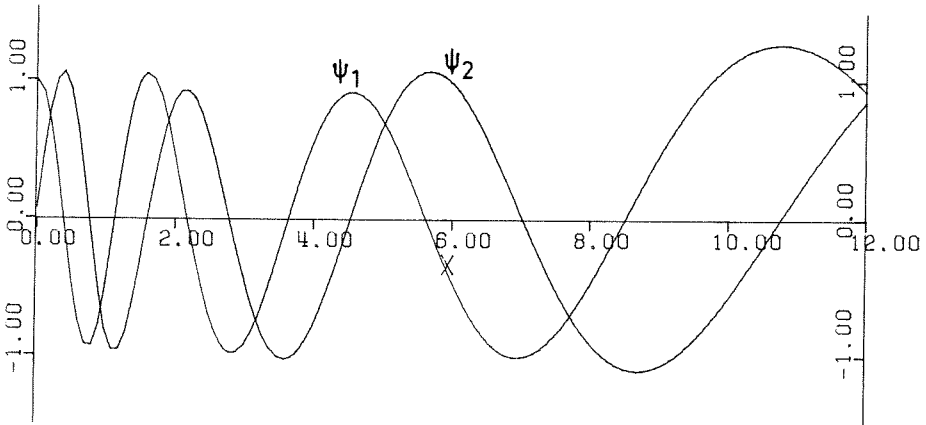to bottom contours, velocity in positive x-di-
rection. m=1.20, Qx=+0.04.

Figure 5.13. Wave system with current velocity perpendicular
to bottom contours, velocity in negative x-di-
rection. m=1.20, Qx=-0.04.

5.2. Propagation along the axis of a wave channel.

This section and the following one deal with wave propaga-
tion parallel to the depth contours. The essential differ-
ence between this case and the one treated in sec. 5.1. is
that now the incident waves run parallel to the depth cont-
ours. As a consequence the value of the wave number compo-
nent m is not known a priori, but it follows from the compu-
tation as an eigenvalue. The problem having become an
eigenvalue problem, is a result from the fact that both the
differential equation (5.2) and the boundary conditions
(5.14) have a zero right hand side. Now a non-trivial solu-
tion is only possible for a set of discrete values of m. In
the case considered first the value of m is real, which cor-
responds to waves which maintain their amplitude as they
propagate. In other cases, considered in sec. 5.3, it may
be complex, which corresponds to waves decreasing in the
direction of propagation; this occurs if wave energy is
radiated sideways.

The case considered in this section, is a prismatic wave
channel of finite width, bounded by vertical side-walls.
These are parallel to the depth contours. This wave channel
is an interesting study object mainly because there exists a
continual balance between shoaling and diffraction effects.
The shoaling tends to push the wave energy towards the shal-
lower part of the channel, the diffraction tends to smooth
the energy distribution. A laboratory experiment with which
the results could be compared, seems possible, but it has
not been carried out. Another type of verification has been
done, thanks to the fact that a fully 3-dimensional computa-
tion is possible in this case. In this way the effect of
integrating over the vertical can be studied.

A channel of finite width is assumed, bounded by side-walls

which completely reflect the waves. Thus the boundary conditions are:

$$\frac{\partial \psi}{\partial x} = 0 \qquad \text{at } x = 0 \text{ and } x = L \qquad (5.14)$$

The way in which the eigenvalue m and the corresponding eigenfunction $\psi(x)$ are determined, is discussed in appendix 2. For the 3-dimensional model the eigenvalue has been determined in the same way. This 3-dimensional model was discussed in more detail in the previous section. Only the boundary conditions at the lateral sides are different. In analogy with (5.14) they read:

$$\frac{\partial P}{\partial x} = 0 \qquad \text{at } x = 0 \text{ and } x = L$$

In this comparison between the mild-slope equation and the 3-dimensional model a series of channel cross-sections with increasing maximum slope is considered. These cross-sections consist of two flat sections with non-dimensional depths of 0.2 and 0.6, with a transition zone in between. The channel has a total non-dimensional width of 2., and the slope in the transition zone ranges between 0.2 and 0.8. The cross-sections and the resulting wave forms are presented in figure 5.14 through 5.17. The corresponding eigenvalues are shown in table 5.1. Not only the eigenvalues, also the wave forms are in surprisingly good accordance. It could hardly be expected that a model for small slopes would produce such accurate results for slopes near to 1. No explanation is found for the remarkable fact that the correspondence is best for the steepest slope in the range of values considered.

| slope	eigenvalue m	
	vert.int.mod.	3-dim. model
0.2	1.785	1.777
0.4	1.906	1.894
0.8	1.959	1.955

Table 5.1.   (non-dimensional) eigenvalue
as function of lateral slope

A few examples with current are shown, this time only computed by the vertically integrated model. A current in the direction perpendicular to the channel axis is not possible, so only a current parallel to this axis is considered. The current velocity is calculated from the formula $V=C_f/h$, more or less in analogy with the Chezy law of friction.   The coefficient C_f is variable in the computer program.   The results for three values of C_f are presented in figure 5.18: $C_f=-0.2$, 0. and 0.2. The corresponding maximum non-dimensional velocities are -0.15, 0., and 0.15.

It follows from figure 5.18 that the current has a limited influence on the shape of the wave propagating in the channel. It has a stronger influence on the eigenvalue, which is closely related to the propagation velocity. The propagation velocity is 1/m, or 0.70 and 0.425, resp.   For the case of zero current it is 0.56. This shows that the differences in propagation velocity are close to the differences in current velocity averaged over the cross-section.

(a)

2.0

0.2

0.6

max. slope = 0.2

(b)

1.0

max. slope = 0.4

(c)

0.5
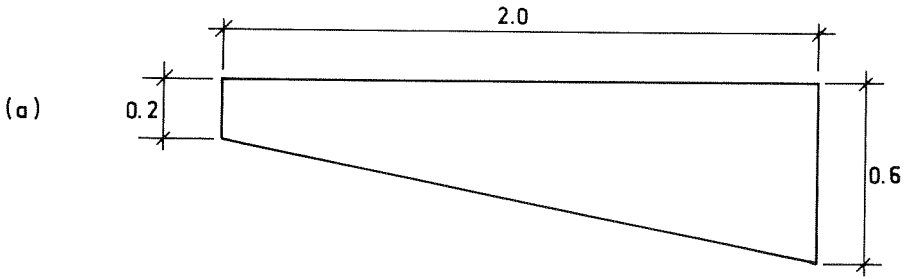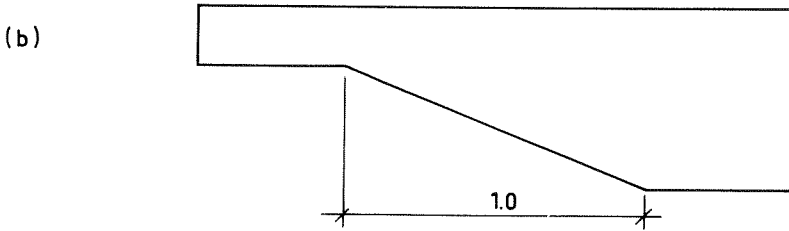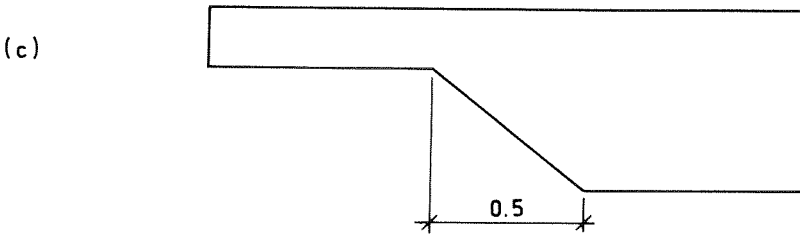
max. slope = 0.8

Figure 5.14. Cross-sections of three wave channels, on non-distorted scale. Measures are non-dimensional.

Figure 5.15. Wave system in channel with maximum bottom steepness 0.2 (see cross-section (a) in figure 5.14)

Figure 5.16. Wave system in channel with maximum bottom steepness 0.4 (see cross-section (b) in figure 5.14)
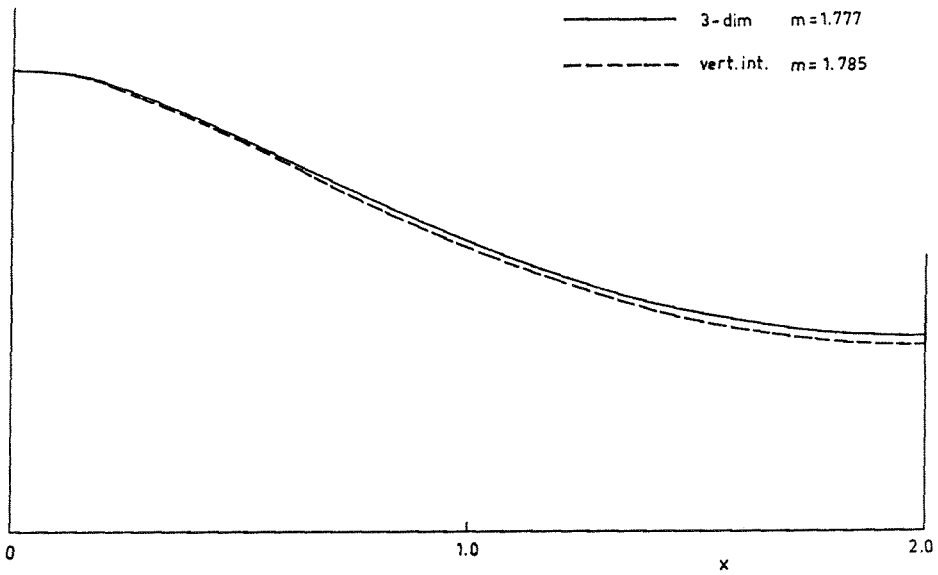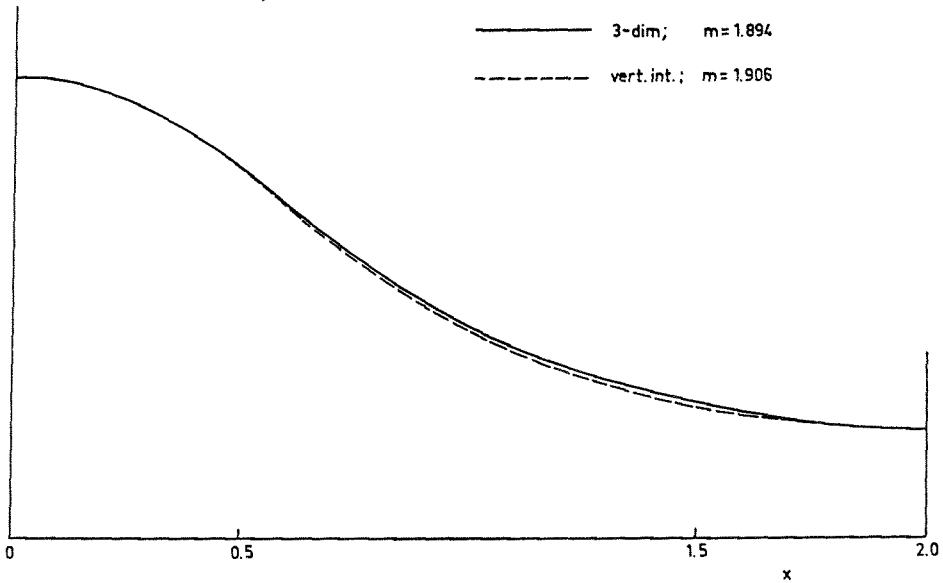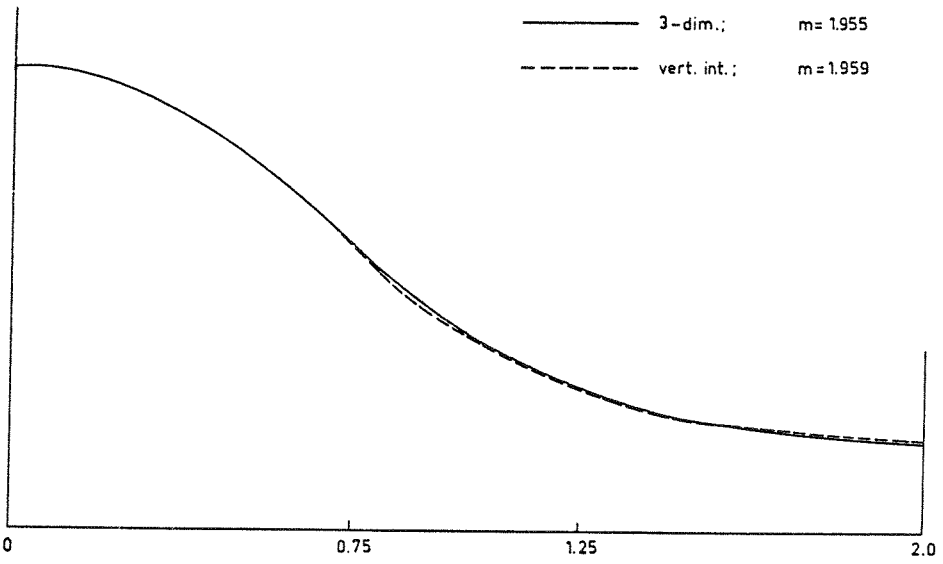
Figure 5.17. Wave system in channel with maximum bottom
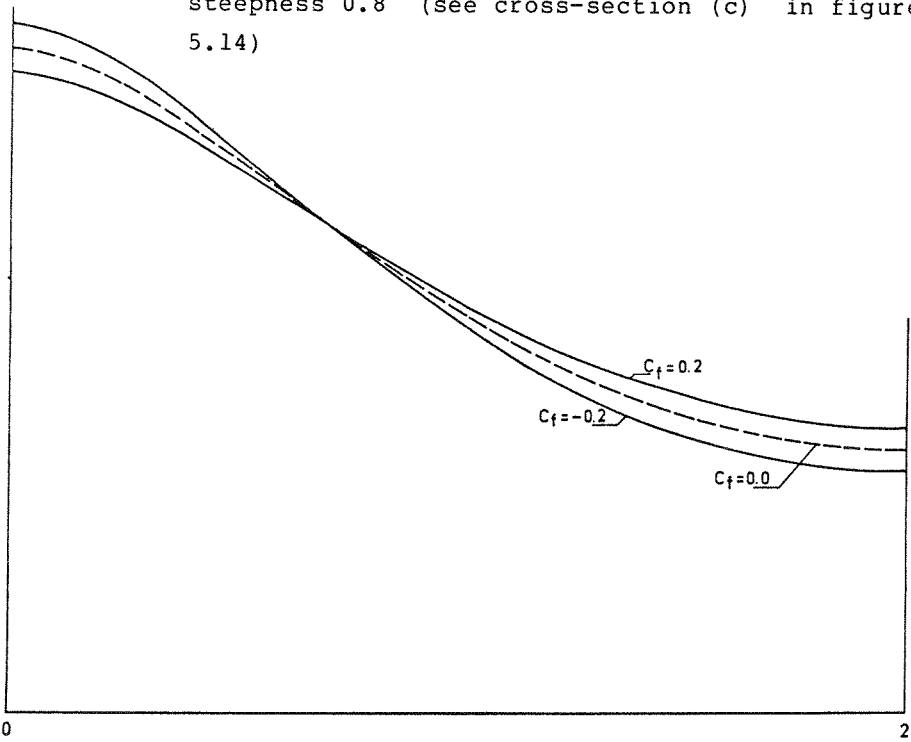steepness 0.8 (see cross-section (c) in figure
5.14)

Figure 5.18. Wave system in channel with current. Cross-
section (a) in figure 5.14. $V = C_f \sqrt{h}$

5.3. Waves propagating along an undersea gully.

This section deals again with waves propagating in a direction parallel to the depth contours. This time however, in contrast to the previous section, there are no reflecting side-walls along the channel, but shallower regions extending to infinity which can absorb wave energy (see figure 5.19). This results in an eigenvalue m which is no longer purely real. Its imaginary part shows the rate of decay of the waves along the y-axis.

HUITENGA and VAN DRIEL (1974) carried out a series of experiments in which they tried to measure the decay of the waves propagating along a gully. Obviously the experiment had to be done in a wave tank of finite width, so the shallow regions were bounded by beaches that had to absorb the wave energy penetrating onto the shallows. Their experimental set-up is sketched in figure 5.20. They measured, among other quantities, the shapes of the wave fronts that developed in the wave tank, and the decay of the wave amplitude along the axis of symmetry. They carried out measurements with 4 different wave frequencies and 2 different water levels.

Since in these experiments both shoaling and diffraction effects play a role, they are very suitable for a validation of the mild slope equation. As before, eq. (5.2) is used to compute the wave system, with the radiation condition (5.3) as boundary condition at x=L. This boundary is located somewhere in the shallow region. The boundary x=0 is chosen on the axis of symmetry, so the other boundary condition reads:

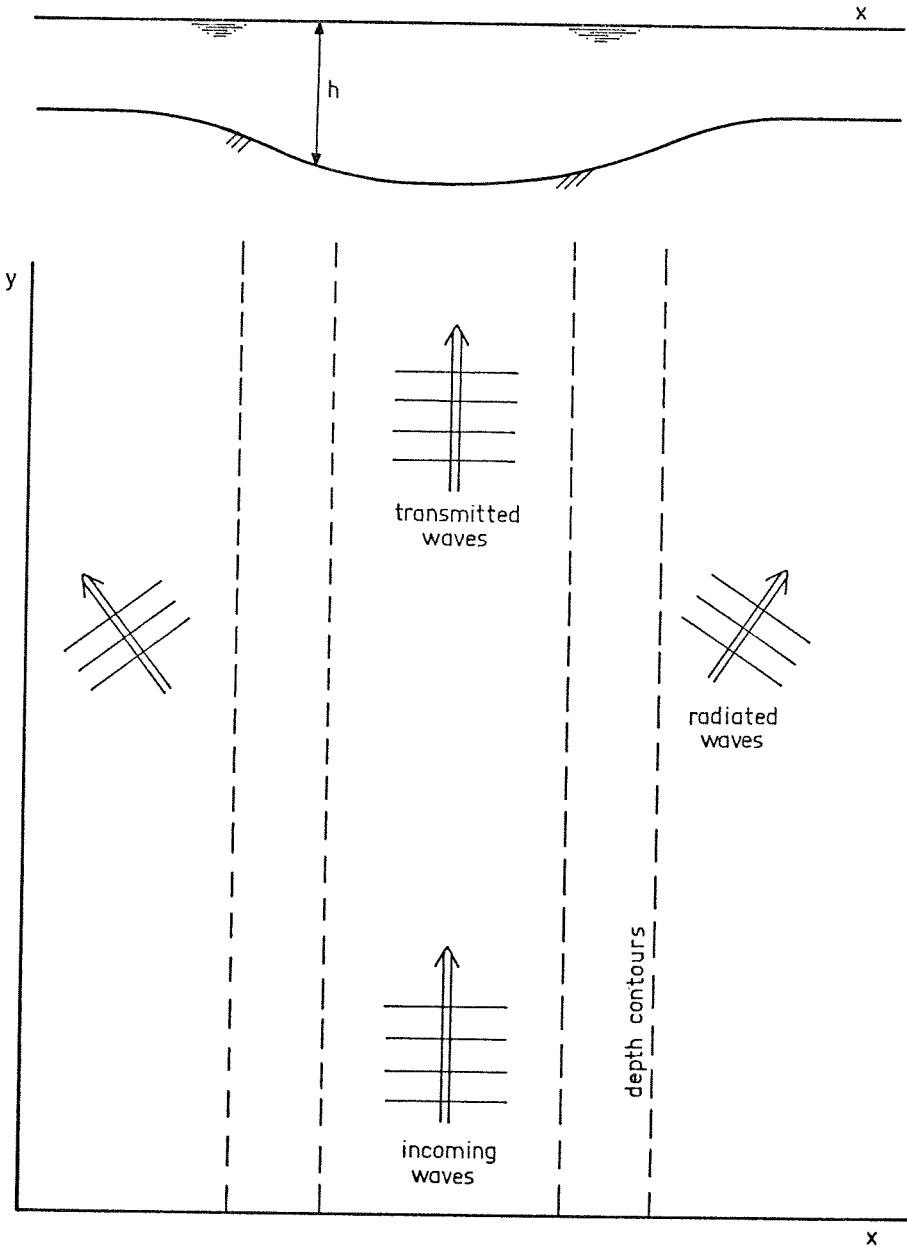$$\frac{\partial \psi}{\partial x} = 0 \qquad \text{at } x = 0 \ .$$

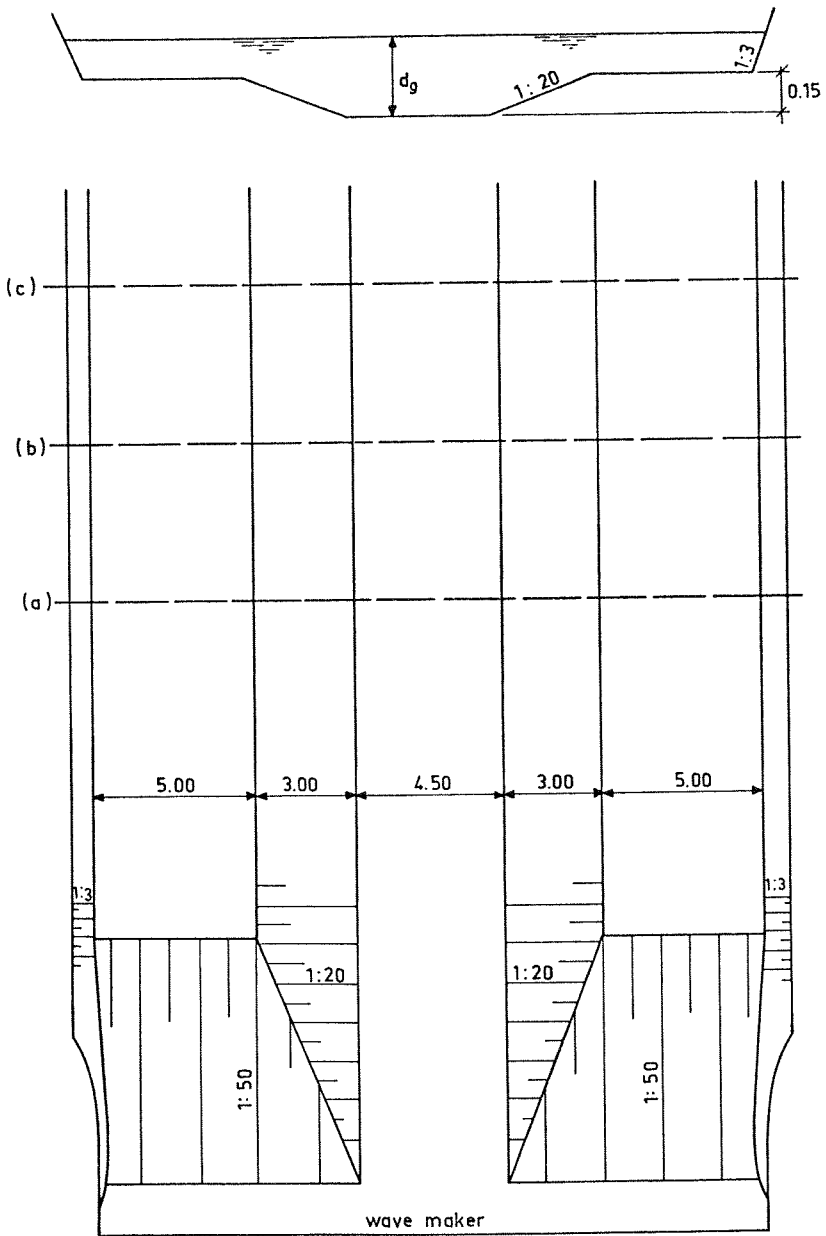Figure 5.19. Cross-section of a gully and sketch of the wave system (plan view)

Figure 5.20. Cross-section and plan view of the wave tank used in the experiment by Huitenga and Van Driel.

The solution of this set of equations provides a value for m
and the function $\psi(x)$. The projection on the horizontal
plane of the wave fronts is now determined by:

$$y = - \frac{1}{Re^-(m)} \, \text{arg} \, (\psi) .$$

In figure 5.21 through 5.24 each computed wave front is com-
pared with wave fronts observed by Huitenga and Van Driel.
The wave fronts are based on measurements of the phase in
three cross-sections indicated in figure 5.20 by the labels
(a), (b) and (c). It is concluded that although the agree-
ment is not very close, there is no indication of any syste-
matic error. The measured wave fronts show many irregulari-
ties, perhaps due to reflections from the boundaries of the
model. The large discrepancies at the sides may be due to
waves propagating over the shallows in the direction of the
axis. These waves are generated by the outer parts of the
wavemaker. They do not penetrate into the gully itself
because they are reflected at the top of the slope.

The decay rate of the waves is related to the imaginary part
of m. The decay rate was determined by the experimenters
taking into account the energy loss due to bottom friction.
A formula derived by IWAGAKI and TSUCHIYA (1966) was used to
determine the rate of energy loss due to bottom friction per
unit area:

$$E_{fb} = \frac{\rho\nu}{2} \left(\frac{\omega}{2\nu}\right)^{\frac{1}{2}} (\omega\hat{\zeta})^2 \quad \frac{1}{(\sinh(\kappa h))^2} \, (1 - 0.197 \, \varepsilon + 0 \, (\varepsilon^2)) .$$

This formula was derived for laminar flow conditions. $\hat{\zeta}$ is
the wave amplitude, and ν the viscosity, for which Huitenga
and Van Driel took $10^{-6} \, m^2/s$. The quantity ε, which repre-
sents the ratio of the orbital velocity and the propagation
velocity was small enough to be ignored.

The decay rate r_m was determined by comparing the energy

transports (E_t) through consecutive cross-sections. Let F be the friction loss integrated over the width of the gully, and integrated in axial direction:

$$F_i = \int_0^{y_i} \int_0^W E_{fb} \, dy \, dx$$

Now for one interval (y_i, y_{i+1}) the decay ratio is equal to

$$r_i = \frac{E_{t,i+1} + F_{i+1}}{E_{t,i} + F_i}, \quad i = 1, 2, \ldots, N-1 \ .$$

The energy transport is found from the wave heights measured in each of the cross-sections.

For each experiment the average of the numbers r_i is used as a measure of the overall decay rate.

In the mathematical model the decay rate is related with the imaginary part of m according to: $r_m = \exp(-2*Im(m)*\Delta y)$, Δy being the distance between two consecutive cross-sections, 5 m in this case.

In table 5.2 the computed value of r_m is compared with the value that results from the measurements. It can be concluded that there is a good agreement between the measurements and the mathematical model.

The computations referred to above, have also been carried out by means of the 3-dimensional model. The results from this model are not shown separately, because they are always very close to the results of the vertically integrated model, both with respect to the eigenvalue and to the shape of the wave front. For instance for a depth of 0.35 m and a period of 1.62 s the three-dimensional model gave m=2.2700-0.0390i, and the vertically integrated model m=2.2714-0.0393i. This discrepancy is insignificant com-

wave period in sec.	gully depth at x=0, in m	r_m measured	r_m computed
2.2	0.35	0.67	0.62
1.62	0.35	0.64	0.68
1.4	0.35	0.72	0.72
1.2	0.35	0.74	0.78
2.2	0.275	0.59	0.62
1.62	0.275	0.69	0.70
1.4	0.275	0.76	0.74
1.2	0.275	0.77	0.78

Table 5.2. measured and computed decay rates

pared with the discrepancy between measurement and computa-
tion. As regards the wave fronts there is no visible dis-
crepancy between the two mathematical models, if these
fronts are plotted on the scale used in figures 5.21 through
5.24.

Figure 5.21. Comparison of computed and measured wave
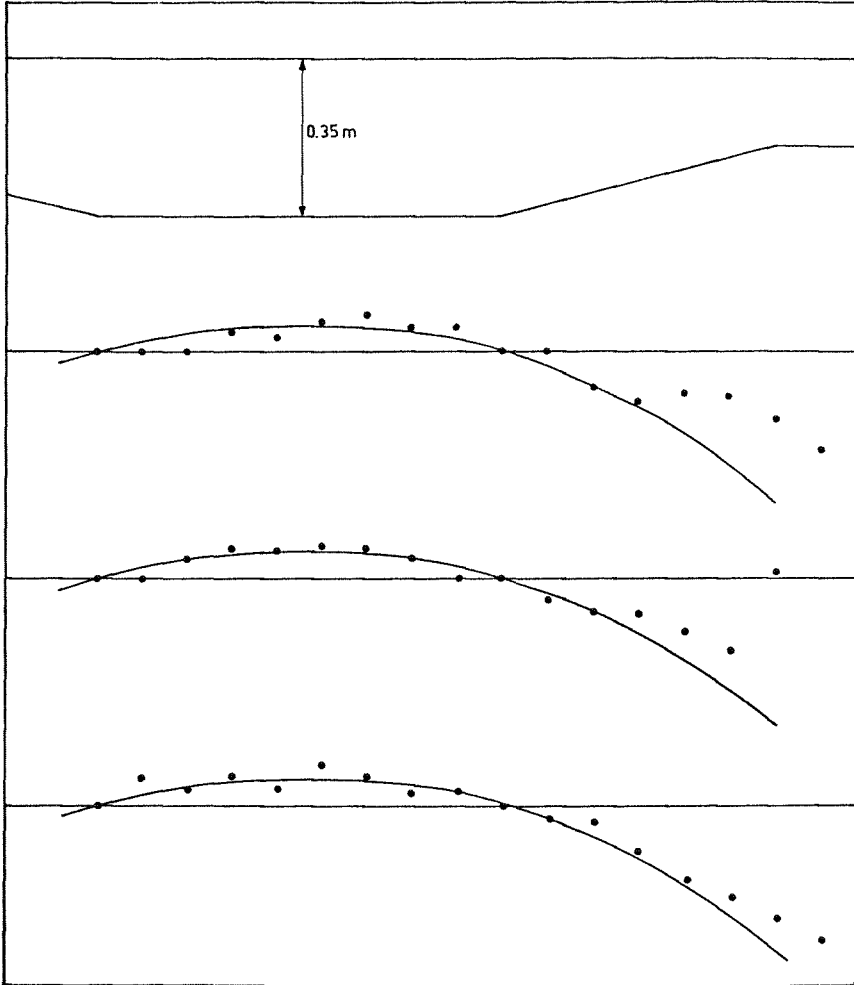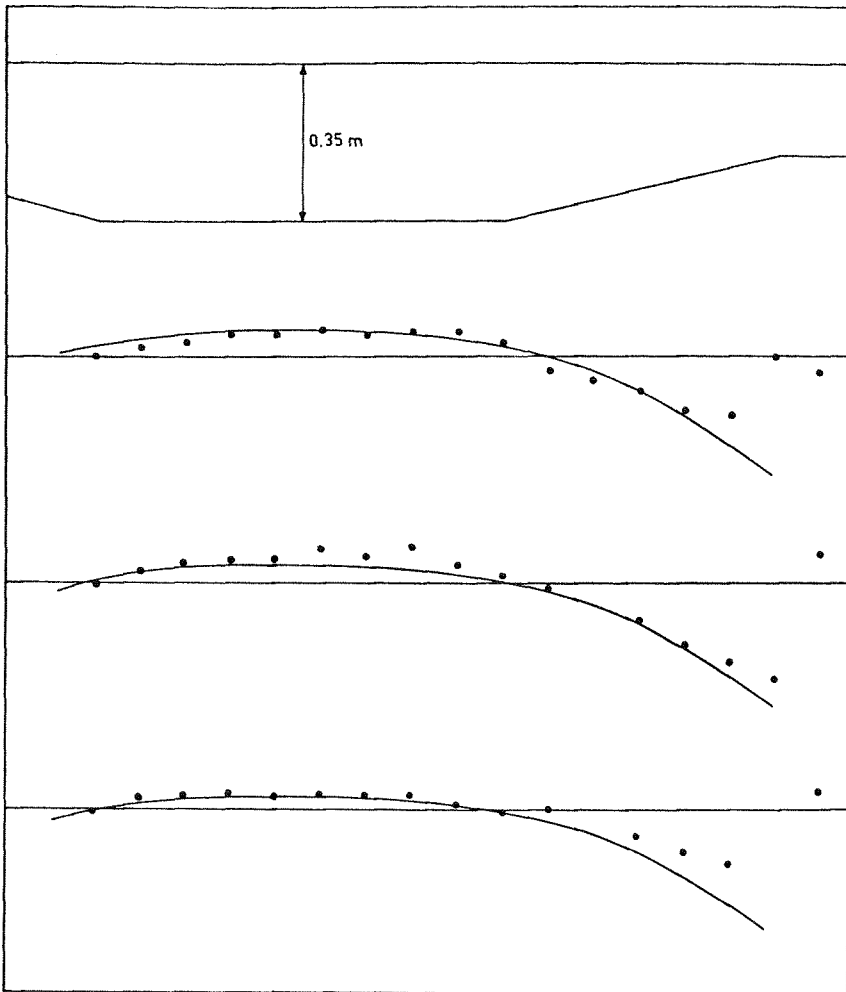fronts. Wave period 2.2 s, gully depth 0.35 m.

Figure 5.22. Comparison of computed and measured wave
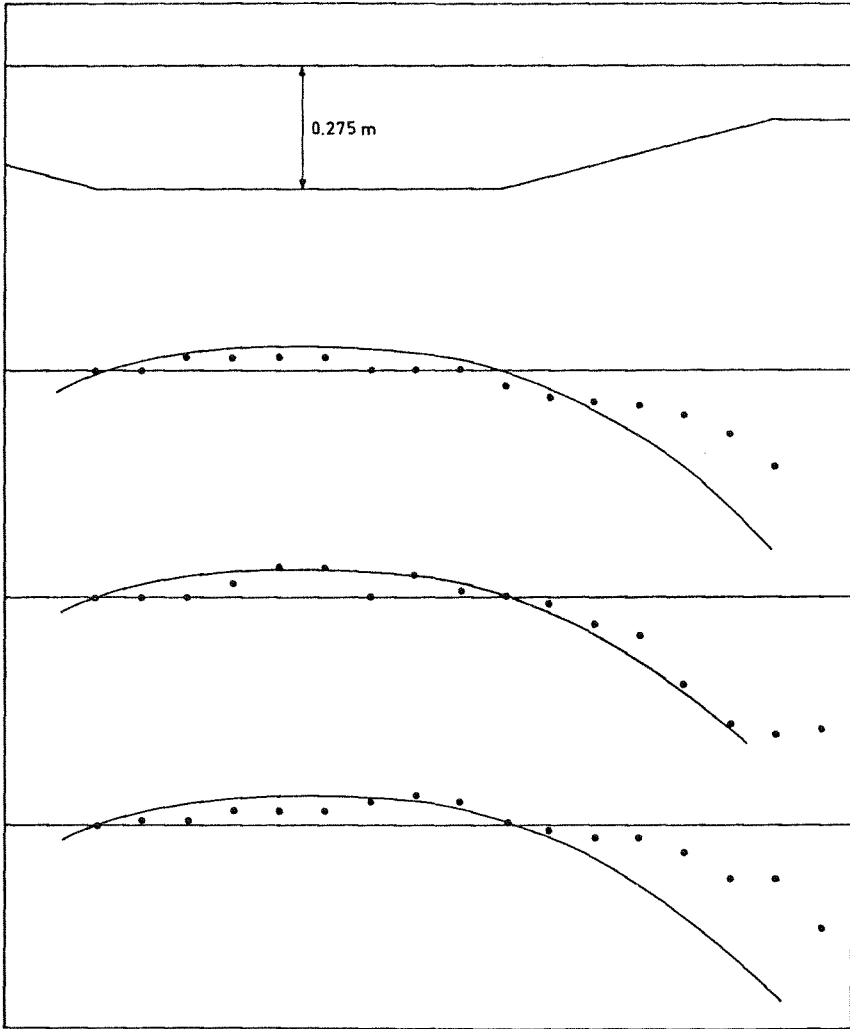fronts. Wave period 1.2 s, gully depth 0.35 m.

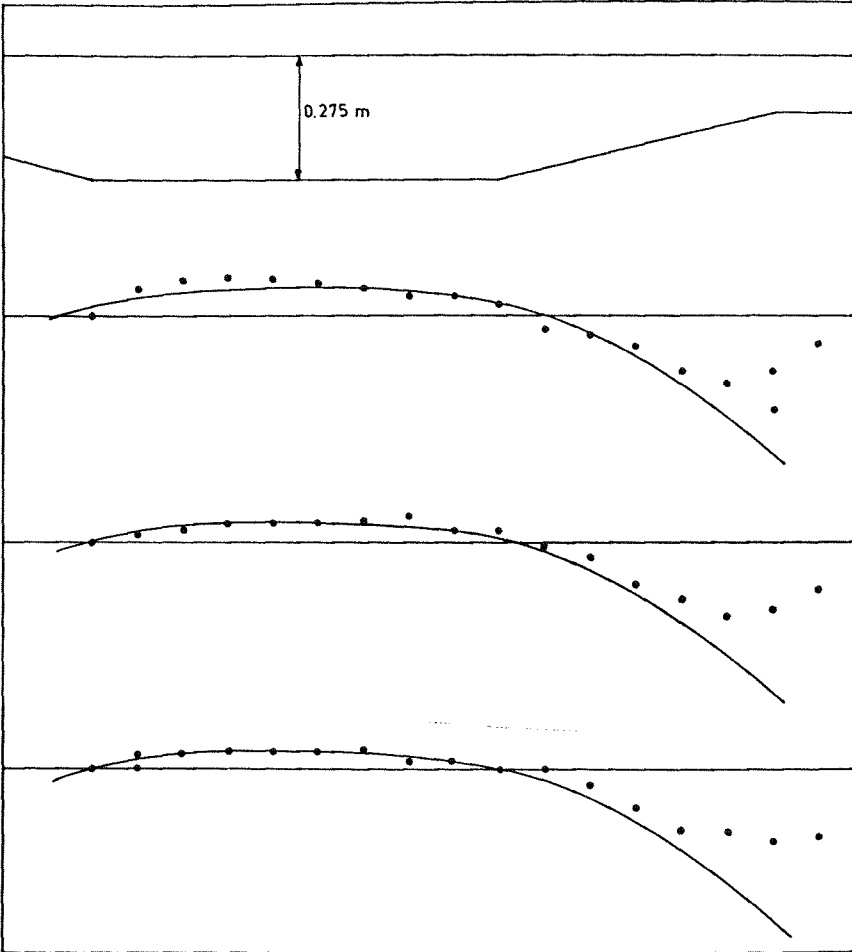Figure 5.23. Comparison of computed and measured wave fronts. Wave period 2.2 s, gully depth 0.275 m.

Figure 5.24. Comparison of computed and measured wave fronts. Wave period 1.2 s, gully depth 0.275 m.

CHAPTER 6. PARABOLISATION OF THE PROPOSED MODEL

6.1. An alternative method for the parabolisation of the
     Helmholtz equation

It was argued in sec. 4.5 that the parabolic approximation
provides the most feasible way to obtain numerical solutions
for the wave equation. In the approach taken by RADDER
(1979) to obtain the approximation, the equation is first
transformed into a Helmholtz equation, usually with varying
coefficients. A rectangular coordinate system is con-
structed of which one coordinate is roughly in the direction
of the main wave propagation. This coordinate will be
called s in the sequel. The wave field is split into a
transmitted and a reflected field, and equations for both
fields are derived. In the most simple approximation the
reflected field is then completely neglected. The result is
a partial differential equation of parabolic type for the
transmitted field. The order of the equation has been
reduced in the sense that second derivatives with respect to
s have disappeared and first derivatives have emerged
instead.

The approach sketched above is not entirely followed in the
case of the equation with current. An approach will be pre-
sented which avoids the somewhat arbitrary splitting of the
wave field. The wave equation is brought, as well as possi-
ble, into the form of an equation that can be split exactly.
There results an equation which involves so-called pseudo
operators which are then developed into derivatives with
respect to the coordinate n, which is perpendicular to s.
The method is first demonstrated by means of the Helmholtz

equation in order to facilitate comparison with other
approximations.

Similar pseudo operators have been used by ENGQUIST and
MAJDA (1977) in a paper on wave absorbing boundary condi-
tions. It is hardly surprising that their work is relevant
for the present method, since their aim is to find a boun-
dary equation which produces as little reflection as possi-
ble, whereas in the parabolic approximation the reflection
is neglected in the whole computational region.

The present method is based on the observation that the dif-
ferential equation

$$\frac{\partial}{\partial s}\left(\frac{1}{\gamma}\frac{\partial \Phi_m}{\partial s}\right) + \gamma \; \Phi_m = 0 \tag{6.1}$$

can be split exactly into an equation for the transmitted
field and an equation for the reflected field:

$$\frac{\partial \Phi^+}{\partial s} = i \; \gamma \; \Phi^+ \; , \tag{6.2}$$

$$\frac{\partial \Phi^-}{\partial s} = - \; i \; \gamma \; \Phi^- . \tag{6.3}$$

These relations are easily verified by means of substitu-
tion. It is the aim of the analysis to transform a given
wave equation into a form as close as possible to eq. (6.1).
In general this cannot be done in an exact manner. The wave
equation that will be studied in this section, is the Helm-
holtz equation with variable coefficient κ :

$$\frac{\partial^2 \Phi}{\partial s^2} = - \; \kappa^2 \; \Phi - \frac{\partial^2 \Phi}{\partial n^2} \; . \tag{6.4}$$

In order to start the transformation process, we put:

$$\Phi_m = \alpha \; \Phi$$

where α is an as yet unknown variable. α and γ will be cho-
sen in such a way that the equations (6.4) and (6.1) conform
as well as possible. In (6.1) the following term appears:

$$\frac{\partial}{\partial s} \left\{ \frac{1}{\gamma} \frac{\partial (\alpha \Phi)}{\partial s} \right\} =$$

$$= \frac{\alpha}{\gamma} \frac{\partial^2 \Phi}{\partial s^2} + \left\{ \alpha \frac{\partial}{\partial s} \left(\frac{1}{\gamma} \right) + \frac{2}{\gamma} \frac{\partial \alpha}{\partial s} \right\} \frac{\partial \Phi}{\partial s} + \left\{ \frac{\partial}{\partial s} \left(\frac{1}{\gamma} \frac{\partial \alpha}{\partial s} \right) \right\} \Phi \ .$$

Since no first derivative with respect to s appears in eq.
(6.4), the coefficient of $\partial \Phi / \partial s$ must vanish:

$$\alpha \frac{\partial}{\partial s} \left(\frac{1}{\gamma} \right) + \frac{2}{\gamma} \frac{\partial \alpha}{\partial s} = 0$$

So $\qquad \gamma = \alpha^2$

Now eq. (6.1) yields:

$$\frac{\partial^2 \Phi}{\partial s^2} = - \alpha^4 \Phi - \left\{ \frac{\partial}{\partial s} \left(\frac{1}{\alpha^2} \frac{\partial \alpha}{\partial s} \right) \right\} \Phi \ .$$

In the same way as was done by Radder, it is assumed here
that the derivatives of α can be neglected. This is justi-
fied by the assumption that the bottom slope is small, which
causes the derivatives of the wave number κ to be small. It
will appear shortly that α is closely related to the wave
number. One finds

$$\alpha^4 \Phi = \left\{ \kappa^2 + \frac{\partial^2}{\partial n^2} \right\} \Phi \ .$$

so that α is a pseudo differential operator:

$$\alpha = \left\{ \kappa^2 + \frac{\partial^2}{\partial n^2} \right\}^{\frac{1}{4}} \ .$$

Now it is possible to use the method announced in the begin-
ning of this section. From (6.2) it follows that

$$\frac{\partial}{\partial s} (\alpha \ \Phi) = i \ \alpha^3 \ \Phi \ .$$ (6.5)

or: $$\frac{\partial}{\partial s} \left(\kappa^2 + \frac{\partial^2}{\partial n^2} \right)^{\frac{1}{4}} \Phi \ = i \left(\kappa^2 + \frac{\partial^2}{\partial n^2} \right)^{\frac{3}{4}} \Phi \ .$$

The pseudo operators arising in the above expression have to be approximated by differential operators. This can be achieved by means of the power series expansion of a non-integer power of (1+z), which reads

$$(1 + z)^{\beta} = 1 + \beta \ z + \beta \ (\beta - 1) \ z^2 + 0 \ (z^3) \ .$$

Since only the first two or three terms of the series will be used, the error is small if z is small. Consequently one must assume that the derivatives with respect to n are much smaller than the wave number. Under this condition the following approximations can be used:

$$\left(\kappa^2 + \frac{\partial^2}{\partial n^2} \right)^{\frac{1}{4}} = \kappa^{\frac{1}{2}} \left(1 + p_1 \ \frac{1}{\kappa^2} \ \frac{\partial^2}{\partial n^2} \right)$$

$$\left(\kappa^2 + \frac{\partial^2}{\partial n^2} \right)^{\frac{3}{4}} = \kappa^{\frac{3}{2}} \left(1 - p_2 \ \frac{1}{\kappa^2} \ \frac{\partial^2}{\partial n^2} \right)$$

The differential equation (6.5) then is approximated by:

$$\frac{\partial}{\partial s} \left(\kappa^{\frac{1}{2}} \ \Phi + p_1 \ \kappa^{-\frac{3}{2}} \ \frac{\partial^2 \Phi}{\partial n^2} \right) = i \ \kappa^{\frac{3}{2}} \ \Phi + i \ p_2 \ \kappa^{-\frac{1}{2}} \ \frac{\partial^2 \Phi}{\partial n^2} \ .$$ (6.6)

This is the parabolic wave model sought after. The values of the coefficients p_1 and p_2 are 1/4 and 3/4 respectively. A different choice for which $p_2 = p_1 + 1/2$, is possible. If Radder's approximation is followed, p_1 vanishes.

The approximations in eq. (6.6) can be carried one step further. Fourth order derivatives with respect to n appear in that case:

$$\frac{\partial}{\partial s} \left\{ \kappa^{\frac{1}{2}} \Phi + \frac{1}{4} \kappa^{-\frac{3}{2}} \frac{\partial^2 \Phi}{\partial n^2} - \frac{3}{16} \kappa^{-\frac{7}{2}} \frac{\partial^4 \Phi}{\partial n^4} \right\} =$$

$$= i \kappa^{\frac{3}{2}} \Phi + \frac{3}{4} i \kappa^{-\frac{1}{2}} \frac{\partial^2 \Phi}{\partial n^2} - \frac{3}{16} i \kappa^{-\frac{5}{2}} \frac{\partial^4 \Phi}{\partial n^4} \quad . \tag{6.7}$$

One of the criteria by which the various approximations can be compared, is how accurately each describes an obliquely incident wave in a field with homogeneous depth. The wave is described by the expression

$$\Phi = \hat{\Phi} \exp (i \mu s + i \nu n) \quad .$$

The parabolic model is in the form of an initial value problem, so the value of ν is determined by the initial condition. The various approximations yield different values for μ . These values will be compared with the exact value which is obviously

$$\mu = (\kappa^2 - \nu^2)^{\frac{1}{2}}$$

Since the depth is constant, the wave number κ is constant too. The coefficients μ and ν are non-dimensionalised by means of κ :

$$\mu' = \mu/\kappa \quad , \qquad \nu' = \nu/\kappa \quad .$$

Radder's approximation yields

$$\mu' = 1 - \frac{1}{2} \nu'^2 \tag{6.8}$$

Eq. (6.6) yields

$$\mu' = \frac{1 - \frac{3}{4} \nu'^2}{1 - \frac{1}{4} \nu'^2} \tag{6.9}$$

The approximation (6.7) with fourth order derivatives yields

$$\mu' = \frac{1 - \frac{3}{4} \nu'^2 - \frac{3}{16} \nu'^4}{1 - \frac{1}{4} \nu'^2 - \frac{3}{16} \nu'^4} \quad . \tag{6.10}$$

The various approximations are assembled in figure 6.1. Hor-

izontally the exact propagation direction is measured, ver-
tically the various approximations. Expression (6.8) is
indicated with the symbol (A), eq. (6.9) with (B), and
(6.10) with (C). All approximations perform well for angles
under 30°. Eq. (6.9) already gives a significant improvement
compared with (6.8), and (6.10) can be used even for very
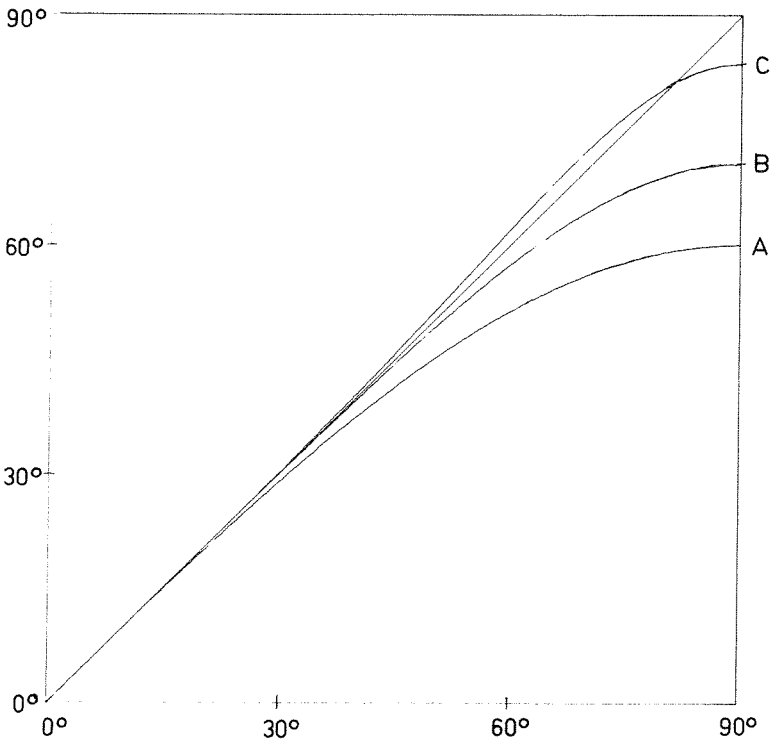large angles between the s-axis and the propagation direc-
tion.

Figure 6.1. Accuracy of various parabolic approximations.
  horizontal axis: $\arcsin(\nu')$
  vertical axis: $\arccos(\mu')$

6.2. Parabolic approximation for refraction-diffraction with current.

The parabolic approximation is based on the equation for time-harmonic wave motion (3.23). For the calculation of the coefficients in this equation two alternatives are presented in Chapter 3. One is used if the direction of propagation is known beforehand, the other (which is less accurate) if this is not so. The situations in which the parabolic approximation can be used, form a compromise between these two extremes. It is known that the waves propagate mainly in s-direction, but locally they can deviate appreciably. The wave number component in s-direction is equal to κ or somewhat less, depending on the direction of the waves. The wave number component in n-direction is completely unknown. Consequently a compromise is used for the calculation of the coefficients:

$$\sigma_o = \omega_o - r_f \kappa U_s \qquad (6.11)$$

r_f is a reduction factor expressing the fact the waves do not exactly follow the s-direction. Its value must be between 0 and 1. In the example discussed later in this chapter, a value of 0.9 is used. This is consistent with the assumption underlying the parabolic approximation, viz. that the waves propagate nearly parallel to the s-direction.

Approximate coefficients can be used if the current velocity is small compared with the propagation velocity. It is therefore realistic, but by no means necessary for the following derivation, to neglect the term with U^2 in eq. (3.23). So there remains:

$$- i\omega_o (\underline{U} \cdot \nabla \tilde{\Phi} + \nabla \cdot (\underline{U} \, \tilde{\Phi})) - \nabla \cdot (a \nabla \tilde{\Phi}) + (\sigma_o^2 - \omega_o^2 - a \kappa^2) \, \tilde{\Phi} = 0 \qquad (6.12)$$

This equation will be reduced to a parabolic form in the same way as discussed in the previous section. It is brought into a form comparable with (6.1). To this end it is written as

$$\frac{\partial}{\partial s} \left(a \frac{\partial \tilde{\Phi}}{\partial s} \right) + 2 i \omega_o U \frac{\partial \tilde{\Phi}}{\partial s} + a \kappa^2 \tilde{\Phi} +$$

$$+ (\omega_o^2 - \sigma_o^2 + i \omega_o \nabla \cdot \underline{U}) \tilde{\Phi} + \frac{\partial}{\partial n} \left(a \frac{\partial \tilde{\Phi}}{\partial n} \right) + 2 i \omega_o V \frac{\partial \tilde{\Phi}}{\partial n} = 0 \quad . \tag{6.13}$$

This is in accordance with (6.1) if the coefficients are proportional. Consider at first the terms in (6.1) and (6.13) which contain second and first order derivatives with respect to s:

$$\frac{\gamma}{\alpha} \cdot \frac{1}{\alpha} \frac{\partial}{\partial s} (\alpha^2/\gamma) = \frac{1}{a} \left(\frac{\partial a}{\partial s} + 2 i \omega_o U \right) \quad . \tag{6.14}$$

This results in

$$\beta \equiv \frac{\alpha^2}{a\gamma} = \exp \left\{ \int 2 i \omega_o U \, ds \right\} \quad . \tag{6.15}$$

Consider now the terms in which the function is not differentiated with respect to s. Again the derivatives of α and γ are neglected.

$$\frac{\gamma}{\alpha} \cdot \alpha \gamma = \kappa^2 + \frac{M}{a} \quad . \tag{6.16}$$

The operator M introduced here is defined by:

$$M \tilde{\Phi} = (\omega_o^2 - \sigma_o^2 + i \omega_o \nabla \cdot \underline{U}) \tilde{\Phi} + \frac{\partial}{\partial n} \left(a \frac{\partial \tilde{\Phi}}{\partial n} \right) + 2 i \omega_o V \frac{\partial \tilde{\Phi}}{\partial n} \quad . \tag{6.17}$$

From (6.15) and (6.16) it follows that

$$\alpha^4 = \beta^2 \{ (a\kappa)^2 + aM \} \quad . \tag{6.18}$$

Now the parabolic model results from eq. (6.2) after devel-

opment of the pseudo operators, under the assumption that

$$|M \, \tilde{\Phi}| \; << \; |\kappa^2 \, \tilde{\Phi}|$$

It reads

$$\frac{\partial}{\partial s} \{ \beta^{\frac{1}{2}} \, ((a\kappa)^{\frac{1}{2}} \, \tilde{\Phi} + \frac{P_1}{a} \, (a\kappa)^{-\frac{1}{2}} \, M \, \tilde{\Phi}) \} \; =$$

$$= \beta^{\frac{1}{2}} \, (i\kappa (a\kappa)^{\frac{1}{2}} \, \tilde{\Phi} + i \, p_2 \, (a\kappa)^{-\frac{1}{2}} \, M \, \tilde{\Phi}) \quad .$$

Using expression (6.15) this becomes

$$\left(\frac{i\,\omega_o\,U}{a} \; + \frac{\partial}{\partial s} \right) \left\{ (a\kappa)^{\frac{1}{2}} \, \tilde{\Phi} + \frac{P_1}{\kappa} \, (a\kappa)^{-\frac{1}{2}} \, M \, \tilde{\Phi} \right\}$$

$$- \, i\kappa (a\kappa)^{\frac{1}{2}} \, \tilde{\Phi} - i \, p_2 \, (a\kappa)^{-\frac{1}{2}} \, M \, \tilde{\Phi} = 0 \quad . \tag{6.19}$$

This is the parabolic approximation to the refraction-diffraction equation with current, that will be used as the basis for a numerical model. This model will be developed in the next section.

It is noted that for a zero current velocity and with the choice $p_1 = 0$, eq. (6.19) reduces to the parabolic model developed by RADDER (1979).

The solution of a parabolic differential equation requires the availability of initial and boundary conditions. The initial values can be derived from the incoming wave field; the conditions along the lateral boundaries are more difficult to establish. Obviously the boundary condition should be such that waves approaching a boundary are not reflected there. Furthermore there is a possibility of waves entering the computational region through a boundary, but it is not possible with this type of model to determine such waves. Thus such waves are ignored.

The expressions that ENGQUIST and MAJDA (1978) used to simu-
late wave absorbing boundary conditions, cannot be applied
in the case at hand, because they considered waves leaving
the computational region in direction approximately normal
to the boundary. In the parabolic method however, it is
assumed that the waves run parallel or nearly parallel to
the s-axis and thereby also nearly parallel to the lateral
boundaries. So the waves approaching the boundary will make
a small angle with it. A simple boundary condition that
also can easily be incorporated into the numerical method
discussed in the next section, is the following:

$$\cos \chi \, \frac{\partial \tilde{\Phi}}{\partial s} + \sin \chi \, \frac{\partial \tilde{\Phi}}{\partial n} = i \kappa \tilde{\Phi} . \tag{6.20}$$

This boundary condition absorbs waves under an angle χ
exactly, and waves in other directions partially. This
boundary condition with a value of 20° for χ, was used in
the computations discussed later in this chapter.

As a result of the fact that the boundary conditions give a
rather poor representation of reality, there will be a zone
along each boundary in which the wave field is disturbed.
The shape of the disturbed zone has been determined by
visual inspection and by varying the place of the boundary.
The zone is found to have roughly the shape of a triangle,
with its vertex on the corner of the computational region,
and a top angle of approximately 10° to 20°. This will
impose a requirement on the choice of the computational
region, because the disturbed zones should be disjunct from
the region of interest.

6.3. A finite difference approximation for the parabolic model.

The final result of the previous section is a partial differential equation of the parabolic type, with first order derivatives with respect to s and second order derivatives with respect to n. The coordinate system is assumed to be Euclidian. The most obvious choice for the discretization is a finite difference approximation using rectangular meshes. The computational molecule will comprise at least one mesh in the s-direction, and at least two meshes in the n-direction, due to the order of the equation.

The equation is in the form of an initial value problem with values for a certain s, say s=0, acting as initial values. These stem from the (given) incoming wave field. A choice exists between explicit and implicit schemes. Implicit schemes are preferred in this application because of their inherent stability, and because the resulting set of equations can be solved in an extremely efficient manner using the Thomas algorithm.

Two implicit schemes are fit for the purpose, viz. the Stone and Brian scheme, and the Crank-Nicholson scheme. A mixture of the two is chosen, and it is investigated which is the most accurate for the type of equation at hand. The selection of the numerical scheme is done in two steps. First the discretization in s-direction is considered, later the one in n-direction.

The equation in its original state only allows steps small compared with the wavelength. In s-direction larger steps can be taken if an unknown function is used which has a smaller s-derivative. This is achieved by incorporating the wave character into the function Φ a priori. To this end

an ansatz of the form

$$\tilde{\Phi} = e^{i \kappa_1 x} \Phi_o$$

is often used. This expression has a disadvantage in that the variations of κ often are so large that the s-derivative of Φ^o still are not small. A little more general expression for $\hat{\Phi}$ enables a better adaptation to the variation of the wave number.

Let $\qquad \tilde{\Phi} = \Phi_1 \, e^{i S(s)}$.

Then

$$\frac{\partial}{\partial s} \{ (a \kappa)^{\frac{1}{2}} \, \tilde{\Phi} + \frac{P_1}{\kappa} \, (a \kappa)^{-\frac{1}{2}} \, M \, \tilde{\Phi} \} =$$

$$= e^{i S} \{ i S' ((a \kappa)^{\frac{1}{2}} \Phi_1 + \frac{P_1}{\kappa} (a \kappa)^{-\frac{1}{2}} M \Phi_1) + \frac{\partial}{\partial s} ((a \kappa)^{\frac{1}{2}} \Phi_1 + \frac{P_1}{\kappa} (a \kappa)^{-\frac{1}{2}} M \Phi_1) \} \ .$$

By resubstitution of the original $\hat{\tilde{\Phi}}$ a computational scheme is arrived at in which a different value for S' can be chosen in every computational molecule. The same terms of the equation for $\hat{\tilde{\Phi}}$ become

$$\frac{\partial}{\partial s} \left\{ (a \kappa)^{\frac{1}{2}} \Phi_1 \, e^{i S} + \frac{P_1}{\kappa} \, (a \kappa)^{-\frac{1}{2}} \, M \, \Phi_1 \, e^{i S} \right\} =$$

$$i S' ((a \kappa)^{\frac{1}{2}} \tilde{\Phi} + \frac{P_1}{\kappa} (a \kappa)^{-\frac{1}{2}} M \tilde{\Phi}) + e^{i S} \frac{\partial}{\partial s} ((a \kappa)^{\frac{1}{2}} \tilde{\Phi} \, e^{-i S} + \frac{P_1}{\kappa} (a \kappa)^{-\frac{1}{2}} M \tilde{\Phi} e^{-i S})$$

For S' a value can be chosen related to the local wave number, such as: $S' = const \ast \kappa$.

It was the purpose of the above manipulation to obtain an equation in which the quantity to be differentiated with respect to s would be slowly varying, at least in s-direction. Now the equation is ready to be discretized with respect to s. The usual central differencing is employed:

$$\frac{\partial p}{\partial s} \to \frac{p^+ - p^-}{\Delta s} \quad , \quad p^+ = p\,(s + \tfrac{1}{2}\Delta s), \quad p^- = p\,(s - \tfrac{1}{2}\Delta s)$$

$$q \to \frac{q^+ + q^-}{2} \quad , \quad q^+ = q\,(s + \tfrac{1}{2}\Delta s), \quad q^- = q\,(s - \tfrac{1}{2}\Delta s)$$

The equation discretized with respect to s then reads:

$$((a\,\kappa)^{\frac{1}{2}}\,\tilde{\Phi})^+ \; e^{-iS'\Delta s} \left\{ \frac{1}{\Delta s} + \frac{iS'}{2} - \frac{i\kappa^+}{2} + \frac{i\,\omega_o\,U}{2a} \right\}^+ +$$

$$+ \; ((a\,\kappa)^{\frac{1}{2}}\,\tilde{\Phi})^- \left\{ -\frac{1}{\Delta s} + \frac{iS'}{2} - \frac{i\kappa^-}{2} + \frac{i\,\omega_o\,U}{2a} \right\}^- +$$

$$+ \; M\,\tilde{\Phi}^+ \; e^{-iS'\Delta s} \left\{ \frac{p_1}{\kappa\Delta s}\,(a\kappa)^{-\frac{1}{2}} + \frac{i\,p_1\,S'}{2\kappa}\,(a\kappa)^{-\frac{1}{2}} \right.$$

$$\left. - \frac{i\,p_2}{2}\,(a\kappa)^{-\frac{1}{2}} + \tfrac{1}{2}\,i\,p_1\,\omega_o\,U\,(a\kappa)^{-\frac{3}{2}} \right\}^+ +$$

$$+ \; M\,\tilde{\Phi}^- \left\{ -\frac{p_1}{\kappa\Delta s}\,(a\kappa)^{-\frac{1}{2}} + \frac{i\,p_1\,S'}{2\kappa}\,(a\kappa)^{-\frac{1}{2}} - \frac{i\,p_2}{2}\,(a\kappa)^{-\frac{1}{2}} + \tfrac{1}{2}\,i\,p_1\,\omega_o\,U\,(a\kappa)^{-\frac{3}{2}} \right\}^-$$

$$= 0 \quad .$$

The discretization with respect to n is done such that only 3 nodes in that direction are needed. The Stone and Brian scheme and the Crank-Nicholson scheme differ only in the representation of the zero order terms in n. Both schemes will represent a term

$$\frac{\partial}{\partial n} \left(a\,\frac{\partial \tilde{\Phi}}{\partial n} \right)$$

by $\quad \{ (a_2 + a_3)(\tilde{\Phi}_3 - \tilde{\Phi}_1) - (a_1 + a_2)(\tilde{\Phi}_2 - \tilde{\Phi}_1) \} \,/\, (2\,\Delta n^2) \quad .$

Here: $\quad \tilde{\Phi}_1 = (n - \Delta n) \;,\; \tilde{\Phi}_2 = \tilde{\Phi}\,(n) \;,\; \tilde{\Phi}_3 = \tilde{\Phi}\,(n + \Delta n) \quad .$

A term with a first order derivative will be represented as

$$(\tilde{\Phi}_3 - \tilde{\Phi}_1) \,/\, (2\,\Delta n) \quad .$$

A zero order term such as Φ will be represented by the Crank-Nicholson scheme as: Φ_2.

The Stone and Brian scheme represents the same term by:

$$\frac{1}{6} \tilde{\Phi}_1 + \frac{2}{3} \tilde{\Phi}_2 + \frac{1}{6} \tilde{\Phi}_3 \quad .$$

The compromise scheme contains an as yet unknown parameter r:

$$r \tilde{\Phi}_1 + (1 - 2r) \tilde{\Phi}_2 + r \tilde{\Phi}_3 \quad .$$

The influence of the parameter r on the accuracy is investigated not by means of the full equation (6.7), but a reduced equation containing only the main terms, also taking into account the ansatz introduced above. Naturally this reduced equation is the Schrödinger equation:

$$\frac{\partial \tilde{\Phi}}{\partial s} = \frac{i}{2\kappa} \frac{\partial^2 \tilde{\Phi}}{\partial n^2} \quad . \tag{6.21}$$

The numerical model for this equation would be:

$$\frac{1}{\Delta s} \{ r \tilde{\Phi}_1^+ + (1 - 2r) \tilde{\Phi}_2^+ + r \tilde{\Phi}_3^+ - r \tilde{\Phi}_1^- - (1 - 2r) \tilde{\Phi}_2^- - r \tilde{\Phi}_3^- \} =$$

$$= \frac{i}{4\kappa \Delta n^2} \quad \tilde{\Phi}_1^+ - 2 \tilde{\Phi}_2^+ + \tilde{\Phi}_3^+ + \tilde{\Phi}_1^- - 2 \tilde{\Phi}_2^- + \tilde{\Phi}_3^- \} \quad .$$

Δs and Δn are the mesh sizes in s- and n-direction respectively. The accuracy will be studied by means of the function:

$$\tilde{\Phi} = \exp(i\mu s + i\nu n) = \rho^{s/\Delta s} \sigma^{n/\Delta n} \tag{6.22}$$

If μ and ν are real numbers, this function represents a wave-like solution. Note that

$$\rho = \exp(i\mu \Delta s), \qquad \sigma = \exp(i\nu \Delta n) \quad .$$

ρ is known as the propagation factor. Its value is used as the criterion for the accuracy. The values of either ν or σ are assumed to be known, due to the initial conditions.

Substituting eq. (6.22) into the numerical model, one obtains an expression from which ρ can be calculated.

$$\frac{\rho - 1}{\Delta s} \left\{ \frac{r}{\sigma} + (1 - 2r) + r\sigma \right\} = \frac{i}{2\kappa} \frac{\rho + 1}{2} \frac{1}{\Delta n^2} \left(\frac{1}{\sigma} - 2 + \sigma \right) \quad .$$

Let $\qquad \beta = \sigma^{\frac{1}{2}} - \sigma^{-\frac{1}{2}} = 2 i \sin \left(\frac{1}{2} \nu \Delta n \right) \quad .$

Then $\qquad 2 \frac{\rho - 1}{\rho + 1} = \frac{i \Delta s}{2 \kappa \Delta n^2} \frac{\beta^2}{1 + r \beta^2} ,$

or $\qquad 2 \tan \left(\frac{1}{2} \mu \Delta s \right) = - \frac{1}{2} \cdot \frac{\Delta s}{\kappa \Delta n^2} \cdot \frac{\left(2 \sin \left(\frac{1}{2} \nu \Delta n \right) \right)^2}{1 - r. \left(2 \sin \left(\frac{1}{2} \nu \Delta n \right) \right)^2} \quad .$

From the fact that the right hand side of this equation is real valued it is seen that a real value for μ will be found. This means that the numerical model is unconditionally stable, and that the wave amplitude is conserved, i.e. there is no numerical damping. Thus the criterion for the accuracy must rely on the propagation of the wave. This question is investigated by developing both sides in powers of μ and ν :

$$\mu + \frac{1}{12} \mu^3 \Delta s^2 + 0(\Delta s^4) =$$

$$= - \frac{1}{2} \nu^2 / \kappa + \nu^4 \left(\frac{1}{12} - r \right) \Delta n^2 / \kappa + 0 \, (\Delta n^4) \quad .$$

Since $\qquad \mu = - \frac{1}{2} \nu^2 / \kappa + 0 \, (\Delta s^2, \Delta n^2) \quad ,$

this is equal to

$$\mu = - \frac{1}{2} \frac{\nu^2}{\kappa} + \frac{\nu^4}{2\kappa} \left(\frac{1}{12} - r \right) \Delta n^2 + \frac{1}{96} \frac{\nu^6}{\kappa^3} \Delta s^2 + 0 \, (\Delta s^4, \Delta n^4) \quad .$$

This is close to the exact value μ_0 resulting from the Schrödinger equation:

$$\mu_0 = - \frac{1}{2} \frac{\nu^2}{\kappa} \quad .$$

The value of r that makes the term with Δn^2 disappear, is
r=1/12. A term with Δs^2 remains. It may be assumed that
the mesh sizes are of the same order of magnitude. It is in
accordance with the parabolic approximation to assume that
$\nu \ll \kappa$. Since moreover the coefficient 1/96 appearing
before this term is a small number, the term with Δs^2 will
in fact be quite small. Thus, although with r =1/12 the
scheme is theoretically still of second order, the error
involved is relatively small.

6.4. Some additional physical effects.

The wave propagation model developed in Chapter 3 entails the main effects in the phenomenon, viz. the influence of bottom and current on the direction of propagation. Many effects are not yet taken into account, such as: dissipation due to bottom friction, wave breaking, growth of the waves due to wind, influence of the wave amplitude on the propagation velocity. Most of these effects introduce mild non-linearity.

Growth of the waves due to wind is an effect which is fundamentally hard to build into the model, because the wind generates waves of many frequencies and many directions, not just the frequency and direction of the wave under consideration. However the generation of waves requires long distances, and in coastal regions the generation is a minor effect compared with the dissipation. It is therefore not considered in the sequel.

Wave breaking naturally is an important phenomenon in coastal regions, obviously near the beaches, but also on shallows that may exist in such regions. It is important that this effect is taken into account, because without it wave heights would tend to infinity near the beach. This would make the result unacceptable to engineers using the model. There are two ways to introduce breaking. One is to limit the wave amplitudes; once a wave height has been calculated it is checked against the local breaker height. If it surpasses this breaker height, it is reduced to that value. The other way is to recognize that wave breaking is a mechanism, which causes energy dissipation. BATTJES (1978) shows how this dissipation can be modeled for periodic waves, BATTJES and JANSSEN (1978) show the same for irregular waves. The latter is important if the wave field that

is computed, is thought to be representative for a whole spectrum of waves, or perhaps part of such a spectrum.

SKOVGAARD, JONSSON and BERTELSEN (1975) present a model for the dissipation due to bottom friction. It remains to show how energy dissipation can be introduced into the wave propagation equation.

It is well known that in the shallow water equation:

$$\frac{\partial^2 \Phi}{\partial t^2} - \nabla . (gh \nabla \Phi) = 0 \quad ,$$

the energy dissipation due to bottom friction is modeled by adding a term

$$w \frac{\partial \Phi}{\partial t} \quad .$$

Due to the great similarity of eq. (3.21) and the above equation, it is reasonable to suppose that the same would work for eq. (3.21). In the case of eq. (6.12), which is for purely periodic waves, one would add $i\omega_o w\tilde{\Phi}$.

This wave equation then reads

$$i\,\omega_o\,(\underline{U}.\nabla\tilde{\Phi} + \nabla.(\underline{U}\,\tilde{\Phi})) - \nabla.(a\nabla\tilde{\Phi}) + (\sigma_o^{\,2} - \omega_o^{\,2} - a\kappa^2)\,\tilde{\Phi} + i\,\omega_o\,w\,\tilde{\Phi} = 0 \quad .$$

A conservation law for the wave action density can immediately be found from this equation by considering the product of the differential equation and the complex conjugate of $\tilde{\Phi}$, denoted by $\tilde{\Phi}^x$. If the imaginary part of this product is taken, the conservation principle immediately results.

If $\qquad \tilde{\Phi} = \hat{\Phi}\,e^{iS}$

then $\qquad \mathrm{Im}\,(\frac{1}{\tilde{\Phi}}\nabla\tilde{\Phi}) = \nabla S$

So

$$\text{Im} \left[\tilde{\Phi}^* \{ i\omega_o (\underline{U}.\nabla\tilde{\Phi} + \nabla.(\underline{U}\,\tilde{\Phi})) - \nabla.(a\nabla\tilde{\Phi}) + (\sigma_o^2 - \omega_o^2 - a\kappa^2) + i\omega_o w\,\tilde{\Phi} \} \right] =$$

$$= \nabla.\{ a\,\hat{\Phi}^2\,\nabla S + \omega_o\,\underline{U}\,\tilde{\Phi}^2 \} + \omega_o\,w\,\tilde{\Phi}^2 =$$

$$= \nabla.\{ c_g\,E/\omega_o + \underline{U}\,E/\omega_o \} + w\,E/\omega_o = 0 \ .$$

or $\qquad \nabla.\{ (c_g + \underline{U})\,E \} = -\,w\,E \quad .$

This shows that the divergence of the energy transport does not vanish. The term wE is the energy dissipation per unit surface and per unit of time, so that the added term has indeed the effect aimed at.

In the parabolic approximation the addition of the dissipation term leads to the addition of the following terms to eq. (6.19)

$$\left(\frac{i\omega_o U}{a} + \frac{\partial}{\partial s} \right) p_1 \frac{i\omega_o w}{\kappa(a\kappa)^{\frac{1}{2}}} \cdot \tilde{\Phi} + p_2 \frac{\omega_o w}{(a\kappa)^{\frac{1}{2}}} \tilde{\Phi} \quad .$$

The coefficient w used in the model is the sum of a dissipation coefficient due to breaking and one due to bottom friction. Both contributions can be derived from the papers referred to in the beginning of this section.

It was shown by WALKER (1976) that the influence of the wave amplitude on the propagation velocity can have an important effect on the concentration of waves on a shoal. The fact that this addition to the model brings in non-linearity, is not harmful to the numerical process, because the equations can be locally linearized. Walker shows that the concentration of waves on a shoal is diminished since higher waves have a greater propagation velocity. He advises a formula for the propagation velocity that is derived from the one in

the linear model by multiplication with a factor depending on the local wave height:

$$c = (1 + \frac{H}{4h}) \, c_a \quad ,$$

where c_a is the propagation velocity that follows from the linear model. The above is equivalent to calculating the wave number κ from the following equation:

$$\sigma_o^{\,2} = g\kappa \, (1 + \frac{H}{4h}) \, \tanh\{\kappa(h + \tfrac{1}{4}H)\} \tag{6.23}$$

HEDGES (1976) arrives at a slightly different formula by a comparison with cnoidal waves:

$$\sigma_o^{\,2} = g\kappa \, \tanh\{\kappa(h + Z)\} \tag{6.24}$$

The paramater Z can still be chosen. Hedges proposes Z=H. The argument for this choice is not strong, because the wave height of a sinusoidal wave is simply equated to the wave height of a cnoidal wave. Walker on the other hand supports his choice with measurements, so that it may be assumed that the overall effect is represented correctly. His experiment however pertained only to waves in relatively shallow water. In shallow water his formula is nearly identical with the one by Hedges if for Z the half of the wave height is chosen. For deeper water Hedges' formula is presumably better; although it overestimates the difference between the linear and the nonlinear model (HEDGES, 1976), Walker's formula does even more so. It is for this reason that eq. (6.24) is used for this nonlinear effect, in combination with Z=H/2.

It can be seen that for deep water both these formulae do not agree with the dispersion relations for the second order Stokes wave on deep water (see e.g. YUEN and LAKE, 1975). This is not important for the present research since it is concerned with waves in shallow regions near the coast. It

would be very useful if an easy-to-handle relation for restricted depth could be developed based on second (or higher) order Stokes theory.

6.5. Alternative model based on complex phase function

The result of the foregoing section is a partial differential equation of parabolic type, which is to be solved numerically. With the parabolic approximation a numerical solution has become feasible, but the computational effort is still considerable. For instance the entrance to the Oosterschelde estuary (figure 6.2) would require a computational grid of 24 km times 24 km, leading to at least 2000 times 3000 grid points. The computational effort can be reduced again if the complex phase is used as the unknown quantity, as was done by RADDER (1979). This function is related to the wave potential by:

$$\tilde{\Phi} = \exp{(\Gamma)} = \exp{(\Gamma_1 + i\,\Gamma_2)} \tag{6.25}$$

Γ_1 is the usual phase function and Γ_2 is related to the amplitude. The calculation can be carried out with larger meshes since the function Γ is essentially smoother than Φ which oscillates rapidly. In the absence of crossing waves the gradient of Γ varies over the same distance as the medium does, whereas Φ varies with the wavelength.

The equation for Γ is based on eq. (6.19) with $p_1 = 0$ and $p_2 = 1/2$, the coefficients as used by RADDER (1979). After some calculations which are not reproduced here, it appears to be:

$$\frac{\partial}{\partial s}\left(\Gamma + \tfrac{1}{2}\log{(a\kappa)}\right) - \tfrac{1}{2}\frac{i}{a\kappa}\left\{\frac{\partial}{\partial n}\left(a\frac{\partial\Gamma}{\partial n}\right) + a\left(\frac{\partial\Gamma}{\partial n}\right)^2\right\} +$$

$$+ \frac{i\,\omega_o U}{a} + \frac{\omega_o V}{a}\frac{\partial\Gamma}{\partial n} - i\kappa - \tfrac{1}{2}i\,\frac{\omega_o^2 - \sigma_o^2 + i\,\omega_o\,\nabla.\underline{U}}{a\kappa} = 0 \quad . \tag{6.26}$$

Now the same region can be covered by a grid consisting of 1000 times 1500 grid points.

The transition from the wave potential to the complex phase function has not only advantages. The latter leads to a nonlinear model in which instabilities may develop. Such instabilities are damped by adding a numerical diffusion term to the model, thereby reducing its accuracy. Details are found in RADDER (1979).

6.6. Example of a practical application

The parabolic model using the complex phase was applied to the entrance of the Oosterschelde estuary in the Southwest of the Netherlands, where extensive coastal defense works are undertaken. This region is chosen, because the necessary data were relatively easily accessible. The region is moreover representative for practical problems in coastal engineering. The computations can show whether results of practical importance can be obtained. Furthermore the influence of a current can be computed in physically realistic circumstances.

The necessary current data were provided by the WAQUA model, a two-dimensional tidal computations program (see LANGERAK et al., 1978). The same bottom data that were used as input to this program, served for the parabolic wave computation. The bottom contours are displayed in figure 6.2 and the current vectors in figure 6.3. A typical velocity in the entrance region is 0.70 m/s, leading to a value for U/c of about 0.08. Figure 6.2 also shows the contour of the computational grid as a dashed line. The size of the computational region is 24 km by 24 km. Further data were: wave period 8 s, incident amplitude 0.8 m, direction of the incoming waves under an angle of 20 with the x-axis of the bottom grid, or between West and Northwest. The s-axis of the computational grid was chosen parallel to the direction of the incident waves.

Two computations were performed, one taking the current influence into account, the other without current. Results are shown not for the entire region, but for a subregion of the computational grid, also indicated by a dashed line in figure 6.2. For comparison the results of the refraction model (without current) are shown in figure 6.4. The fol-

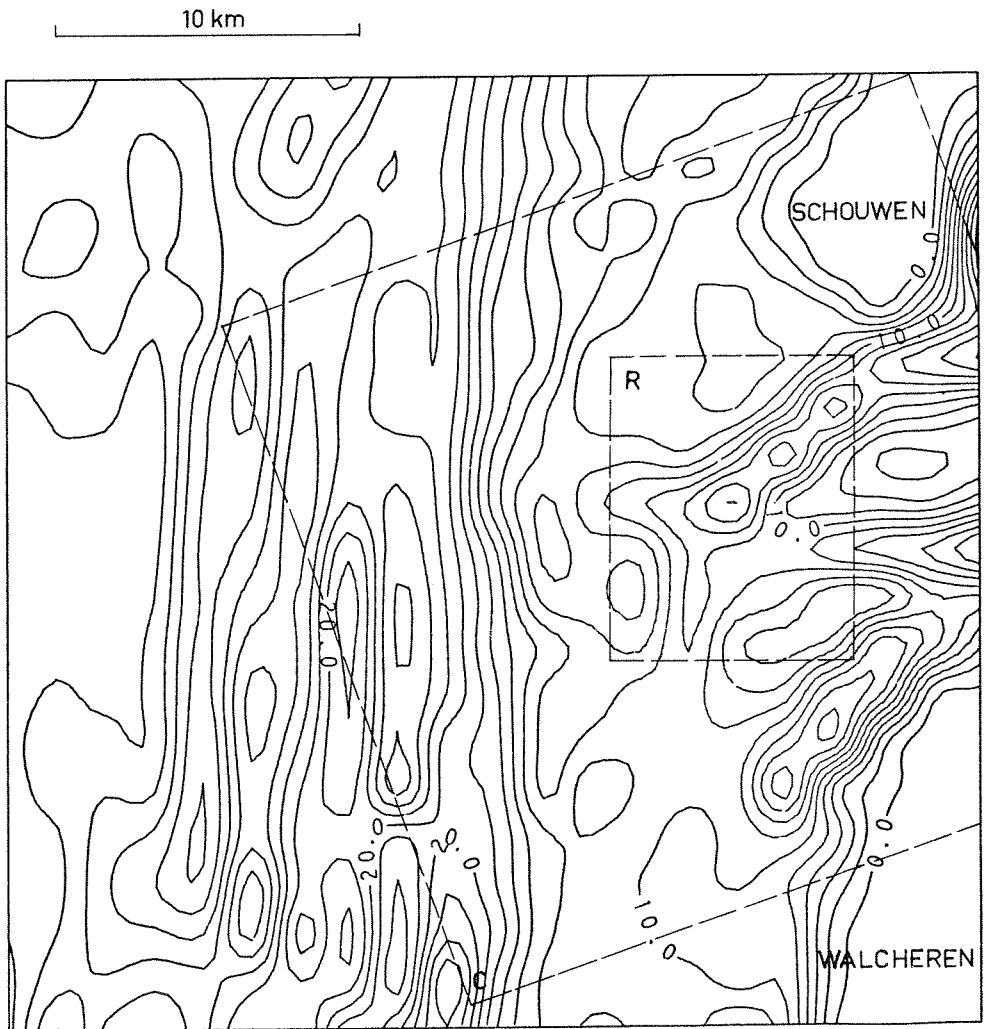Figure 6.2. Bottom map of the region in the Oosterschelde
estuary, showing also the circumference of the
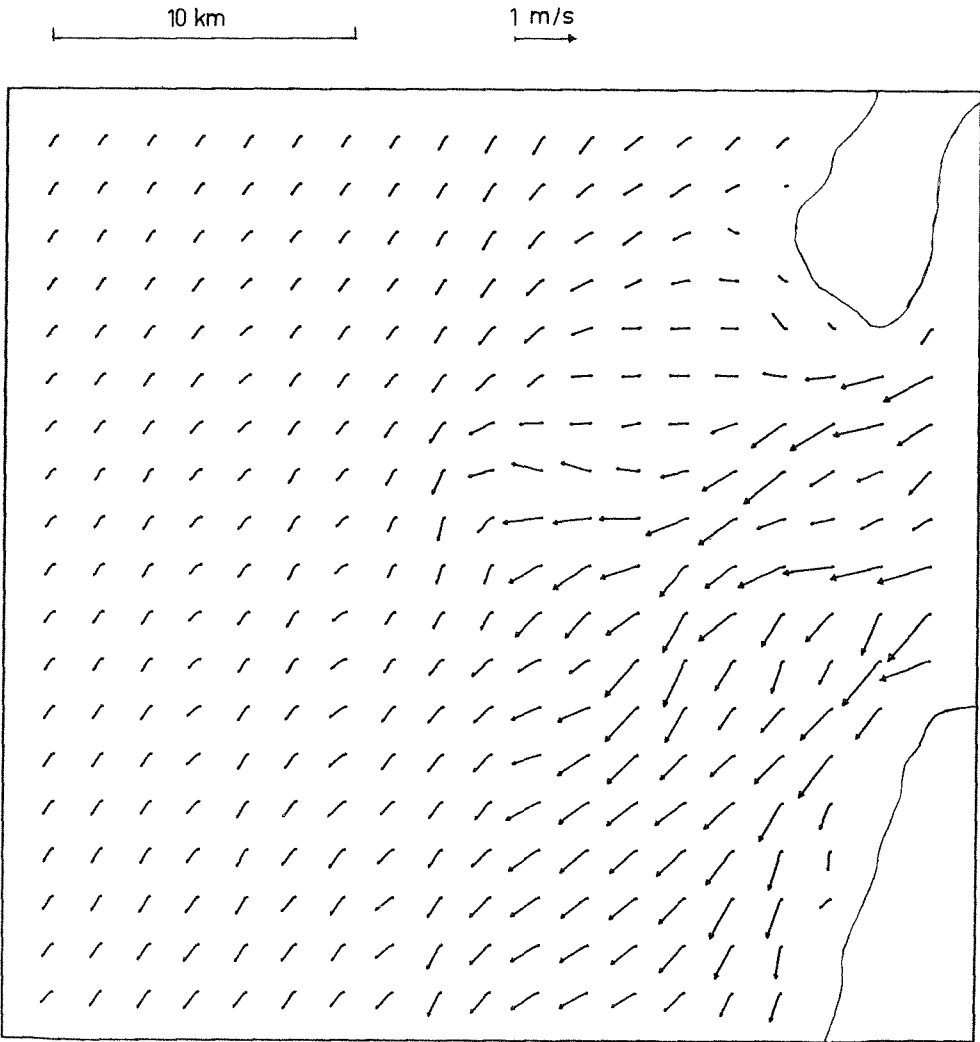computational grid (C), and the output rectangle
(R).

Figure 6.3. Current vectors in the region shown in figure
6.2 (ebb flow)

lowing figures give results of the refraction-diffraction
model. Figures 6.5 and 6.6 show the lines of constant wave
amplitude, 6.6 for the computation with current, and 6.5

without. This computation was carried out by means of the
alternative model using the complex phase function. Figures
6.7 and 6.8 show the lines of constant phase resulting from
the same two computations. The graphs indicate that the
current does not have a spectacular influence. Locally
there may be some deviation but the overall patterns are
much alike. This holds for amplitudes as well as wave
directions. It is noted that U/c is approximately 0.08, a
small value, but probably representative for estuaries with
a sandy bottom.

The current-free parabolic model by RADDER (1979) has been
applied to the same region. VRIJLING and BRUINSMA (1980)
report that its results are in good agreement with observa-
tions. Radder's model produces the same results as the
model presented in this thesis, if no current is assumed in
the latter. It can therefore be concluded that in the case
of a zero current the model agrees with observations.
Vrijling and Bruinsma also show how the wave height in a
point in the estuary depends on the tidal level. The direc-
tion of the tidal flow is also of interest, mainly because
it influences the amount of breaking on the shallows in
front of the point under consideration. The difference in
wave height between ebb and flood situations reported by
Vrijling and Bruinsma is larger than is found in the mathe-
matical model. However the incoming wave height assumed in
the example (0.8 m) is much less than the incident wave
height in the rough-wheather conditions considered by
Vrijling and Bruinsma, so that the amount of breaking is
much smaller too. A better agreement may be expected if the
same wave height is used in the mathematical model.
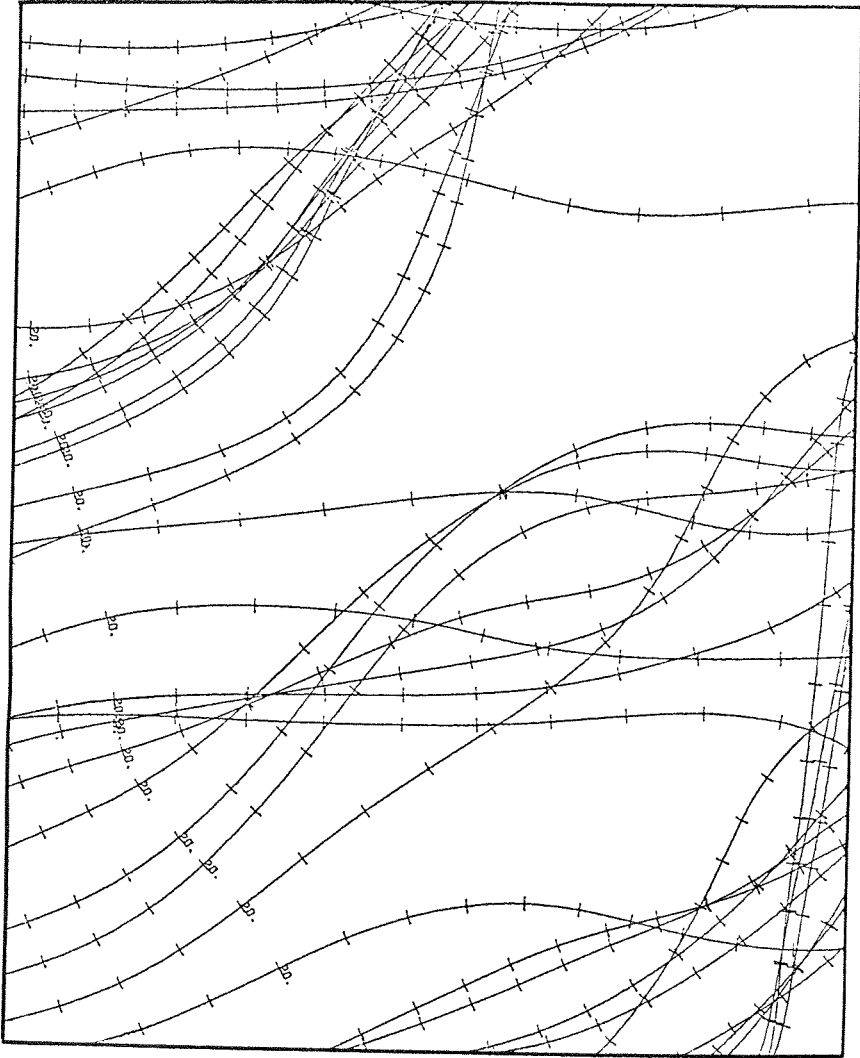
Figure 6.4. Ray pattern in output rectangle R (see figure
6.2). No current influence.

Figure 6.5. Amplitude contours, computed with complex phase
function, in region R. No current influence.

Figure 6.6. Amplitude contours, computed with complex phase
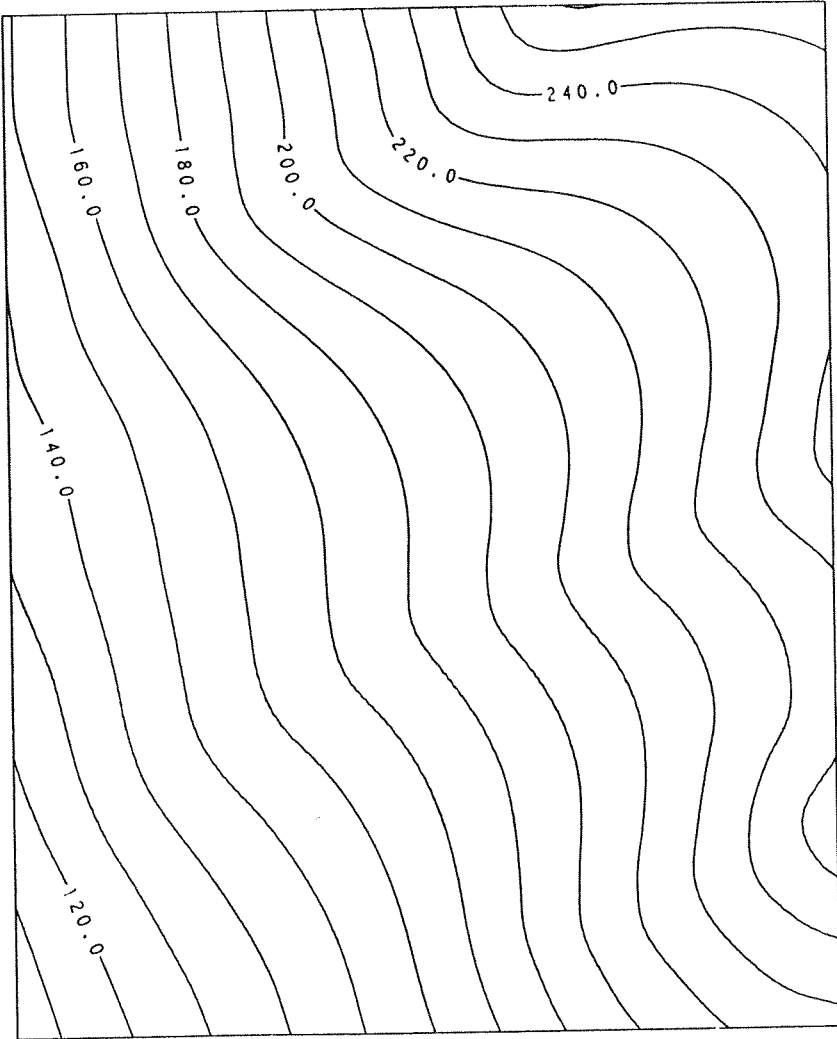function, in region R. Current field assumed as
shown in figure 6.3.

Figure 6.7. Phase contours, computed with complex phase function, in region R. No current influence.
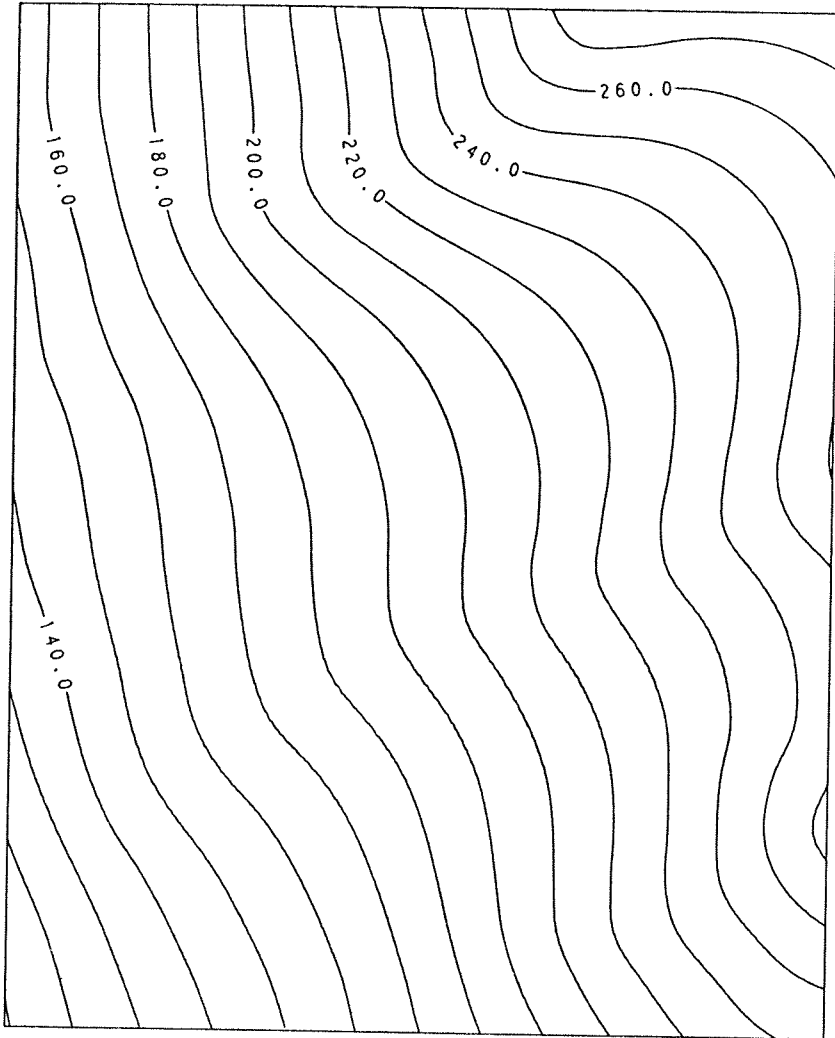
Figure 6.8. Phase contours, computed with complex phase function, in region R. Current field assumed as shown in figure 6.3.

CHAPTER 7. CONCLUSIONS

An equation for combined refraction and diffraction in
regions with variable depth and current is developed.
Strictly speaking, the derivation is only valid for current
fields with zero rotation. From a practical point of view,
the use of the equation for current fields occurring in
reality is allowed. Rotation in the vertical plane is res-
tricted to a thin layer near the bottom, which has little
influence on the wave propagation. It is justified to allow
rotation in the horizontal plane by a comparison with the
refraction model, which is also frequently used for regions
with a rotational current. The agreement between both
models regards the dispersion as well as the conservation
equation.

If one is about to apply the refraction-diffraction model to
areas very large compared with the wavelength, such as occur
in coastal engineering, the only feasible method is through
the use of a parabolic approximation. Such an approximation
is developed and compared with an existing parabolic model
for the current-free case. Dissipation terms are added to
the model to bring it closer to physical reality.

An alternative version of the parabolic model uses the
logarithm of the wave potential as the unknown function.
This allows for larger meshes, at the expense of giving an
incorrect picture of what happens at the downwave side of a
wave crossing.

Both versions of the parabolic model are such that a 6-point
numerical scheme can be employed. This allows a very effi-
cient solution algorithm. The results of the computations
are in the form of plots of iso-amplitude contours and iso-
phase contours. In an example shown the current was found

to have only a small influence on the overall pattern of
these contours. It remains useful to check this for any new
problem for which the model is to be applied.

The full equation, i.e. without resorting to a parabolic
approximation, is applied to some situations in which the
wave field is independent of one of the horizontal coordi-
nates. Such a reduced model can be used to study subjects
like reflection due to an undersea slope, wave propagation
in a wave channel, and wave propagation in a gully with
lateral energy loss.

Partial reflection of waves travelling obliquely accross an
undersea slope is one of the reasons why one might refrain
from using the refraction method. This method predicts
either full reflection or no reflection at all, whereas the
refraction-diffraction equation can also predict partial
reflection. However, it turns out that the range of angles
of incidence for which the reflection coefficient is above,
say, 0.05 and under 0.95, is limited to only a few degrees,
so that the refraction method is reasonably accurate in this
respect.

Waves incident in a direction normal to a slope can also be
reflected partially if the slope is steep enough. According
to the refraction-diffraction equation the reflection is
under 0.05 if the steepness is lower than 0.10. In practice
one will seldom meet bottom slopes steeper than 0.10, so
that this again is a justification for the use of the
refraction method. It also justifies the use of the para-
bolic method, since it assumes that the reflections counter
to the computational direction are negligible.

It can be questioned however whether the mild-slope equation
itself may be used at all for slopes steeper than 0.1, since
the bottom slope was assumed to be small in deriving the

equation. Therefore a comparison with a three-dimensional computation for the same case was made, leading to the conclusion that the mild-slope equation is accurate for slopes with a steepness lower than 0.2. Unlike the refraction method it gives results which are in the right order of magnitude for an inclination in the neighbourhood of 1.

The case of propagation parallel to the depth contours is treated separately. This is done because the equations now lead to an eigenvalue problem. Solutions are presented pertaining to a prismatic wave channel bounded by reflecting side-walls. The waves propagate in axial direction in this set of examples. In this case the eigenvalue is real, which means that the waves do not lose energy as they propagate.

The comparison of the vertically integrated refraction-diffraction equation with the three-dimensional model is made for waves perpendicular to the depth contours, and for waves parallel to these contours. The first case is discussed above. For the other case the prismatic wave channel is used. This time the vertically integrated model proves to be accurate for a bottom inclination up to the order of 1.

A second case of propagation parallel to depth contours is formed by a gully bounded by shallows on each side. The eigenvalue is now complex, which means that the waves are damped in axial direction. This damping is due to the transfer of wave energy from the gully to the shallows. Laboratory measurements were available for such a configuration. The decay of wave energy in the gully that is caused by the energy transfer, is reproduced well by the refraction-diffraction model. The shape of the wave fronts in the gully was reproduced less well, but it seems that these measurements were subject to a large uncertainty.

In conclusion it can be said that the parabolic approxima-

tion of the refraction-diffraction equation is a feasible tool for the prediction of waves in regions up to a few hundreds of wavelengths in size. For larger regions the refraction method is still indispensable.

In ordinary use the refraction-diffraction model is much more expensive than the refraction model. Then why would one use the refraction-diffraction model at all? The possibility of partial reflection can hardly be a reason as was explained above. The most important reason, illustrated by figure 6.4, is that the rays tend to occur in bundles, leaving large areas which are hardly covered by rays. According to the refraction-diffraction equation, and according to experience there may still be an appreciable wave height in such areas.

A drawback of both the refraction and the refraction-diffraction models is that they are in principle deterministic models. They compute one wave frequency at a time, whereas a real wave field is described by means of a continuous spectrum. Sometimes it is sufficient to know an estimate of the peak of the spectrum at the coast line or elsewhere in the computational region. Then a simple approach can be used. It consists of a computation of the propagation of the wave which has the frequency and direction of the peak of the spectrum of the waves incident from the sea. If this approximation is too crude, one should perform a set of computations with different wave periods and angles of incidence. An estimate of the spectrum is obtained from a superposition of the waves computed at the point(s) of interest. In view of the smoother wave field resulting from the refraction-diffraction model than from the refraction model, probably fewer combinations of incident wave frequency and direction need to be considered when using the refraction-diffraction model.

REFERENCES

ABBOTT, M.B., H.M. PETERSEN and O. SKOVGAARD (1978), On the numerical modelling of short waves in shallow water. J. Hydr. Res., vol.16, pp.173-204.

ANDREWS, D.G. and M.E. McINTYRE (1978a) An exact theory of nonlinear waves on a Lagrangian mean flow. J. Fluid Mech., vol.89, no.4, pp.609-646.

ANDREWS, D.G. and M.E. McINTYRE (1978b) On wave action and its relatives. J. Fluid Mech., vol.89, no.4, pp.647-664.

BATEMAN, H. (1944), Partial Differential Equations. publ: Cambridge Univ. Press.

BATTJES, J.A. (1978) Energy dissipation in breaking solitary and periodic waves, Manuscript, Delft Univ. Techn.

BATTJES, J.A. and J.P.F.M. JANSSEN (1978) Energy loss and set-up due to breaking of random waves, Proc. 16th Int. Conf. on Coastal Engng., held Sept. 1978 in Hamburg, Germany, vol.I, pp. 569-587 publ. ASCE, New York 1979

BERKHOFF, J.C.W. (1972) Computation of combined refraction-diffraction. Proc. 13th Int. Conf. on Coastal Engng. held July 1972 at Vancouver, Canada. publ.ASCE, New York 1973

BERKHOFF, J.C.W. (1976) Mathematical models for simple harmonic linear water waves, report on mathematical investigation.
Delft Hydr. Lab., Report W 154-IV

BETTESS, P. and O.C. ZIENKIEWICZ (1977) Diffraction and refraction of surface waves using finite and infinite elements.
Int. J. Num. Meth. Engng., vol.11, pp.1271-1290

BRETHERTON, F.P. and C.J.R. GARRETT (1969) Wavetrains in inhomogeneous moving media.
Proc. Roy.Soc., A, vol.302, pp. 529-554

CAVALERI, L. and P. MALANOTTE RIZZOLI (1977), A wind waves prediction model in the Adriatic Sea.
Proc. NATO Conf. on Turbulent Fluxes through the Sea Surface, Wave Dynamics, and Prediction; Sept. 1977, Marseille, France.
NATO Conf. Series: V, Air-Sea Interactions, Vol.1, pp.629-646.
publ: Plenum Press, New York 1978.

CONNOR, J.J. and C.A. BREBBIA (1977) Finite Element Techniques for Fluid Flow.
publ: Newnes-Butterworths, London.

DE HAAN, R.H.E. (1980) Wave directions research in the entrance of the Oosterschelde in behalf of the design of the storm surge barrier.
Rijkswaterstaat, Deltadienst, report DDWT-80.015 (in Dutch)

ENGQUIST, B. and A. MAJDA (1977), Absorbing boundary condi-
   tions for the numerical solution of waves.
   Math. Comp., vol.31, pp.629-651.

FINLAYSON, B.A. (1972) The method of weighted residuals and
   variational principles.
   publ: Ac. Press, New York, London.

HAYES, W.D. (1970), Conservation of action and modal wave
   action.
   Proc. Roy. Soc., A, vol.320, pp.187-208.

HEDGES, T.S. (1976) An empirical modification to linear wave
   theory.
   Proc. Instn. Civ. Engrs., vol.61, part 2, 1976,
   pp.575-579.

HUITENGA, I.J. and G.B. VAN DRIEL (1974), Lateral Energy
   Losses of Waves in a Gully.
   Delft Univ. Techn. (Master's thesis, in Dutch)

ITO, Y. and K. TANIMOTO (1972) A method of numerical analy-
   sis of wave propagation - application to wave diffraction
   and refraction.
   Proc. 13th Int. Conf. on Coastal Engng. held July 1972 at
   Vancouver, Canada.
   publ: ASCE, New York 1973

JONSSON, I.G., O. BRINK-KJAER and G.P. THOMAS (1978), Wave-
   action and set-down for waves on a shear current.
   J. Fluid Mech., vol.87, no.3, pp.401-416.

JONSSON, I.G. and O. SKOVGAARD (1979), A mild-slope wave
   equation and its application to tsunami calculations.
   Marine Geodesy, vol.2, no.1, pp.41-58.

LANDAU, L.D. and E.M. LIFSHITZ (1975), The classical theory
   of fields.
   4th English edition, Pergamon Press.

LANGERAK, A., M.A.M. DE RAS and J.J. LEENDERTSE (1978)
   Adjustment and Verification of the Randdelta II Model.
   Proc. 16th Int. Conf. on Coastal Engng., held Sept. 1978
   in Hamburg, Germany, vol.I, pp. 1049-1070
   publ: ASCE, New York 1979

LOZANO, C. and R.E. MEYER (1976) Leakage and response of
   waves trapped by round islands.
   Phys. of Fluids, vol.19, no.8, August 1976, pp.1075-1088.

LUKE, J.C. (1967) A variational principle for a fluid with a
   free surface.
   J. Fluid Mech. vol.27, no.2, pp.395-397

MIKHLIN, S.G. (1964) Variational Methods in Mathematical
   Physics.
   New York.

PEREGRINE, D.H. (1976) Interaction of water waves and cur-
   rents.
   Advances in Appl. Mech, vol.16

PEREGRINE, D.H. and G.P. THOMAS (1976), Finite-amplitude
   waves on non-uniform currents,
   in: Waves on water of variable depth, ed. by D.G.Provis
   and R.Radok. Proc. IUTAM symp. July 1976, Canberra,
   pp.145-153.
   publ: Springer Verlag, Berlin.

RADDER, A.C. (1979) On the parabolic equation method for
   water wave propagation.
   J. Fluid Mech. vol.95, no.1, pp.159-176

SCHONFELD, J.C. (1972) Propagation of two-dimensional waves.
    Delft Univ. Techn. (manuscript, in Dutch)

SKOVGAARD, O., I.G. JONSSON and J.A. BERTELSEN (1975), Com-
    putation of wave heights due to refraction and friction.
    J. Waterways, Harbours and Coastal Engng. Div., A.S.C.E.,
    vol.101, no.WW1, pp.15-32

STIASSNIE, M. and G. DAGAN (1979) Partial reflexion of water
    waves by non-uniform adverse currents.
    J. Fluid Mech., vol.92, no.1, pp.119-129.

STOKER, J.J. (1966) Water waves.
    publ: Interscience, New York.

SVENDSEN, I.A. (1967) The wave equation for gravity waves in
    water of gradually varying depth.
    Coastal Engng. Lab. and Hydraulics Lab., Tech. Univ. Den-
    mark, Progress Rep. no.15, pp.2-7.

VRIJLING, J. K. and J. BRUINSMA (1980), Hydraulic boundary
    conditions.
    in: Hydraulic Aspects of Coastal Structures (ed. A.
    Paape, J. Stuip and W. A. Venis)
    publ: Delft Univ. Press, 1980.

WALKER, J.R. (1976) Refraction of finite-height and breaking
    waves.
    Proc. 15th Int. Conf. on Coastal Engng., held July 1976
    at Honolulu, Hawaii.
    publ: A.S.C.E., New York 1977.

WHITHAM, G.B. (1965) A general approach to linear and nonli-
    near dispersive waves using a Lagrangian.
    J. Fluid Mech., vol.22, no.2, pp.273-284.

WHITHAM, G.B. (1971) Dispersive waves and variational prin-
    ciples.
    in: Studies of Applied Mathematics, vol.7 (ed. A.H.Taub),
    pp.181-212
    Math. Ass. of America.

WHITHAM, G.B. (1974) Linear and nonlinear waves
    publ: Wiley, New York.

YUEN, H.C. and B.M. LAKE (1975) Nonlinear deep water waves:
    theory and experiment.
    Phys. of Fluids, vol.18, no.8, August 1975, pp.956-960.

ZIENKIEWICZ, O.C. (1977) The Finite Element Method.
    publ: Mc Graw-Hill, London.

APPENDIX 1. NUMERICAL APPROXIMATION OF THE WAVE EQUATION

The wave equation that appears in Chapter 5 (eq. 5.2), is written here somewhat more compact:

$$(-i\sigma + U\frac{\partial}{\partial x})(-i\sigma\psi + \frac{\partial U\psi}{\partial x}) - \frac{\partial}{\partial x}a\frac{\partial\psi}{\partial x} + b\psi = 0 \quad . \tag{A.1}$$

According to the method of weighted residuals this equation is integrated with a weighting function $W(x)$ (see FINLAYSON, 1972). Integration by parts is applied to those terms in which second order derivatives appear.

$$\int_0^L W(x) \{ (-i\sigma + U\frac{\partial}{\partial x})(-i\sigma\psi + \frac{\partial U\psi}{\partial x}) - \frac{\partial}{\partial x}a\frac{\partial\psi}{\partial x} + b\psi \} dx =$$

$$= \left[UW(-i\sigma\psi + \frac{\partial U\psi}{\partial x}) - aW\frac{\partial\psi}{\partial x} \right]_0^L + \tag{A.2}$$

$$+ \int_0^L \{ (-i\sigma W - \frac{\partial U W}{\partial x})(-i\sigma\psi + \frac{\partial U\psi}{\partial x}) + a\frac{\partial W}{\partial x}\frac{\partial\psi}{\partial x} + bW\psi \} dx = 0 \quad .$$

In the discretizing procedure the unknown function is approximated by a linear combination of shape functions $q_j(x)$:

$$\sum_{j=1}^N \psi_j \, q_j(x) \quad .$$

In the Galerkin version of the finite element method a set of weighting functions is used which coincides with the set of shape functions. Furthermore the interval $(0,L)$ of the x-axis is divided into N-1 segments, called finite elements. The shape functions q are chosen linear within each element (x_{i-1}, x_i); and $q_j(x_i) = \delta_{ji}$.

The numbers ψ_j can be calculated from a set of equations of the form:

$$\sum_{j=1}^N A_{ij} \, \psi_j = 0 \tag{A.3}$$

where

(A.4)

$$A_{ij} = \int_0^L \left\{ \left(-i\sigma q_i - \frac{\partial U q_i}{\partial x} \right) \left(-i\sigma q_j + \frac{\partial U q_j}{\partial x} \right) + a \frac{\partial q_i}{\partial x} \frac{\partial q_j}{\partial x} + b q_i q_j \right\} dx \ .$$

The equation (A.3) holds for $i=2,3,\ldots,N-1$; for $i=1$ and $i=N$ terms must be added to account for the boundary conditions at $x=0$ and $x=L$, resp.. These terms follow immediately from the terms in square brackets in eq. (A.2).

For the three-dimensional model the same procedure is applied. The (x,z)-plane is divided into triangular elements, with shape functions linear over each element. The integration by parts is replaced by an application of Gauss' divergence theorem.

APPENDIX 2. SOLUTION OF THE EIGENVALUE PROBLEM

The linear system of equations (A.3) derived in appendix
1, is homogeneous. Often it becomes inhomogeneous if the
additions due to the boundary conditions are taken into
account. In Chapter 5 several examples are treated in
which the boundary conditions are such that the system
remains homogeneous. In that case the problem becomes an
eigenvalue problem, with m as eigenvalue. This is the
case if one is dealing with homogeneous boundary condi-
tions. The matrix elements A_{ij} depend in some, often
nonlinear, way on the value of m. Ready-made subroutines
for the computation of eigenvalue problems usually assume
that A_{ij} depends linearly on m. A new method must be
found or an existing method adapted. Preferably this
method should take advantage of the bandedness of the
matrix A.   The solution method chosen is based on the
Newton-Raphson iteration method for systems of nonlinear
equations. In this method the system

$$\sum_{j=1}^{N} A_{ij}(m)\, \psi_j = 0 \qquad i = 1, 2, \ldots, N \quad . \qquad (B.1)$$

is approximated by

$$\sum_{j=1}^{N} \left\{ A_{ij}(m^{(k)})\, \psi_j^{(k+1)} + \frac{dA_{ij}}{dm}(m^{(k+1)} - m^{(k)})\, \psi_j^{(k)} \right\} = 0 \quad . \qquad (B.2)$$

Now m is introduced as an ordinary unknown just as the
number ψ_j. The consequence is that an additional equa-
tion is necessary. This has to secure that the vector
is finite; so it might read

$$\sum_{j=1}^{N} \psi_j^2 = N \quad . \qquad (B.3)$$

which is iteratively approximated· by

$$\sum_{j=1}^{N} \left\{ 2 \, \psi_j^{(k)} \, \psi_j^{(k+1)} - (\psi_j^{(k)})^2 \right\} - N = 0 \quad . \tag{B.4}$$

It is seen that the set of equations (B.2) together with (B.4) forms a band matrix with one added row and one added column (see the figure below).

```
++                        +
+++                       +
 +++                      +
  +++                     +
   +++                    +
    +++                   +
     +++                  +
      +++                 +
       +++                +
        +++               +
         +++              +
          +++             +
           +++            +
            +++           +
             +++          +
              +++    +
               ++++
                +++
++++++++++++++++++++
```
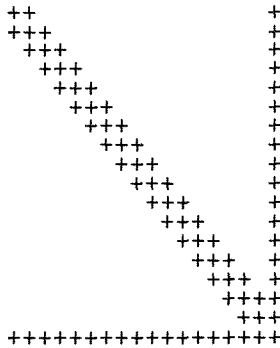
Figure B.1. distribution of non-zero coefficients
in the system of equations

This type of matrices is called profile matrix; such sets of equations can be solved efficiently. In its present form the set of equations is non-symmetric. Some computational effort can be saved if the system is made symmetric; a condition for this is of course that A is symmetric. The system can then be symmetric if the added row reads

$$\sum_{j=1}^{N} \frac{dA_{ij}}{dm} \, \psi_j^{(k)} \, \psi_i^{(k+1)} - N = 0 \quad . \tag{B.5}$$

The method described in this appendix converges rapidly if the initial approximation $\psi_j^{(0)}$ and $m^{(0)}$ is not too far away from the final solution. Otherwise it will often diverge. The method is only efficient if one is interested in not more than a few principal eigenvalues.

SAMENVATTING

Zwaartekrachtsgolven in water met niet-uniforme diepte en stroming.

De dissertatie heeft tot doel een verbetering te bereiken van de berekening van golven in gebieden nabij de kust. Het gaat hierbij in het bijzonder om gebieden in de ingang van estuaria, omdat de veelgebruikte refractie-methode door het onregelmatige verloop van de ondiepten stralenpatronen oplevert die zich slecht lenen voor interpretatie (zie bijvoorbeeld figuur 6.3).

Een model dat aan het bovengenoemde bezwaar tegemoet komt, is het refractie-diffractie model. In het reeds bestaande model van dit type, dat bekend staat als de mild-slope equation, is de invloed van bodemoneffenheden op de golfvoortplanting verwerkt; de invloed van stroming nog niet. Echter men mag aannemen dat juist in de ingang van estuaria de invloed van stroming belangrijk kan zijn. In het proefschrift wordt een model afgeleid, dat gezien kan worden als een uitbreiding van de mild-slope equation. Er zijn termen aan toegevoegd die de invloed van de stroming weergeven.

Het model wordt afgeleid met behulp van de variatierekening (hoofdstuk 3). Daartoe worden eerst de 3-dimensionale differentiaalvergelijking en de randvoorwaarden voor de golfbeweging bekeken. Deze worden gelineariseerd en vervolgens wordt hieruit een variatieprincipe afgeleid. Dit principe is geldig voor willekeurig steile bodemhellingen. Een gereduceerd model voor flauwe hellingen wordt afgeleid met behulp van de methode-Ritz. Hierbij wordt een benaderde oplossing verkregen door het minimum-principe toe te passen

op een deelverzameling van alle toegelaten functies. In dit
geval is de deelverzameling gedefinieerd door aan te nemen
dat lokaal het verloop van de golfpotentiaal over de diepte
is alsof de bodem horizontaal zou zijn. Uit het
gereduceerde minimum-principe kan de partiele
differentiaalvergelijking worden afgeleid.

Deze partiele differentiaalvergelijking bevat een aantal
coefficienten, die afhangen van de golffrequentie, de lokale
diepte en de lokale stroomsnelheid. Ook de
voortplantingsrichting speelt een rol bij de bepaling van de
coefficienten, en dit kan problemen geven in gebieden waar
golven uit verschillende richtingen elkaar kruisen. In dat
geval moet met benaderde coefficienten gewerkt worden.
Aangetoond wordt dat de vergelijking een redelijk
nauwkeurige uitkomst levert ook als van benaderde
coefficienten gebruik gemaakt wordt.

Hoofdstuk 4 laat zien dat de aldus afgeleide vergelijking
goed overeenkomt met andere reeds bestaande modellen.
Besproken worden in dit verband: het variatie-principe van
Luke, de mild-slope equation, de ondiep-watervergelijking,
en het refractie-model.

De golfvoortplantingsvergelijking wordt in hoofdtuk 5
toegepast op een aantal gevallen, waarvan het
gemeenschappelijk kenmerk is dat de dieptelijnen evenwijdig
zijn, terwijl ook de stroomsnelheid niet verandert in de
richting van de dieptelijnen. Bij deze configuratie is een
golfveld mogelijk dat periodiek is in de richting van de
dieptelijnen. Mathematisch betekent dit dat het aantal
onafhankelijke veranderlijken afneemt van 2 tot 1; de
overgebleven coordinaat is de horizontale coordinaat
loodrecht op de dieptelijnen. Met dit model wordt de
partiele reflectie bestudeerd bij scheve of loodrechte inval
op een geul of een onderzeese helling. De uitkomst is dat

een aanzienlijke partiele reflectie slechts in een beperkt aantal gevallen optreedt.

Het bedoelde model is eveneens toepasbaar als de golven evenwijdig lopen aan de dieptelijnen, zoals gebeurt in een prismatische golfgoot. Hierbij wordt het stelsel vergelijkingen mathematisch gezien een eigenwaarde-probleem, waarbij het golfgetal in axiale richting als eigenwaarde optreedt. Iets dergelijks geldt voor golven evenwijdig aan de as van een geul gelegen tussen twee ondiepten. Nu echter is uitstraling van golfenergie in zijdelingse richting mogelijk. Hiermee houdt verband dat de eigenwaarde nu complex kan worden, waarbij het imaginaire deel van de eigenwaarde gerelateerd is aan de mate van vermindering van golfhoogte in axiale richting. Voor dit geval zijn metingen beschikbaar. Er is een vergelijking gemaakt tussen de gemeten en de berekende daling van de golfhoogte. In dit geval is een goede overeenstemming gevonden. Ook is gekeken naar de vorm van de golffronten in de geul. Door de grote variabiliteit van de metingen is geen sterke overeenkomst gevonden; systematische afwijkingen zijn echter niet geconstateerd.

Bij de hiervoor genoemde gevallen is een vergelijking mogelijk van de uitkomsten van het vertikaal geintegreerde model en het oorsponkelijke niet vertikaal geintegreerde (z.g. 3-dimensionale) model. Dit laatste is ook geldig bij grote bodemhellingen, zodat nagegaan kan worden bij welke bodemhellingen het vertikaal geintegreerde model zijn geldigheid verliest. De vergelijking is gemaakt voor een geval van golfinval loodrecht op een helling, en een geval van voortplanting evenwijdig aan een helling. De afwijkingen zijn het grootst bij het eerstgenoemde geval; tot een helling van 0.2 blijkt het vertikaal geintegreerde model goed te voldoen.

In paragraaf 4.5 wordt besproken dat de toepassing van een refractie-diffractie model in een gebied voor de kust zonder verdergaande benaderingen niet uitvoerbaar is. Dit is een gevolg van de grootte van de gebieden die men in de praktijk ontmoet; deze zijn meestal honderden golflengten groot. Bij een numerieke berekening moet dan gewerkt worden met een rekenrooster van duizenden bij duizenden punten. Een stelsel van miljoenen vergelijkingen met miljoenen onbekenden moet hierbij opgelost worden. Dit is een onmogelijke opgave voor hedendaagse computers, zowel bij gebruik van directe als van iteratieve oplossingsmethoden. De uitweg uit het probleem is gebruik te maken van een parabolische benadering. Daarom wordt in hoofdstuk 6 een parabolische benadering afgeleid voor het in hoofdstuk 3 ontwikkelde golfvoortplantingsmodel. Daarna worden enkele fysische effecten aan het model toegevoegd, opdat het de werkelijkheid realistischer weergeeft, met name energiedissipatie ten gvolge van breking, en de invloed van de golfhoogte op de voortplantingssnelheid. De rekenwijze bij het parabolische model is zodanig dat deze effecten zonder problemen in het model opgenomen kunnen worden. Naast het parabolische model waarin de potentiaal als onbekende fungeert, wordt een alternatief model gebruikt met de logarithme van de potentiaal als onbekende. Hiermee is een wijdmaziger rekenrooster mogelijk.

Uitkomsten van het parabolische model met de logarithme van de potentiaal worden getoond voor een gebied gelegen in de mond van de Oosterschelde. Er is een berekening met en een zonder de invloed van stroming gedaan. In het geval met stroming is bekeken een ebstroming met snelheden ter grootte van ong. 0.70 m/s. De invloed van de stroming op het golfveld blijkt in dit geval slechts klein te zijn. Geconcludeerd kan worden dat het model bruikbaar is voor in de praktijk van de kustwaterbouwkunde voorkomende gevallen.

DANK

De tekst van dit proefschrift is vervaardigd met behulp van
tekstverwerkende apparatuur van het Rekencentrum T.H.D.

De typekamer van de afdeling Civiele Techniek heeft de
formules verzorgd.

Tekeningen zijn gemaakt door de tekenkamer van de afdeling
Civiele Techniek.

De berekeningen betreffende de Oosterschelde zijn uitgevoerd
met het programma CREDIZ van de Dienst Informatie Verwerking
van de Rijkswaterstaat.